Solar energy as a renewable resource for cooling

SOLAR ENERGY AS A RENEWABLE RESOURCE FOR COOLING

Yingying YANG

SUPERVISOR: Prof. Gian Vincenzo FRACASTORO

PhD Thesis, 2012

Energy Department

Politecnico di Torino

ACKNOWLEDGMENT

The writing of this PhD thesis has been one of the most significant academic challenges I have ever had to face. And this thesis would not have been possible without the supervising of Prof. G. V. Fracastoro. I am grateful for his support, patience and guidance.
I owe my deepest gratitude to Prof.Gianni Coppa, who inspired my final effort despite the enormous work pressures I was facing and gave me technical support of Matlab.
It is a pleasure to thank all my work mates for their help and collaborations: Marco Simonetti, Luca Degiorgis, Jacopo Toniolo, and Abdul Ghafoor.
My friends: Dong Wei, Xie Ning, Roberta Mulas, Laura Bottino, Shi Hongxia, have given me great support during my study in Italy, and I will forever be grateful for it.
I thank my parents, who have always supported, encouraged and believed in me. And this thesis is dedicated to them.
Special thanks go to the China Scholarship Council, who gave me financial support during my study in Italy.

ABSTRACT

The thesis contains mainly two parts: 1) the solar energy resource assessment through measurements and comparison of solar irradiance models and analysis of atmospheric turbidity factors; 2) Sensitivity analysis of solar cooling system, monitoring on solar cooling system and pre-design of a solar cooling system test rig in Politecnico di Torino.

Firstly, the solar energy resource assessment is based on the measurements of solar beam normal irradiance and solar global horizontal irradiance in Turin during the whole 2010 with available data from end of January until end of December except two thirds of August when the Politecnico di Torino was closed since the campaign was carried on inside the department of Energy. Measured data have been compared with clear-sky models and the atmospheric turbidity factors have been calculated and compared with that in 1975-6 to evaluate the air-quality variation during the last three decades.

Secondly, a series of sensitivity analysis on solar cooling system with various configurations has been undertaken through simulation software Polysun. Field data of solar cooling system in IPLA (Istituto per le Piante da Legno e l'Ambiente) have been monitored and analyzed.

The main conclusions are: The ASHRAE clear-sky model mostly fits the solar beam normal irradiance while it has been found that the solar diffuse radiation factor 'C' ($C=G_{dh}/G_{bn}$) actually not constant but varies all through the day in a typical way; The turbidity factors are lower in 2010 during winter time due to usage of cleaner fuels and district heating while during summer they increase due to heavier traffic; Solar factor (SF) increases as solar collector area is larger, but its increasing ratio is decreasing and SF decreases as volume size of storage tank is bigger after the demand side is satisfied; the three-week monitoring campaign has shown a satisfactory performance of this solar cooling system in PUEEL, although the solar installation appears oversized.

CONTENTS

CHAPTER 1 INTRODUCTION

1.1 Background of solar heating and cooling

1.1.1 Solar thermal energy

This thesis is focus on solar thermal energy, and it is started from the energy structure.

The International Energy Agency (IEA), founded in 1973/4 in response to oil crisis, including 28 member countries, is an autonomous body which works to ensure reliable, affordable and clean energy within the framework of the Organization for Economic Co-operation and Development (OECD). CERT is IEA Committee on Energy Research and Technology.

CERT includes four working parties: working party on energy end use technologies, renewable energy technologies, fossil fuels and fusion power co-coordinating committee.

Both working parties on energy end use and renewable energy technologies are related to solar thermal energy shown as follows. In the Energy end-use working party, the buildings sector includes District heating and cooling, Energy conservation in buildings and community systems and Energy conservation through energy storage. While in the working party of Renewable energy, there is Solar heating and cooling systems (SHC).

SHC is Solar Heating & Cooling Implementing Agreement, which was established in 1976, and its mission is to facilitate an environmentally sustainable future through the greater use of solar design and technologies.

In Europe, the status of installed solar driven systems until 2007 is: there are about 100-120 systems, around 8-9 MW cooling capacity. The collector area is approximately 20000 m^2. The technologies can be divided as: 60% of absorption, 12% of adsorption, 25% of desiccant solid, and 4% of desiccant liquid.

Solar thermal energy (STE) is a technology for harnessing solar energy for thermal energy, namely heat.

Classified by the United States Energy Information Administration, Solar thermal collectors are with low-, medium-, or high-temperature. Low-temperature collectors are flat plates generally used to heat swimming pools; medium-temperature collectors are also usually flat plates but are used for heating water or air for residential and commercial use, and high-temperature collectors concentrate sunlight using mirrors or lenses and are generally used for electric power production. STE is different from and much more efficient than photovoltaic, which converts solar energy directly into electricity.

1.1.2 Air-conditioning worldwide

Global Industry Analysts (GIA) announces that the global air conditioning systems market

will reach 78.8 million units by 2015. Growth in the short to medium term period will be driven by factors such as focus on energy efficient air conditioners, growing replacement needs and increasing demand for developing markets.

1.1.3 Solar thermal for air-conditioning

Around thirty years ago, there was much development of solar energy systems for air conditioning applications particularly in United States and Japan, such as the components and systems. Those activities were terminated mainly because of economic reasons. Nowadays, solar cooling has been prevalent in Europe for many awhile, while it is just become more common in the United States.

Research and demonstration projects are carried out in many countries and also in international framework of the SHC-IEA (Solar Heating and Cooling Programme of the International Energy Agency). Particularly the development of the market of high efficient solar thermal collectors, which are nowadays produced on a semi-industrial or industrial level, provides a good starting point for new attempts.)

Solar assisted cooling is most promising for large buildings with central air-conditioning systems. However, the growing demand for air-conditioned homes and small office buildings is opening new sectors for this technology. In many regions of the world, air-conditioning represents the dominant share of electricity consumption in buildings, and will only to continue to grow. The current technology, electrically driven chillers, unfortunately do not offer a solution as they create high electricity peak loads even if the system has a relatively high energy efficiency standard.

Also, from the environment point of view, solar cooling systems have advantages over conventional air-conditioning ones which use problematic coolants (CFCs), furthermore, less CO_2 emissions from solar cooling systems.

1.2 Potential of Solar heating and cooling

Since 1990 there has been a favorable development in the solar thermal market in many countries, mainly in China and Europe (Energy and Communications 2007). In this thesis, the potential of solar cooling is focus on Europe and China markets.

The worldwide installed capacity of solar heating and cooling systems in total have increased four-fold from 2000 to 2008, with the global industry growing an average of 20.1% annually. The trend of growth has been significant fluctuations from year to year. (Roselund s.d.)

The solar thermal collector capacity in operation worldwide equaled 171 GW_{th} corresponding to 244 million square meters at the end of 2008. China alone accounted for more than half

global capacity, with 101 GW_{th}. Other countries with a large number of collectors in operation are the United States (unglazed collectors), Germany and Turkey. With respect to the capacity installed per 1000 inhabitants, the leading countries are Cyprus (651 kW_{th}), Israel (499 kW_{th}) and Austria (651 kW_{th}) (Renewable Energy Essentials: Solar Heating and Cooling s.d.).

Solar thermal energy for domestic hot water is common all over the world and the so-called solar combi-systems for combined hot water and space heating show a rapidly growing market in European countries. In Germany and Austria, the predominant share of the annual installed collector area is already for combi-systems. Large-scale (producing 1MW or more) solar systems for district heating show considerable growth rates in the Scandinavian countries, Germany and Austria. While new applications for low temperature process heat, air-conditioning and cooling, as well as desalination, are now entering the market. Low temperature solar collectors for water and space heating are very efficient. High temperature solar collectors for refrigeration, industrial process heat and electricity generation, require improvements. Heat storage (both seasonal and compact) represents a key technological challenge. (Renewable Energy Essentials: Solar Heating and Cooling s.d.)

China boasts the largest installed capacity of solar heating and cooling systems in the world, furthermore, it has been expanding to take up an even greater share of the market. China possesses 57.6% of the world's recorded solar heating and cooling capacity with 125 million square meters of collector area until 2008, and in total 2008, there were 21.7 GWth of new installations which makes up 74.6% of the solar heating and cooling market.

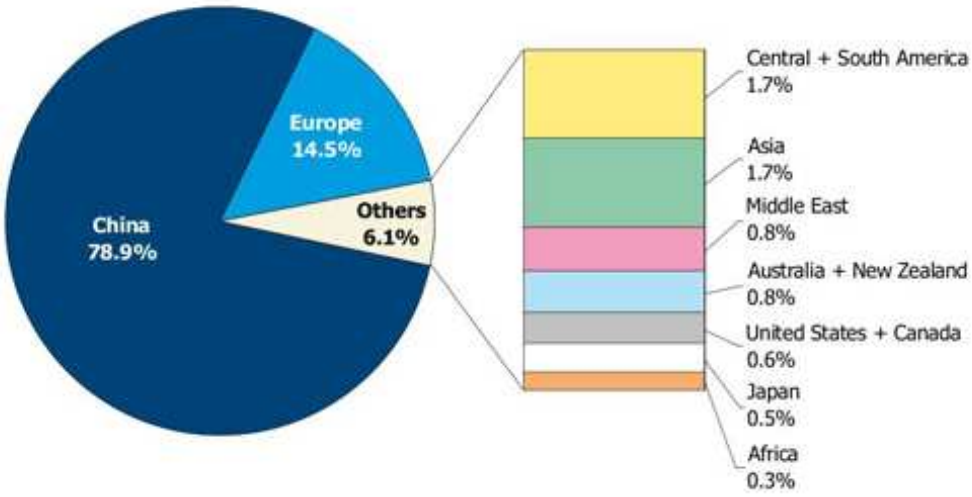

Figure 1Solar heating and cooling market in 2008

1.2.1 Solar thermal market in Europe

European market is the most important secondary market at 14.5% of the market for glazed and evacuated tube collectors, with Germany as the largest European national market. Until 2008, there are around 200 systems including installations of solar cooling with small capacity in Europe. However German demand has been volatile, and in 2009 slipped by 23% to 1.61 million square meters of collectors sold, leading to an overall decrease of 10% for the European industry in 2009. Fortunately for European producers, a number of secondary markets are emerging, led by Italy, which installed 400,000 square meters of collectors in 2009 and which is showing much more stable market growth (Roselund s.d.).

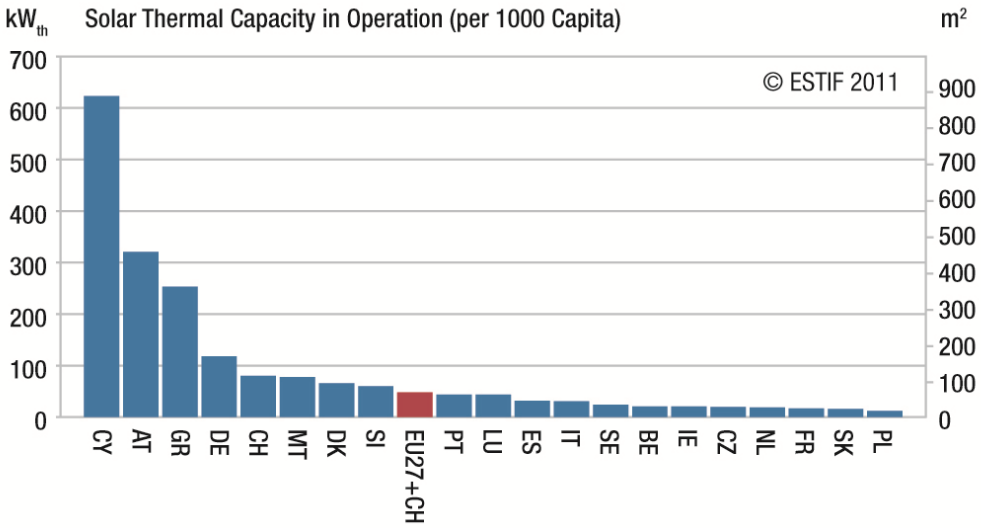

Figure 2thermal capacity in operation until 2011 in Europe

Feed-in tariffs in European nations do not apply to solar heating and cooling, and globally these technologies do not have the policy support that PV and other renewable energy technologies do. This means that a stable market is not guaranteed by strong policies (Roselund s.d.).

Figure 3Solar cooling installation examples in Europe

(Henning s.d.)

It is important to have reliable market data, and ESTIF is dedicated to consolidating its expertise in this field. ESTIF is the voice of the solar thermal industry, actively promoting the use of solar thermal technology for renewable heating and cooling in Europe. With around 100 members from 19 European countries, ESTIF represents the entire supply chain.

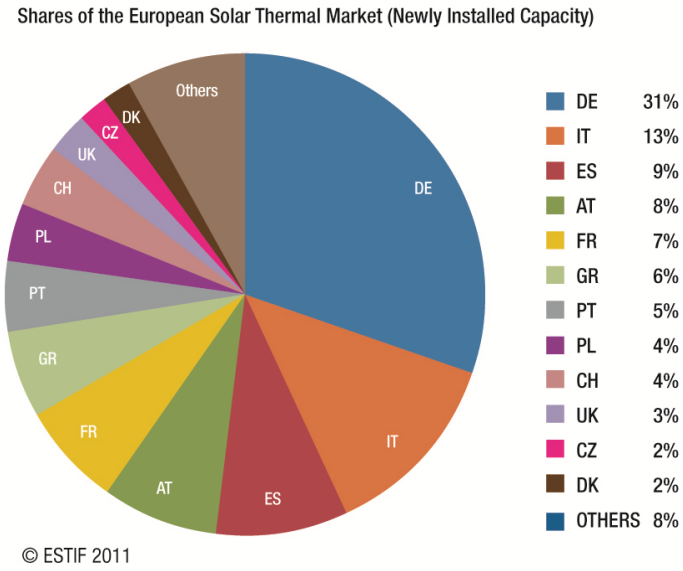

Figure 4Shares of European solar thermal market in 2010

The 2008 financial crisis and the subsequent economic recession have effected on solar thermal fully in 2010, particularly in the construction sector.

The second consecutive decrease of nearly 13% following a 10% drop in 2009 dealt a severe blow since companies had adjusted their production capacities to the peak sales of the decade in 2008. In 2010, companies have implemented strict manufacturing capacity reduction; there was even a concentration in the industry in some countries and, for the first time in a decade, there have been redundancies.

In 2010, the European solar thermal market totaled 2586 MW_{th} (3694940 m^2) of newly installed capacity, decreasing by an estimated 13% in comparison with 2009. Although there is a drop during 2008-2010, the whole level is still above that before 2007.

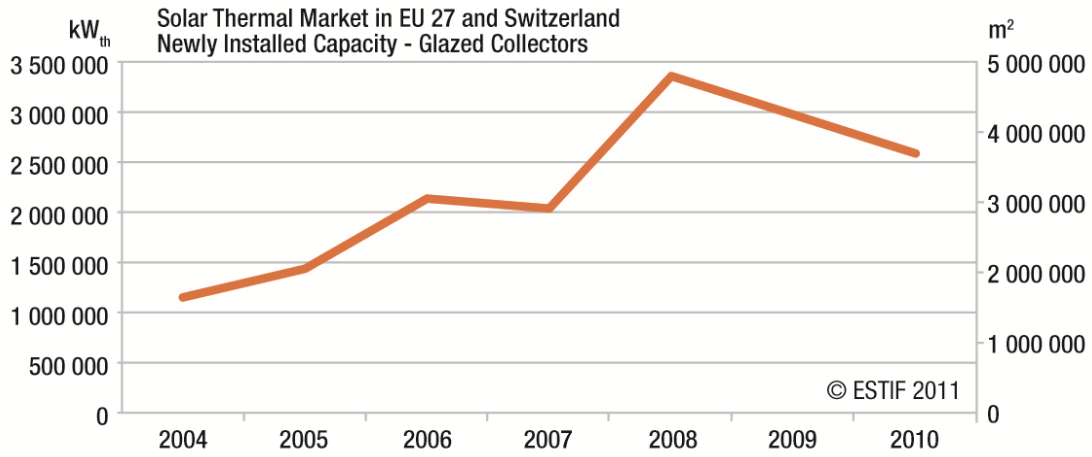

Figure 5Newly installed capacity (glazed collectors) of solar thermal market in EU 27 and Switzerland (ESTIF, European Solar Thermal Industry Federation. s.d.)

From 2010, for better analysis, the European solar thermal markets are divided into three categories according to size, and these three categories are: 50 to 200,000 m^2, above 200,000 to 500,000 m^2, and above 500,000 m^2 of newly installed capacity of glazed collectors.

It is interesting to note that some markets within each group presented similar features.

Figure 6European solar thermal markets by categories

The overall European market reliance on Germany is diminishing. The largest market represents now only one third of the total European market. The dramatic changes in the German market have contributed strongly to the fluctuations in the EU solar thermal market. The relative share of Austria, France, Greece, Italy and Spain is also decreasing. Opposite trends are emerging with Spain facing strong market decrease and Italy consolidating its level.

German market dropped by almost 29% in 2010. This decrease, combined with the 23% downturn in 2009, brings the market almost back to its 2007 level, with 805 MW_{th} of newly installed capacity (1,150,000 m^2).

During 2010, the Italian, Spanish, Austrian, French and Greek markets behaved very differently. While the Italian market confirmed its 2009 level (around 500,000 m^2), the Spanish market continued to decline, increasing the gap between the second and third European markets in terms of newly installed capacity. In previous years, Austria managed to successfully overcome the market downturn but is now following the trend set by its northern neighbor, with a significant decrease of 21%. France also experiences a second year of decline, though more modest than Spain (-3.4%). Finally, the Greek market recovered after a bad performance in 2009, in spite of the difficult situation faced by the country.

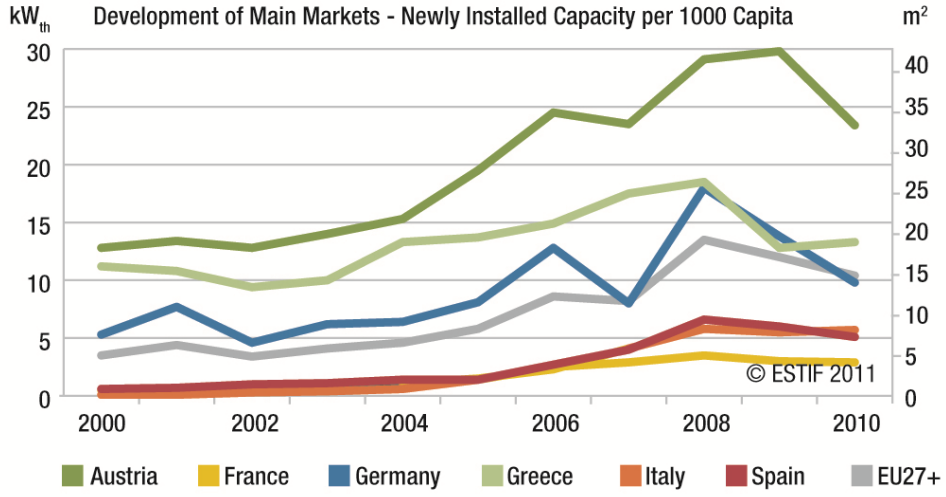

Figure 7Development of main newly installed capacity markets in Europe

Overall, markets below 200,000 m^2 and above 50,000 m^2 grew by 8.8%. Their combined increase of 40,000 m^2 does not quite compensate for the decrease recorded in larger markets. However, it illustrates a different dynamic, triggered by new support schemes in some cases or possibly an increased awareness of solar thermal. (ESTIF, Solar thermal markets in Europe: Trends and market statistics 2010 2011)

Solar Certification Fund is to finance projects of general interests for solar standardization, quality as well as the promotion of the Solar Keymark and its acceptance.

The Solar Keymark, the main quality label for solar thermal, is a voluntary third-party certification mark for solar thermal products, demonstrating to end-users that a product conforms to the relevant European standards and fulfills additional requirements.

Before 2003, it was very complicated and expensive to sell collectors to different countries in Europe as it was needed for the collectors to undergo several different tests and gain additional certificates and approvals.

In 2003, the European Solar Thermal Industry and major testing institutes formulated the Solar Keymark Scheme rules whose major goal is to reduce the wild growth of testing requirements and certificates in order to reduce trade barriers and open the European market for solar thermal products.

All national subsidy schemes and regulations in the EU accept the Solar Keymark with a few exceptions where some additional requirements may apply. Also the Solar Keymark is increasingly recognized worldwide.

The Solar Keymark is a CEN/CENELEC European mark scheme, and is dedicated especially to:

1. Solar thermal collectors (based on European standard series EN 12975)
2. Factory made solar thermal systems (based on European standard series EN 12976)

The Solar Keymark (Solar Keymark brochure s.d.) was developed by the European Solar Thermal Industry Federation (ESTIF) and CEN (European Committee for Standardization) in close co-operation with leading European test labs and with the support of the European Commission. It is the main quality label for solar thermal products and is widely spread across the European market and beyond.

On 1 January 2011, over 1200 Solar Keymark licenses were granted.

Note that the difference between the Solar Keymark and the CE-mark is: The Solar Keymark is a quality label and the CE-mark just attests that the product fulfills minimum legal requirements according to specific European directives.

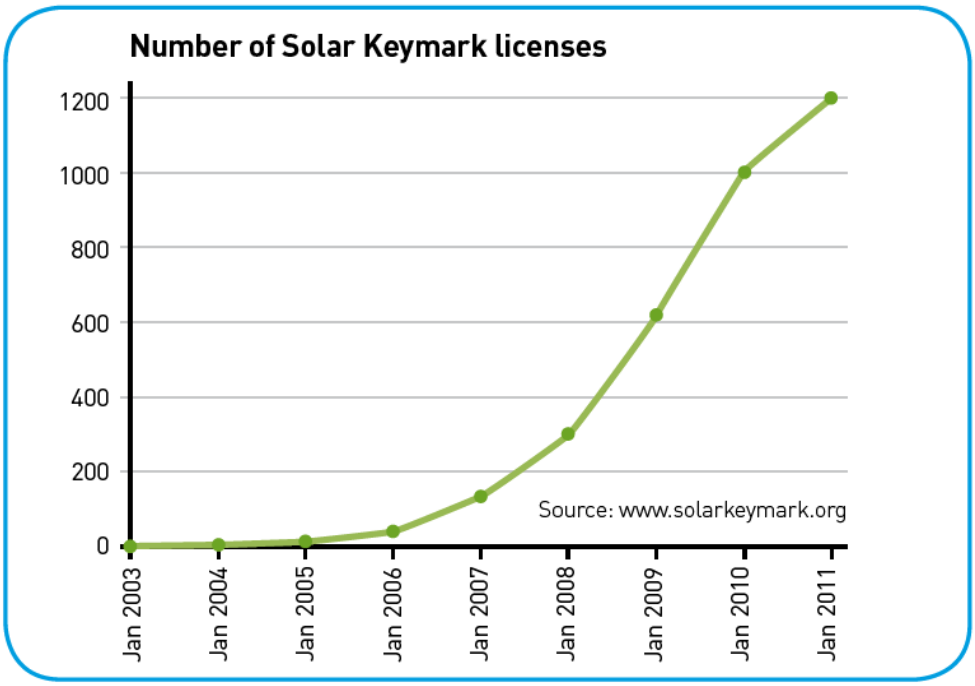

Figure 8Number of Solar Keymark licenses

The Solar Keymark was created to certify solar thermal products of high quality at European level. The aim is to reduce trade barriers and promote the use of high quality solar thermal products in the European market and beyond. (Solar keymark s.d.)

During 2010, the estimated solar yield was 17.3 TWh allowing a contribution of nearly 12 million tons of CO_2 saved thanks to solar thermal.

The European thermal industry needs to adapt strategies and the way to make solar thermal to a competition which also comes from other renewable energy sources.

There would be a benefit from the a renewable boom because of the combined implementation of the binding renewable targets and the higher energy performance standards, but this process is only beginning with the last National Renewable Energy Action Plan (NREAP) delivered in early 2011 and the implementation of the Energy Performance of Buildings Directive (EPBD) still ongoing.

In 2011, the solar thermal industry needs a strong voice at European level, and they focus on the southern European and Mediterranean markets.

1.3 Example of successful installations

1.3.1 Sun-Moon Mansion in China Solar Valley in Dezhou, China

Figure 9 Sun-Moon Mansion in China Solar Valley in Dezhou, Shandong Province, China

At the center of China Solar Valley in Dezhou, Shandong Province, is the Sun-Moon Mansion, the headquarters of Himin Solar Energy found in 1995 by Ming Huang, ISES Vice President for Solar Industry, who received the Right Livelihood Award 2011 (ISES Membership newsletter 2011 (No.6)) 'for his outstanding success in the development and mass-deployment of cutting-edge technologies for harnessing solar energy, thereby showing how dynamic emerging economies can contribute to resolving the global crisis o f anthropogenic climate change.'

Until 2009, the Sun-Moon Mansion was the largest solar structure in the world. It provided the main conference hall for the fourth International Solar Cities Conference in 2010. Covering an area of 750,000 m^2, the building uses solar technologies for hot water supply, space heating and cooling, PV power generation, etc., for the utilization of displays, research and development, work, meetings, education, hotel and recreation.

1.3.2 Air-conditioning of a factory

The site is in Inofita Viotias (approximately 50 km far from Athens from northeast direction). The air conditioning of the production facilities is for a cosmetics factory. It used to be the largest system until 2007.

The flat plat collector field is 2700 m^2. There are two adsorption chillers with 350 kW cooling capacity each, and three compression chillers with 350 kW capacity each.

Figure 10A cosmetics factory using solar cooling system near Athens

1.3.3 Wine store cooling

In Banyuls, south France, there is one of the oldest solar cooling systems in a wine store which has operated this system for more than 12 years without problems.

The evacuated tube collector area is 130 m^2, and there is the single-effect absorption chiller with 52 kW cooling capacity without any back-up system.

In the wine store, there are about 3 million bottles needed to be cooled with three air handling units (25,000 m^3/h air flow).

Figure 11Wine store cooling in Banyuls, France

The solar cooling system is solar autonomous and there is no buffer storage, hence the storage is on load side.

1.3.4 Air-conditioning of a seminar room

The seminar room and the cafeteria are in the building of the chamber for trade & commerce in Freiburg, Germany.

The solar air collector, with an area of 100 m2, is the only heat source, and there is no back-up system or storage tank.

Figure 12A solar desiccant cooling system in Freiburg, Germany

It is a simple solar system because there is only a simple integration into the air-conditioning plant. Nevertheless, it is a promising concept for buildings with a high similarity of cooling loads and solar heat gains.

1.3.5 Hotel air-conditioning

The site is in Dalaman, long the Mediterranean coast of Turkey. The solar thermal collector is parabolic trough collector which produces heat at 180 °C, with an aperture area of 180 m2.

There is a double effect absorption chiller with cooling capacity of 116 kW, 4 bar saturated steam, and the COP reaches higher than 1.2. There is also a LPG-fired back-up steam boiler as an auxiliary system.

Figure 13Air-conditioning of a hotel with parabolic trough collector in Turkey

This system is the first one using double effect chiller. The whole installation has high overall conversion efficiency, which can be an interesting concept for locations with high solar beam radiation. (H.-M. Henning, Solar air-conditioning and refrigeration-Introduction 2007)

1.4 Motivation

1.4.1 Renewable target for 2020 in Europe

The EU Renewable Directive is a unique creation which addresses two of the biggest challenges of our time, energy security and climate change. The 20% renewable target for 2020 is now firmly embedded in the psyche of Europe's decision makers.

In Europe, within only a few years, more than one third of the power from renewable sources of electricity is needed to be generated and a significant part of heating and transport should be based on renewable fuels. Huge practical and concrete initiatives involving society as a whole are needed.

The National Renewable Energy Action Plans (NREAP), which was delivered in early 2011, makes the bridge between ambition and reality. The European Commission is determined that these plans should be coherent, comprehensive and effective. These plans will take the Europe towards a new era of energy security if done well, while Europe will be paying the price for generations to come if not.

Europe's industry and particularly the renewable energy industry, including many small and medium companies, are major players in the policies. Ultimately, the renewable targets will be delivered by them. Hence, to generate the low-carbon revolution and to create jobs, skills, and prosperity in Europe, the key is to make a close collaboration between the EU, Member States and business. In this thesis, the Helios-HP is project between Politecnico di Torino and two companies.

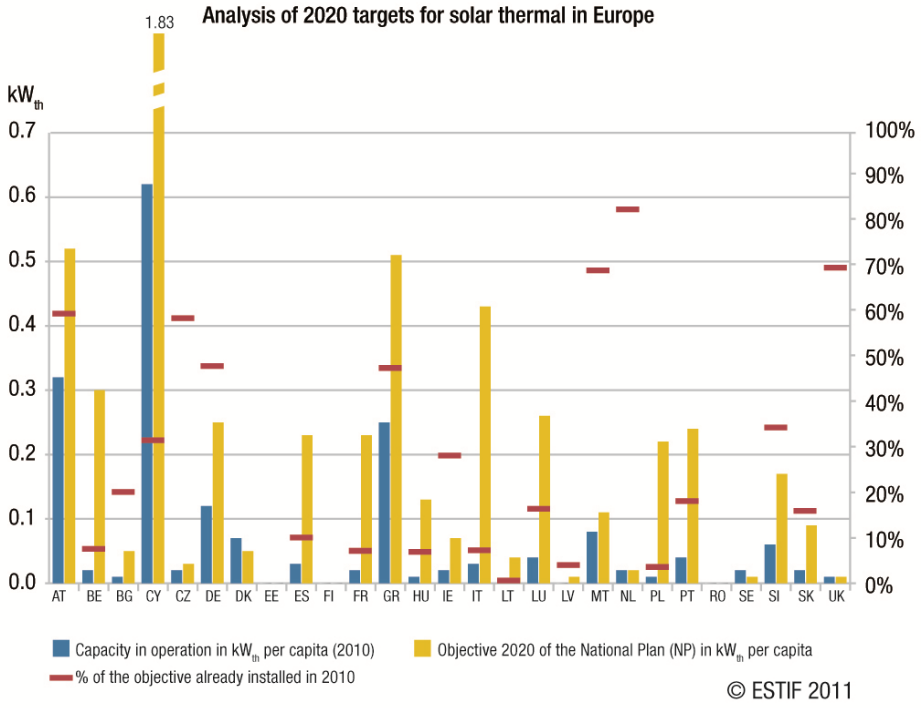

Figure 14Analysis of 2020 targets for solar thermal in Europe

In June 2009, the European Parliament and Council adopted the Directive on the promotion of the use of energy from Renewable Energy Sources (RES), which provides the necessary legislative framework to ensure that the target of 20% renewable energy in Europe becomes a reality by making it mandatory that by 2020 each member state incorporates a share of renewable in its energy mix. Only the overall renewable target is legally binding. This Directive closes a legislative gap, for the first time, heating and cooling accounting for half of the final energy demand will be covered by a European directive promoting renewable energies.

To create a positive climate for the long-term development of solar thermal technologies in Europe is expected. The Directive 2009/28/EC requires each Member State to adopt a National Renewable Energy Action Plan, in which each Member States' national targets for the share of energy from renewable sources consumed in transport, electricity and heating and cooling in 2020 and adequate measures to achieve these targets should be set out. By February 2011, all the 27 Member States had submitted a National Renewable Energy Action Plan (NREAP). In the figure below, the capacity in operation and target for each country is shown.

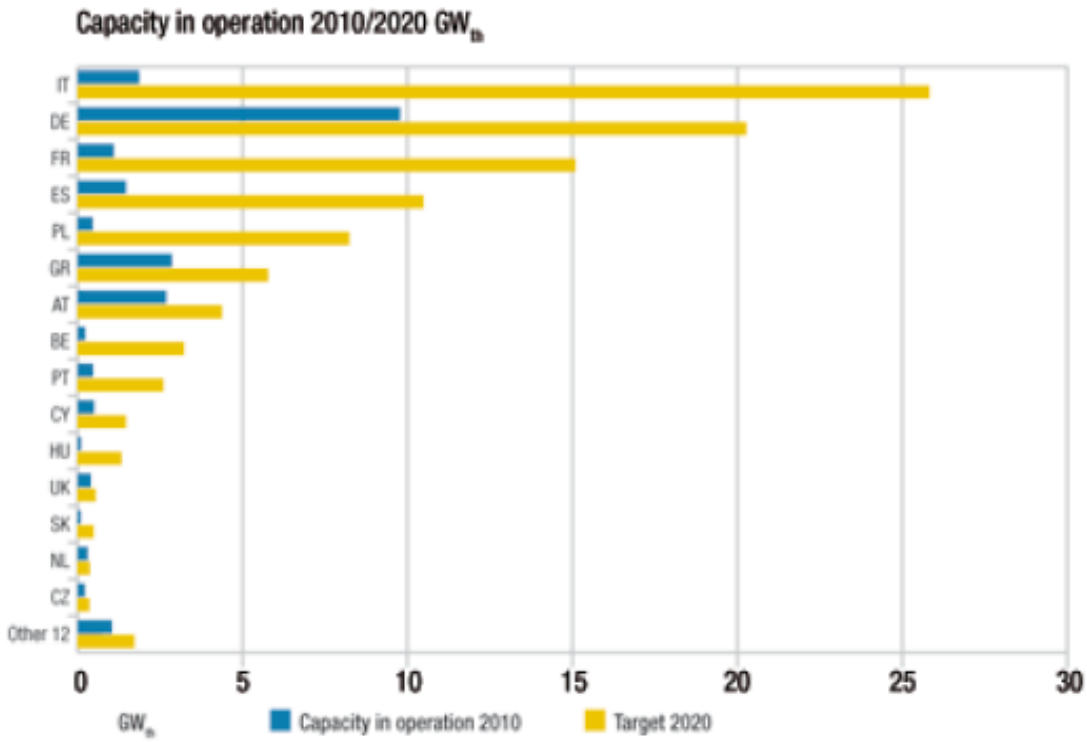

Figure 15Capacity in operation and targets for each country in EU 2010/2020

1.4.2 Energy Performance of Buildings Directive (EPBD)

EPBD's objective is to improve energy efficiency and reduce carbon emissions as part of the government's strategy to achieve a sustainable environment and meet climate change targets agreed under the Kyoto Protocol.

The EPBD introduced higher standards of energy conservation for new and refurbished buildings from April 2006 and will require energy performance certification for all buildings when sold or leased. In addition it will introduce regular inspections for larger air conditioning systems and advice on more efficient boiler operation for commercial property.

To expect a benefit from a renewable boom because of the combined implementation of the binding renewable targets and the higher energy performance standards and prospects for solar thermal according to these national action plans, it is meaningful to do research and practice on solar cooling.

1.4.3 Italian National Renewable Energy Action Plan

In line with the provisions of Directive 2009/28/EC and Commission Decision of 30 June 2009, Italian National Renewable Energy Action Plan appears on 30 June 2010 taken out by Italian ministry for economic development.

The development of renewable energy sources has been one of the priorities of Italy's energy policy for some time, together with the promotion of energy efficiency.

The objectives of such a policy are: energy supply security, reduction in energy costs for businesses and individual citizens, promotion of innovative technology, environmental protection (reduction in polluting and greenhouse gas emissions), and therefore, ultimately, sustainable development.

In the medium to long term, Italy aims to redress the balance of its energy mix, which is currently too dependent on imported fossil fuels. This process will also involve significant measures to re-launch the use of new-generation nuclear power.

Italy's primary objective is to make an extraordinary commitment to increasing energy efficiency and reducing energy consumption. This strategy will also be a determining factor in reaching the targets for reductions in greenhouse gas emissions and the proportion of total energy consumption to be covered by renewable sources.

The recent Italian Law No 99/2009 provided for the publication of an Extraordinary Plan for Energy Saving and Efficiency. This will involve various methods: promotion of distributed cogeneration, measures aimed at encouraging small and medium enterprises to produce their own energy, strengthening the energy efficiency credits scheme, promoting new buildings with significant energy-saving measures and energy retrofits of existing buildings, providing incentives for energy service companies, and promotion of new high-efficiency products.

About the Italy's gross final energy consumption in 2020, there are some different ways to predict it. European Commission has taken the PRIMES model as a reference point. According to the baseline trend scenario of this model, Italy's gross final energy consumption in 2020 could reach a value of 166.50 M_{toe}, compared with the value of 134.61 M_{toe} recorded in 2005. The 2009 update to the PRIMES model, which also takes into account the effect of the financial crisis, estimates Italy's 2020 gross final energy consumption at 145.6 M_{toe}. In a more efficient scenario, which takes into account more energy efficiency measures than the baseline scenario, Italy's gross final consumption in 2020 could remain within a maximum of 133.0 M_{toe}.

According to Directive 2009/28/EC, 17% of Italy's final energy consumption must be covered by renewable sources. Taking the efficient scenario as a reference point, this means that in 2020 the final consumption of renewable energy must be 22.62 M_{toe}.

In order to reach the objectives, there must be a consistent increase in the mobilization of resources available within Italy, and particularly the use of renewable energy sources for heating and cooling and the use of bio-fuels in the transport sector.

Therefore, solar cooling systems combined with domestic hot water (DHW) and space heating is a great option for this target in Italy.

1.5 Objective of study

This thesis consists of several parts: solar energy resource assessment, atmospheric turbidity calculation, solar cooling test rig and one case of solar cooling under monitoring.

First of all, the solar energy resource assessment is carried on through several steps. After a period of trial of the measurement of solar irradiance with Pyrheliometer and Pyranometer, a one-year measurement of solar beam normal irradiance and solar total horizontal irradiance is carried on the roof of the department of Energy in Politecnico di Torino from end of January until end of December in 2010.

Models of clear-sky irradiance are calculated and compared with the measurement data to evaluate the classic models' adaption in Torino or the area with similar climate or atmospheric quality.

Linke turbidity factor is defined and atmospheric turbidity factors are calculated by using the measured solar irradiance in 2010 and a comparison is performed with the turbidity factors measurements during 1975-1976 which were carried on both in center of Torino and in Pino Torinese (10 km far from the center and 380 m above the center).

Furthermore, the air quality is analyzed by specially evaluating the SO_2 concentration during the last three decades in Torino which shows the variation of polluting situation in the city.

The second main part of the work is on solar cooling simulations with software Polysun.

Helios-HP is a project of solar cooling test rig in the department of Energy in Politecnico di Torino and the work includes the pre-design of the solar cooling installation and simulation with Polysun to predict the performance of the solar cooling system.

A solar cooling case in IPLA (Istituto per le Piante da Legno e l'Ambiente) is monitored from 2011 to obtain the related parameters to evaluate the solar cooling system efficiency. And, a simulation of the same scheme as the real installation in IPLA with Polysun is performed to establish a comparison.

CHAPTER 2 RESOURCE ASSESSMENT

2.1 Extraterrestrial solar radiation

2.1.1 Solar system and fusion of Sun

The Solar System consists (Selfe 2006) of the Sun and all objects such as the planets and associated satellites, the asteroids, the Kuiper Belt Objects (KBOs) and the comets that orbit the Sun in the far off Oort Cloud. All these objects are gravitationally bound to the Sun.

The Solar System was formed approximately five billion years ago when a cloud of dust and gas was disturbed and coalesced to form the Sun, the planets and a handful of dwarf planets.

The light and heat that reach the Earth is essential for the human being's survival and the survival for every creature on the planet.

2.1.2 Solar spectra with zero atmosphere

For calculating the turbidity factor, it is necessary to know the spectral distribution of the extraterrestrial radiation, which is the radiation that would be received without atmosphere.

There are several data of solar spectra with zero air mass, and the two main standard ones are 2000 ASTM Standard Extraterrestrial Spectrum Reference E-490-00 (ASTM E-490) and 1985 Wehrli Standard Extraterrestrial Solar Irradiance Spectrum.

The ASTM E-490 was developed for use by the aerospace community in 2000 by the American Society for Testing and Materials (ASTM), and the solar spectral irradiance is based on data from satellites, space shuttle missions, high-altitude aircraft, rocket soundings, ground-based solar telescopes, and modeled spectral irradiance. As for the integrated spectral irradiance, it has been made to conform to the solar constant value, 1366.1 W/m^2, which is accepted by the space community.

The 1985 Wehrli Standard Extraterrestrial Solar Irradiance Spectrum (also called WMO/WRDC Wehrli Air Mass Zero solar spectral irradiance) was constructed in 1985, and the curve has often been cited for the use of extraterrestrial solar spectral irradiance distribution.

To evaluate the two standard spectra, a plot of the two standard spectra was done, and there are slightly small differences between ASTM E490 and Wehrli 1985.

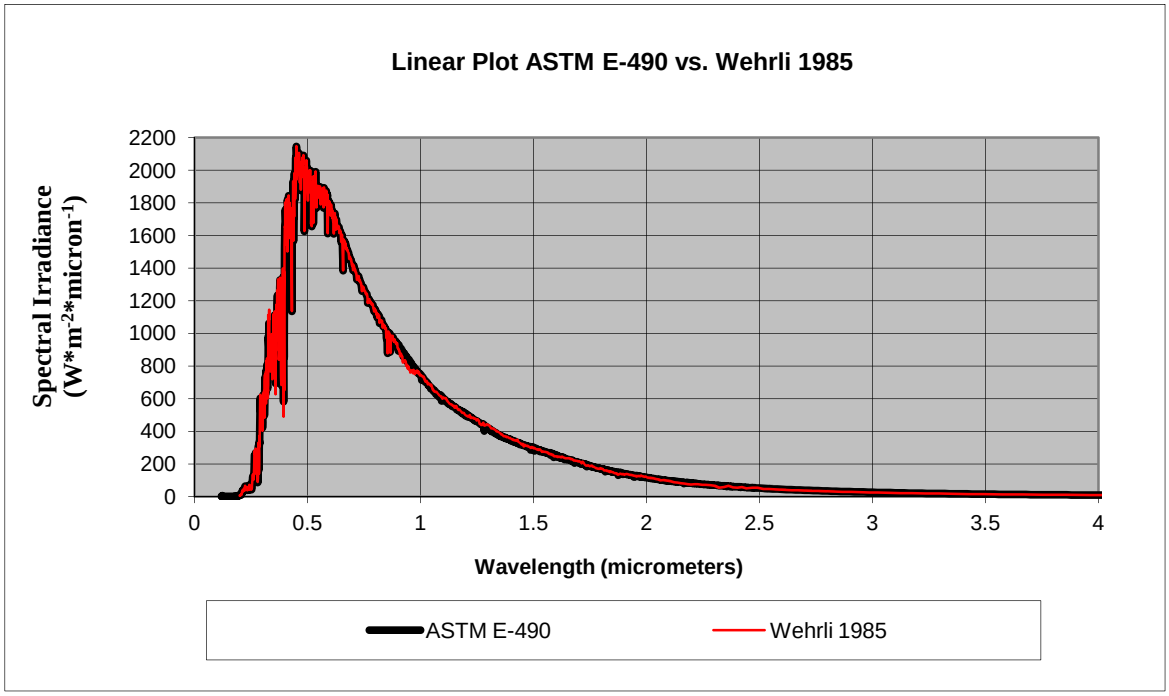

Figure 16Linear plot of wavelength and spectral distribution for ASTM E490 and Wehrli 1985 on top of the atmosphere for a mean Sun-Earth distance

(htt)

Solar constant (G_{sc}) is the energy from the sun per unit time received on a unit area of surface perpendicular to the direction of propagation of the radiation at mean earth-sun distance outside the atmosphere.

In the calculation, the ASTM E-490 is used as the solar extraterrestrial irradiance source, and the solar constant can be found by summing up all products of delta wavelength($\Delta\lambda$)and spectral irradiance:

$$G_{st} = \sum_{\lambda=0.1195}^{400} \Delta\lambda \times G_{\lambda} = 1367.6\, W/m^2$$

$$\lambda: \mu m$$

$$\Delta\lambda_i = \lambda_{i+1} - \lambda_i \quad i = 1, 2, \cdots, 1696$$

In the reference book of 'Solar Engineering of thermal progress' (John A. Duffie s.d.), G_{sc}=1367 W/m^2.

2.1.3 The Sun-Earth geometry

The geometrical relationship between the Sun and Earth affects the solar radiation reaching on the Earth and the Earth's climates.

(1) Variation of Sun-Earth distance

The Sun, with a diameter of 1.39×10^{9} *m* (about 109 times that of Earth), is around 1.5×10^{11} *m* from the Earth. As observed from the Earth, the Sun rotates on its axis about once every four weeks. The Sun does not rotate as a solid body: the equator takes around 27 days, while the Polar Regions take around 30 days.

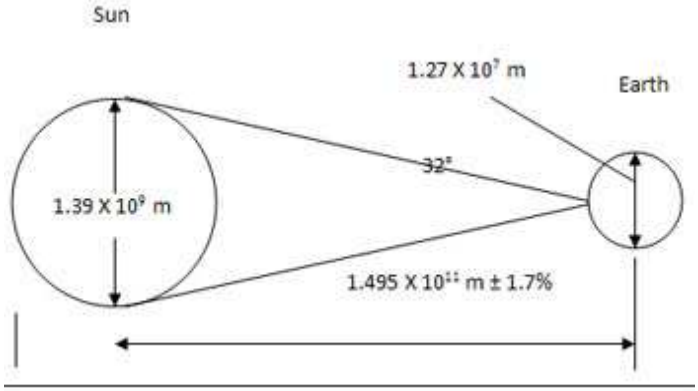

Figure 17The Sun-Earth geometry relationship

a. Celestial sphere

The celestial sphere is a very practical tool for positional astronomy. It is an imaginary sphere of arbitrarily large radius, concentric with the Earth and rotating upon the same axis. Projected upward from the Earth's equator and poles are the celestial equator and the celestial poles (Wiki:Celestial sphere s.d.).

b. Ecliptic

The ecliptic is the plane of the Earth's orbit around the Sun. More accurately speaking, it is the intersection of the celestial sphere with the ecliptic plane, which is the geometric plane containing the mean orbit of the Earth around the Sun. The name ecliptic arises because eclipses occur when the full or new Moon is very close to this path of the Sun (Wiki: Ecliptic s.d.).

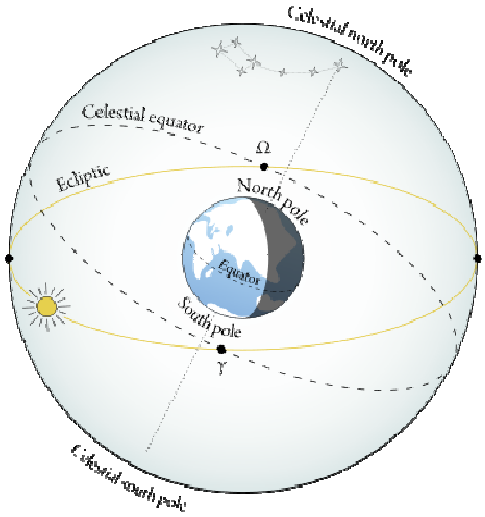

Figure 18Ecliptic

The term ecliptic describes the center-line of Zodiac, which extends some eight degrees above and below the ecliptic. In other words, the Zodiac is a belt 16° wide centered on the ecliptic (Ennis s.d.).

c. Perihelion and Aphelion

The Earth's orbit around the Sun is almost-circular elliptic and the Sun is at the focal point of this ellipse. The Earth moves closer towards and further away from the Sun as it orbits since the Sun is not at the center of the elliptical orbit. The closest point to the Sun in the Earth's orbit is called perihelion which occurs in early January (on January 3rd), while the furthest point is called aphelion which occurs in early July (on July 4th). The terms 'perihelion' and 'aphelion' came from Greek, as 'helios' mean Sun, 'peri' means near, and 'apo' means away from. The distance from Earth to the Sun is about 147 *million km* when Earth is at perihelion, 152 *million km* at aphelion, and the average distance of the Earth from the Sun over a one year period is 150 *million km* (Perihelion and Aphelion s.d.).

The variation of Sun-Earth distance does influence the amount of the extraterrestrial solar radiation intercepted by the Earth, approximately an increase of 6.9% of at perihelion as related to aphelion. Nevertheless, the seasons are not caused by the variation of distance between Sun and Earth. The truth is that the Earth moves fastest at perihelion and slowest at aphelion, and for example, in January the Earth's reaches perihelion when it is winter. The cause of seasons is the tilt angle of Earth's axis which will be explained in the following section.

(2) Earth Revolution

The two principle movements of the Earth are revolution and rotation. Earth rotates on its axis as it revolves around the Sun.

Revolution is the movement of the Earth in an elliptical orbit around the Sun whose average distance is 150 *million km* away.

The elliptical orbit causes the Earth's distance from the Sun to vary at different times of the year. The Earth revolves around the Sun every 365 days and 6 hours which define the astronomical year and also the calendar year. During this time there are 365.25 rotations of the Earth. Due to that extra one quarter day that it takes for the Earth to complete its journey, the calendar of 365 days is corrected once every four years with an additional day to February when the so-called Leap Year arrives.

a. Inclination of the Earth's axis

The Earth's polar axis is not perpendicular to the plane of the ecliptic, but inclined at a fixed angle of about 23.5° from the perpendicular to the ecliptic.

As the Earth revolves about the Sun, the angle of inclination of the earth's axis in relation to the plane of the ecliptic is constant, and this is known as the parallelism of the axis (currently toward Polaris, the North Star). However, the relative position of the Earth's axis to the Sun (The direction of solar irradiance and the direction the Earth's axis leaning towards) does change during this cycle which causes seasons and day lengths of day due to the change of the height of Sun above the horizon annually.

The Earth's axis is tilted relative to the perpendiculars to the ecliptic plane by an angle of 23.5°, which causes the circle of the ecliptic to be tilted relative to the celestial equator again by the same angle, which as a result is called the obliquity of the ecliptic. In fact, the tilt of the Earth changes slightly, with a dominant cycle every 41,000 years (Movements of the Earth s.d.).

The change in angle of inclination is only 1 degree from the present tilt, from 23.5° to 24.5°. However, Earth's tilt is a critical factor in climate resulting in very large differences in solar radiation. Changes in Earth's angle with respect to the Sun often go by the name 'obliquity'.

b. Seasons, Solstice and Equinox

The circumstance of tilt angle of the Earth's axis also causes seasons by controlling the intensity and duration of sunlight the local position receives on the Earth. Without the inclination of the Earth there would be no seasons.

Seasonal time (solstice and equinox) is based on the geometry of the Earth in relation to the Sun during its yearly revolution. Solstice refers to the date when the Sun stands directly overhead of the N-S migration of the location in question, 23.5°N on June 21 or 22 (the summer solstice) and 23.5°S on December 21 or 22 (the winter solstice), while equinox,

refers to the date of equal night and day period and this occurs when the Sun at noon is directly overhead at the equator on March 21 (vernal equinox in the northern hemisphere) or on September 23 (autumnal equinox in the northern hemisphere).

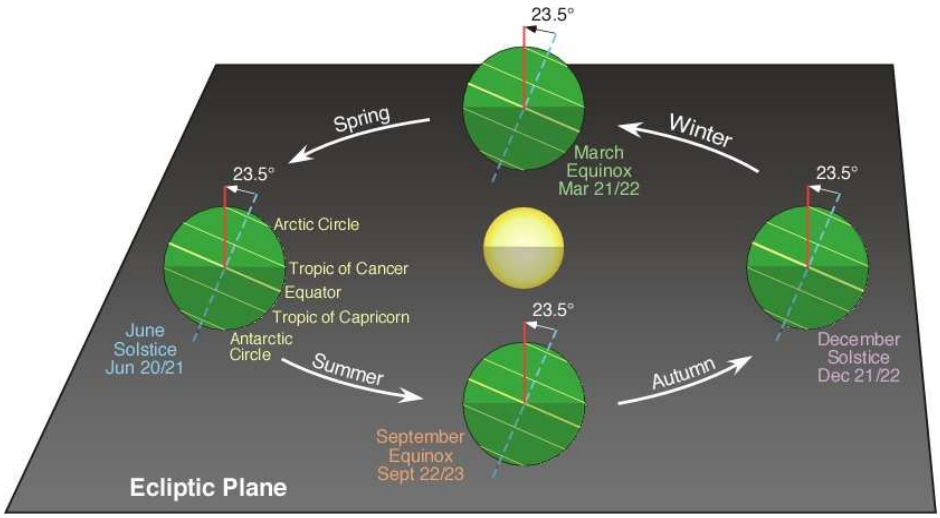

Figure 19The tilt angle of Earth's axis remains unchanged as season changes

At the times of the solstices, the circle of illumination cuts all parallels except the equator unequally, so that days and nights are unequal in length except at latitude 0. For example, during summer solstice in the northern hemisphere, all locations North of the equator have day lengths greater than twelve hours, while all locations South of the equator have day lengths less than twelve hours.

At the times of the two equinoxes, the Sun's noon rays are vertical at the equator, the circle of illumination cuts all parallels in half, so that days and nights are equal (12 hours) over the whole Earth.

The steepest point on the sinusoidal curves is during the equinoxes in March and September.

(3) Earth Rotation

The Earth Rotation refers to the spinning movement of the Earth on its imaginary axis (North and South Pole). One rotation takes 24 hours, which is called a mean (average) solar day and this is why there is a day and night in each 24 hours (Earth-Sun Geometry s.d.).

The direction of Earth rotation is counterclockwise when viewed from above the North Pole, namely, Earth rotates from West to East which explains that the Sun rises in the East and sets in the West apparently.

The rotation produces night and day, and due to the tilt angle of Earth, the lengths of day and night change all through the year. The height of the Sun throughout the year changes. During winter, the Sun has lower height at its highest point, while in summer, the Sun reaches its highest point at the sky for the Northern Hemisphere.

Apparently, the Sun rises in the East and sets in the West, and for a whole year, the Sun rises in the northeast horizon for half of the year, and Southeast for the remainder. This is because the Earth's rotation and the increasing deviation from the eastern horizon with latitude.

In a word, the geometry of Sun-Earth (Revolution, Parallelism, tilt angle of Earth, Earth Rotation, oblate spherical shape of Earth, ect.) produces an unequal distribution of solar energy over the Earth and responsible for lengths of night and day, and changes of seasons.

2.1.4 Extraterrestrial solar radiation reaching on Earth

The solar radiation at normal incidence received at the surface of the atmosphere of the Earth changes due to the variation of extraterrestrial radiation which is inflected by variation in the radiation emitted by the Sun and the one of the Sun-Earth distance. For engineering purposes, the energy emitted by the Sun can be considered to be fixed in a view of the uncertainties and variability of atmospheric transmission, while the variation of the Sun-Earth distance leads to the variation of extraterrestrial radiation flux in the range of ±3.3%.

G_{on} is the extraterrestrial radiation incident on the plane normal to the radiation on the n^{th} day of the year. There are two main equations for calculating G_{on}:

A simple equation (John A. Duffie s.d.) with accuracy adequate for most engineering calculations is given as:

$$G_{on} = G_{sc}(1 + 0.033\cos\frac{360n}{365})$$

And a more accurate equation (±0.01%) is given by Spencer (1971) and cited by Iqbal (1983) as:

$$\mathrm{G_{on}} = \mathrm{G_{sc}}(1.000110 + 0.034221\mathrm{cosB} + 0.001280\mathrm{sinB} + 0.000719\mathrm{cos2B} + 0.000077\mathrm{sin2B})$$

Where B is the fractional year in radians (Declination s.d.), and given by

$$B = \frac{2\pi}{365}(n-1)$$

Or

$$B = (n-1)\frac{360}{365}$$

And n is the n^{th} day of the whole year.

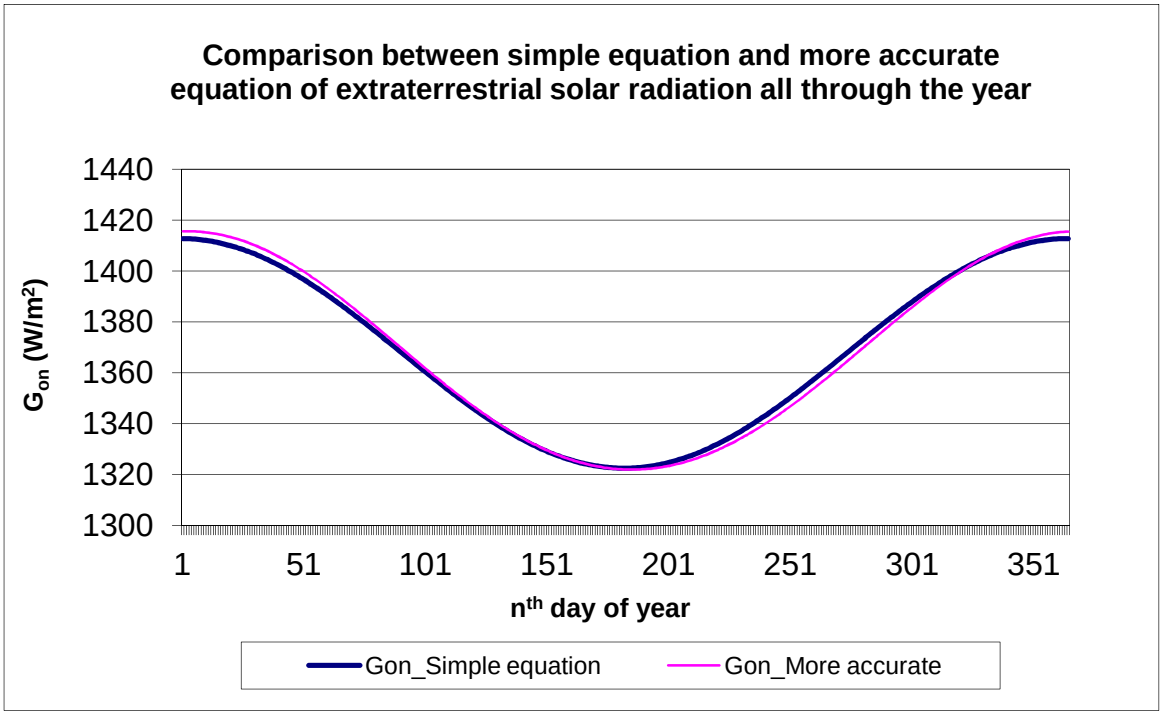

Figure 20Variation of extraterrestrial solar radiation all through the year

2.2 Earth's atmosphere and solar radiation on the ground

The atmosphere is a mixture of 21% oxygen, 78% nitrogen, and approximately 1% other trace gases. It is divided into layers (Atmosphere s.d.), which are the troposphere (including the planetary boundary layer as lowest layer), stratosphere (including the ozone layer), mesosphere, thermosphere, exosphere, and the magnetosphere._Most of the weather and clouds are found in the troposphere layer where three quarters of the atmosphere lies, and the depth of this layer varies between 17 *km* at the equator and 7 *km* at the poles above the sea level. High above the planet, the atmosphere becomes thinner until it gradually reaches space. The Kármán line, which locates within the thermosphere at an altitude of 100 *km*, is commonly used to define the boundary between the Earth's atmosphere and outer space even though the exosphere can extend from 500 up to 10000 *km* above the surface.

The atmosphere is vital for making Earth livable. Firstly, the oxygen is essential for life; secondly, the atmosphere traps heat to make the temperature on Earth comfortable for life, and finally, it blocks some dangerous rays from reaching the surface of Earth (Earth's Atmosphere s.d.). Nevertheless, over several decades, greenhouse gases and air pollutants released into the atmosphere have been causing big changes such as global warming, ozone holes and acid rain.

2.2.1 Scattering and absorption

After solar radiation enters through the top of the atmosphere, the various atmospheric processes operate to change the spectral distribution:

(1) Atmospheric scattering by air molecules, water vapor and droplets, dust, and other aerosol particles inside the atmosphere;

(2) Absorption by atmospheric gases (ozone, water and CO_2) and particulates.

Slanting solar rays deliver less energy at the earth's surface than vertical rays, both because their energy is spread over a larger surface, and because they pass through a thicker layers of reflecting and absorbing atmosphere.

As the solar radiation traverses the atmosphere, the interaction between the radiation and air molecules, water, and dust causes scattering. The number of these particles and the size relative to wavelength of radiation determine the degree to which the scattering occurs and these particles depend on the quantities of dust and moisture present in the atmosphere at different time and location in question and also the air mass which describes the path length of the radiation through air molecules. From the view point of photon, scattering can be explained as the processes in which the photons change direction after an interaction with the light passing through the atmosphere.

Comparing with the wavelength of the solar radiation, the air molecules are very small in size. As a result, the scattering is in accordance with Rayleigh scattering theory (Rayleigh scattering, named after the British physicist Lord Rayleigh, is the elastic scattering of light or other electromagnetic radiation by particles much smaller than the wavelength of the light.) which only has significant effect on atmospheric transmittance relative to the short wavelength band only (below $\lambda = 0.6\mu m$).

Due to water molecules' aggregation and the water's condensation on dust particles of various sizes, the dust and water inside the atmosphere have larger particle sizes. Moreover, the nature and extent of dust and moisture particles are highly variable depending on different location and time. Hence, it is more difficult to treat with these scattering effects caused by dust and water than those of Rayleigh scattering by air molecules. There are two approaches used for dealing with this problem: Moon (1940) and Ångström's turbidity equation. Moon developed different transmission coefficients which are functions of wavelength for water, dust and air molecules, and the overall transmittance due to scattering is the product of the three transmittances. While Ångström's turbidity equation estimates the effects of scattering by dust and water, absorption is caused mainly by water vapor and carbon dioxide in several strong bands in the infrared region, and by high-altitude atmospheric ozone in the ultraviolet

region. When the photons are removed from a beam of light and their energy is converted to an excitation of atoms or molecules, the absorption occurs (Bason s.d.).

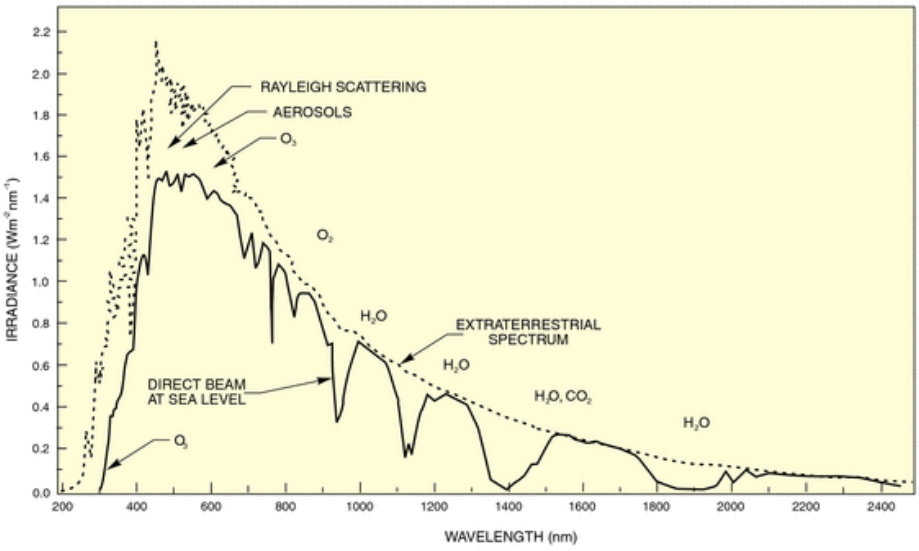

Figure 21Effects of scattering and atmospheric absorption on the spectral distribution of beam irradiance (Introduction to Solar Radiation s.d.)

Scattering by air molecules, water vapour molecules, water droplets, and dust particles causes 6% of solar radiation to be returned to space; 20% of solar radiation reaches the surface of the Earth as diffuse radiation. Air molecules scatter blue light the most and red light the least. This makes the sky blue and the setting sun red. Scattering by large particles (water droplets and dust particles) is independent of wavelength, so mist and haze look white.

Above 40km absorption is mainly by ozone (O_3); this absorbs 3% of solar radiation. At lower levels water vapour absorbs about 14%, mainly in the near infrared. Clouds absorb very little solar radiation, which is why clouds do not evaporate. Their effect on solar radiation is by scattering and reflection. The albedo of the Earth's surface is the fraction of solar radiation reflected. It depends on the colour of the surface. Examples of albedos with the sun overhead are given in Table.

Table 1Albedos of different surfaces

Type of Surface	Normal irradiance Albedo
Vegetation	0.2
Light soil	0.3
Dark soil	0.1
Water	0.1
Clouds	0.5-0.9

It should be noticed that when the Sun is low in the sky the albedo of water is much greater than 0.1.

2.2.2 Rayleigh atmosphere

According to Bouguer-Lambert Law (1760) (variously know as Bouguer's law, Lambert's law, or Beer's law), the incident solar beam irradiance which is transmitted directly by a plane-parallel and horizontal homogeneous atmosphere can be calculated as:

$$G_{bn} = G_{on} e^{-\tau \sec \theta_z}$$

Where G_{bn} and G_{on} are the solar beam irradiance reaching the ground and the extraterrestrial solar irradiance, respectively;

τ is the optical thickness of the atmosphere measured in the local zenith direction;

θ_z is the solar zenith angle.

For an arbitrary height z, the optical thickness of the whole atmosphere above it is defined as:

$$\tau(\lambda, z) = \int_z^{\infty} B(\lambda, z) dz$$

Where $B(\lambda, z)$ is the attenuation coefficient which is a function of both λ and z.

Since the attenuation effect is produced by scattering and absorption, both B and τ include two parts:

$$B = B_s + B_a$$

$$\tau = \tau_s + \tau_a$$

Where the subscripts indicate scattering and absorption respectively.

To evaluate the atmospheric turbidity in real atmosphere, it is convenient to discuss for the case of a clear atmosphere by separating the processes of scattering and absorption, even though in the real atmosphere the effects of scattering and gaseous absorption can not be separated easily.

Rayleigh atmosphere is the simplest atmospheric model which contains scattering particles all with a size much smaller than the wavelength, namely, a non-absorbing medium. In principle, this Rayleigh atmosphere applies to molecules of the atmospheric gases, and the volume scattering coefficient of a Rayleigh atmosphere is:

$$B^R(\lambda) = \frac{32\pi^3}{3\lambda^4} \frac{(n-1)^2}{N}$$

Where *n* is the relative index of refraction of the medium;

N is the number density of particles.

Lord Rayleigh (1842-1919) firstly derived this relation in early 1870s in connection with his famous explanation of the color and polarization of the light from the sunlit sky. According to

Rayleigh's function, the efficiency of the scattering attenuation in the ideal atmosphere depends on $-\lambda^4$ critically, also combining with the spectral sensitivity of human eyes and the spectral distribution of sunlight, this theory explains for the blue color of the clear sky.

If the distribution of the gases in atmosphere with altitude is known, it is possible to compute $B^R(\lambda)$ as a function of altitude. And the Rayleigh optical thickness τ^R of the air above any selected level in atmosphere can be calculated by performing the integration function of the attenuation coefficient $B(\lambda, z)$ which is a function of both λ and z.

2.2.3 Linke turbidity factor theory

Even in the clearest natural atmosphere, there are ample numbers of dust, haze, and other types of non-Rayleigh particles producing important radiation effects. For instance, the significant aerosol effects up to altitudes of at least 24.4 *km* (Eddy, 1961).

The total optical thickness $\tau(\lambda)$ may be composed of several components (B. A. al 1999):

$$\tau(\lambda) = \tau^{R}(\lambda) + \tau^{a}(\lambda) + \tau^{g}(\lambda)$$

where $\tau^{R}(\lambda)$ is the Rayleigh optical thickness;

$\tau^{a}(\lambda)$ is aerosol optical thickness;

$\tau^{g}(\lambda)$ is the optical thickness due to absorption by gases such as O_3, NO_2 and H_2O.

The calculation of Linke turbidity factor will be described in detail in section 2.6.

2.2.4 Definition of solar radiation quantities

The knowledge of the local solar radiation is essential for the proper design of solar cooling for buildings. The best database would be the long-term measured data at the site of the proposed solar system. As the beam component (direct irradiance) is important in designing systems employing solar energy, emphasis is often put on modeling the beam component.

There are two categories of solar radiation models, available in the literature (L.T.Wong 2001), that predict the beam component or sky component based on other more readily measured quantities: Parametric models and Decomposition models.

Beam radiation, which is often referred to as direct solar radiation, is the solar radiation received from the Sun without having been scattered by the atmosphere. To avoid confusion between subscripts for direct and diffuse, the term beam radiation is used in this thesis.

Beam normal irradiance G_{bn} is the beam radiation per unit time received on a unit area of surface perpendicular to the direction of propagation.

Diffuse radiation is the solar radiation received from the Sun after its direction has been changed by scattering by the atmosphere. In some meteorological literature, diffuse radiation

is referred to as sky radiation or solar sky radiation. The definition used here will distinguish the diffuse radiation from infrared radiation emitted by the atmosphere.

Diffuse horizontal irradiance G_{dh} is the diffuse radiation per unit time received on a horizontal surface.

Total solar radiation is the sum of the beam and diffuse solar radiation on a surface. The most common measurements of solar radiation are total radiation on a horizontal surface, which is often referred to as global radiation on the surface.

Irradiance, with unite of W/m^2, is the rate at which radiant energy is incident on a surface per unit area of surface. The symbol *G* is used for solar irradiance, with appropriate subscripts for beam, diffuse, or spectral radiation.

Irradiation or Radiant Exposure, with unit of J/m^2, is the incident energy per unit area on a surface, found by integration of irradiance over a specified time, usually an hour or a day. Insolation is a term applying specifically to solar energy irradiation. The symbol *H* is used for insolation for a day. The symbol *I* is used for insolation for an hour (or other period if specified). The symbol *H* and *I* can represent beam, diffuse, or total and can be on surfaces of any orientation.

Subscripts on *G*, *H*, and *I* are as follows: *o* refers to radiation above the Earth's atmosphere, referred to as extraterrestrial radiation; *b* and *d* refer to beam and diffuse radiation; *T* and *n* refer to radiation on a tilted plane and on a plane normal to the direction of propagation. If neither *T* or *n* appears, the radiation is on a horizontal plane.

2.2.5 Solar time and angles

In all of the Sun-angle relationships, solar time is used. Solar time is the time based on the apparent angular motion of the Sun across the sky, with solar noon which is the time when the Sun crosses the meridian of the observer.

Solar time does not coincide with local clock time, so it is necessary to convert local standard time to solar time by applying two corrections. Firstly, there is a constant correction for the difference in longitude between the observer's meridian (longitude) and the meridian on which the local standard time is based. Apparently the Sun takes around 24 hours to rotate around the Earth, namely, the Sun takes 4 minutes to transverse 1° of longitude. Secondly, there is a correction from the equation of time due to the perturbations in the Earth's rate of rotation which affect the time when the Sun crosses the observer's meridian. The difference in minutes between solar time and standard time is:

$$\text{Solar time} - \text{standard time} = 4\,(L_{st} - L_{loc}) + E$$

where L_{st} is the standard meridian for the local time zone, L_{loc} is the longitude of the location in question, and longitudes are in degree west, that is, 0° < L <360°. The parameter E is the equation of time (in minutes) given by Spencer (1971), as cited by Iqbal (1983):

$$E = 229.2 \times (0.000075 + 0.001868cosB - 0.032077sinB - 0.014615cos2B - 0.04089sin2B)$$

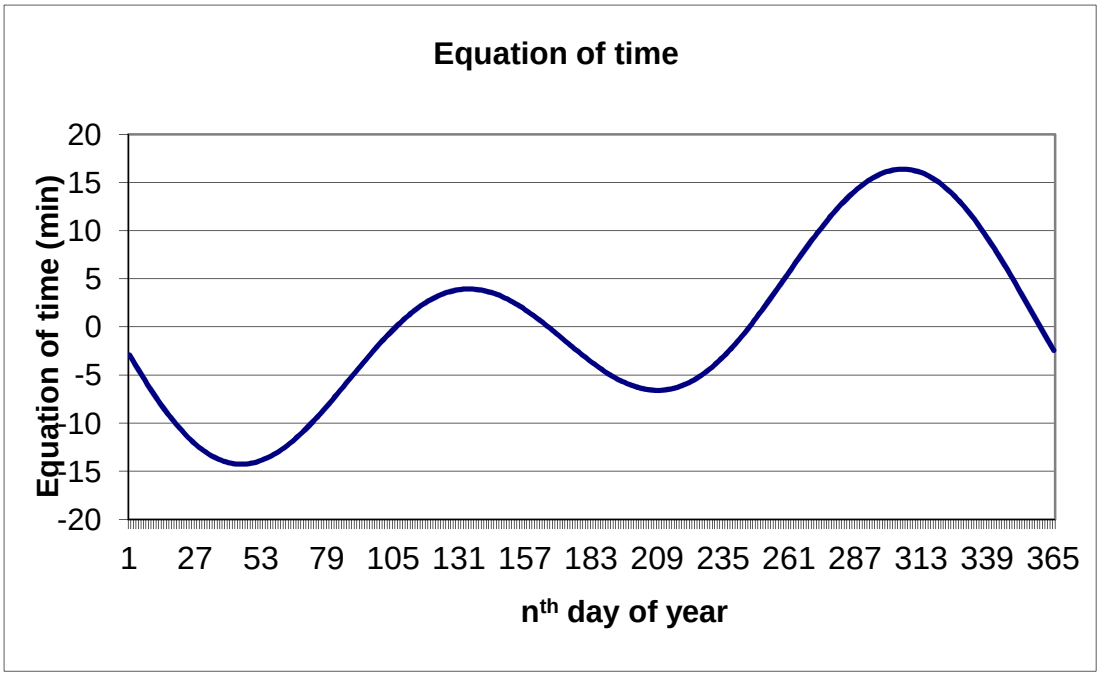

Figure 22Equation of time varies through a year

It is necessary to note that the equation of time and displacement from the standard meridian are both in minutes. Moreover, there is a 60-min difference between daylight saving time (DST) and local standard time. Time is usually specified in hours and minutes.

Air mass (m) is the ratio of the mass of atmosphere through which beam radiation passes to the one it would pass through if the sun were at the zenith. It is a measure of how far the light travels through the earth's atmosphere. One air mass or AM1 is the thickness of the earth's atmosphere. Air mass zero (AM0) describes the solar irradiance in space which is unaffected by the atmosphere. The solar irradiance of AM1.5 is around 1000 W/m^2, while the one of AM0 is considered to be the solar constant G_{sc}.

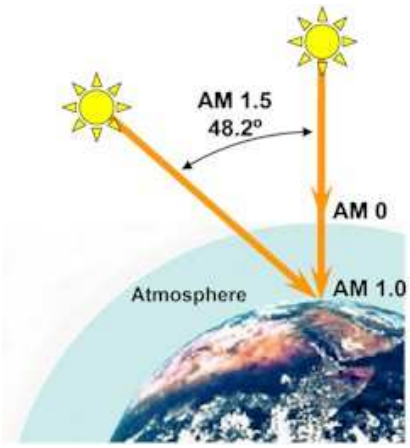

Figure 23Air mass

(Solarlux s.d.)

For zenith angle θ_z from 0° to 70° at sea level, to a close approximation:

$$m = \frac{1}{cos\theta_z}$$

An empirical relationship from Kasten and Young (1989) for air mass that works for zenith angles approaching 90° is:

$$m = \frac{e^{(-0.0001184h)}}{cos\theta_z + 0.5057 \times (96.080 - \theta_z)^{-1.634}}$$

Where *h* is the site altitude in unit of *m*.

The geometric relationships between a plane of any particular orientation relative to the Earth at any time (whether that plane is fixed or moving relative to the Earth) and the incoming beam solar radiation, that is, the position of the Sun relative to that plane, can be described in terms of several angles (Benford and Bock, 1939). Some of the angles are indicated. The angles and a set of consistent sign conventions are as follows:

$\emptyset$ Latitude, the angular location north or south of the equator, north positive; $-90° \leq \phi \leq 90°$

δ Declination, the angular position of the Sun at solar noon (i.e., when the Sun is on the local meridian) with respect to the plane of the equator, north positive, $-23.5° \leq \delta \leq 23.5°$.

ω Hour angle (◦), the angular displacement of the Sun east or west of the local meridian due to rotation of the Earth on its axis at 15° per hour; morning negative, afternoon positive.

$$\omega = \frac{360°}{24hrs} \times (ST - 12) = 15 \times (ST - 12)$$

ST: Standard Time.

γ Surface azimuth angle, the deviation of the projection on a horizontal plane of the normal to the surface from the local meridian, with zero due south, east negative, and west positive;$-180° \leq \gamma \leq 180°$.

θ Angle of incidence, the angle between the beam radiation on a surface and the normal to that surface.

Additional angles are defined that describe the position of the Sun in the sky:

θ_z Zenith angle, the angle between the vertical and the line to the Sun, that is, the angle of incidence of beam radiation on a horizontal surface.

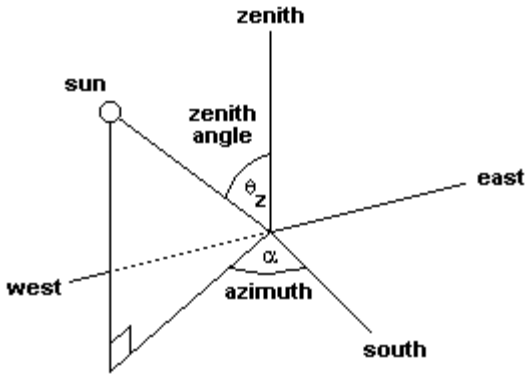

Figure 24Zenith angle and azimuth angle

α_s Solar altitude angle, the angle between the horizontal and the line to the Sun, that is, the complement of the zenith angle.

γ_s Solar azimuth angle, the angular displacement from south of the projection of beam radiation on the horizontal plane. Displacements east of south are negative and west of south are positive.

Declination angle δ which may be calculated, for engineering purposes, from the approximate equation of Cooper (1969):

$$\delta = 23.45 \times \sin\left(360 \times \frac{284 + n}{365}\right)$$

Or from the more accurate equation (error < 0.035°) [from Spencer (1971), as cited by Iqbal (1983)]:

$$\delta = 0.006918 - 0.399912cosB + 0.070257sinB - 0.006758cos2B + 0.000907sin2B - 0.002679cos3B + 0.00148sin3B$$

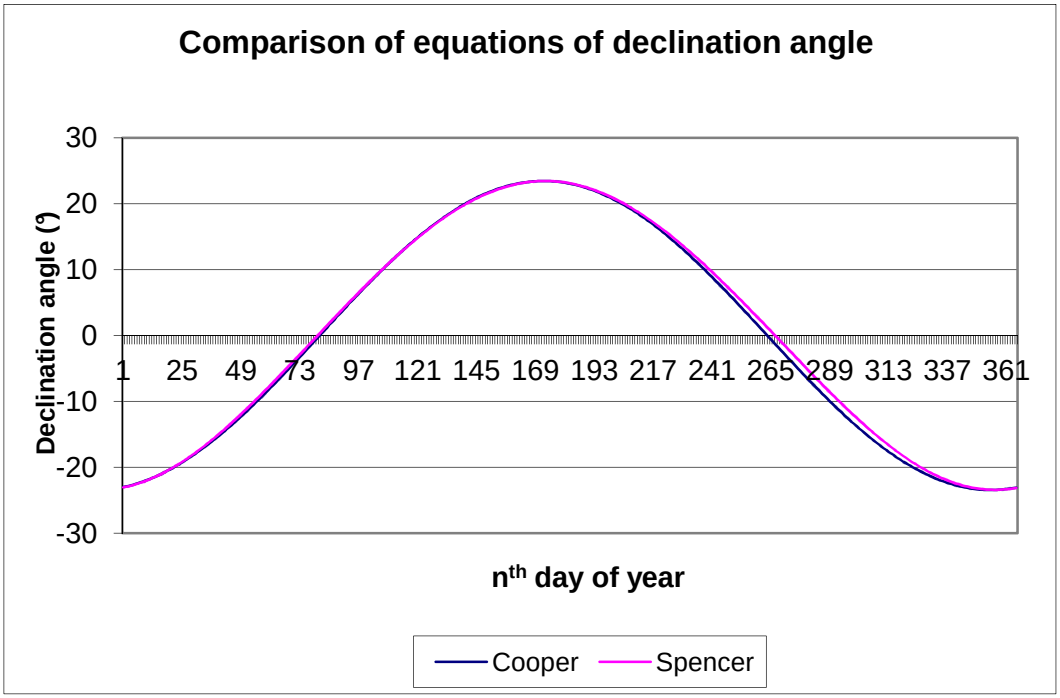

Figure 25Comparison of equations of declination angle

As the variation in Sun-Earth distance, the equation of time E, and declination are all continuously varying functions of time of year, it is customary to express the time of year in terms of n, the day of the year, and thus as an integer between 1 and 365, for many computational purposes. Note that the maximum rate of change of declination is about 0.4° per day. The use of integer values of *n* (n^{th} day of the year) is adequate for most engineering calculations.

There is a set of useful relationships among these angles. Equations relating the angle of incidence of beam radiation on a surface, θ, to the other angles are:

$$\cos\theta = \sin\delta\sin\emptyset\cos\beta - \sin\delta\cos\emptyset\sin\beta\cos\gamma + \cos\delta\cos\emptyset\cos\beta\cos\omega + \cos\delta\sin\emptyset\sin\beta\cos\gamma\cos\omega + \cos\delta\sin\beta\sin\gamma\sin\omega$$

And

$$\cos\theta = \cos\theta_z\cos\beta + \sin\theta_z\sin\beta\cos(\gamma_s - \gamma)$$

When the Sun is behind the surface, the angle θ may exceed 90°. Also, when using the first equation, it is necessary to ensure that the Earth is not blocking the Sun (i.e., that the hour angle is between sunrise and sunset). There are several commonly occurring cases for which the first equation is simplified.

For horizontal surfaces, the angle of incidence is the zenith angle of the Sun,θ_z. Its value must be between 0 and 90 when the sun is above the horizon. For this situation, $\beta = 0$, and the first equation becomes:

$$cos\theta_z = cos\emptyset cos\delta cos\omega + sin\emptyset sin\delta$$

The equation above can be solved for the sunset hour angle ω_s, when $\theta_z = 90°$:

$$\cos\omega_s = -\frac{\sin\emptyset\sin\delta}{\cos\emptyset\cos\delta}$$

The sunrise hour angle is the negative of the sunset hour angle. It also follows that the number of daylight hours is given by

$$N = \frac{2}{15} cos^{-1}(-tan\emptyset tan\delta)$$

A convenient nomogram for determining day length has been devised by Whillier (1965). Information on latitude and declination for either hemisphere leads directly to times of sunrise and sunset and day length.

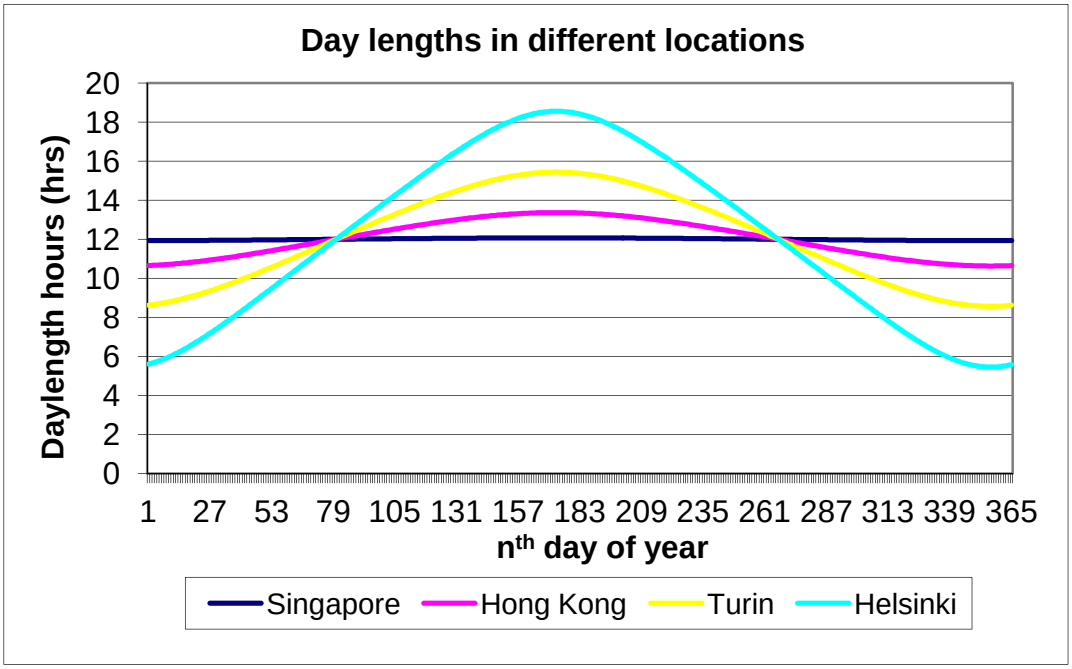

Figure 26Day lengths all through the year in locations with different latitudes

The Figure above shows how the sunlight hours profile changes depending on several cities latitude. Helsinki is just South of the Arctic, while Singapore is just North of the Equator. Hemisphere tilts toward the Sun has longer daylight and beam sunlight, while the other hemisphere which tilts away has shorter ones. And the areas near the equator experience little difference in day length and seasonal temperatures.

$$cos\theta_z = cos\emptyset cos\delta cos\omega + sin\emptyset sin\delta$$

2.3 Models of clear-sky solar irradiance

Due to the change of the atmospheric conditions and air mass, the effects of the atmosphere in scattering and absorbing radiation are variable with time. Therefore, it is necessary to

define a standard clear sky and under standard conditions it is possible to calculate the instantaneous irradiance (W/m^2) and hourly radiation which are expected to be received on a horizontal surface.

2.3.1 ASHRAE Clear-sky model

The American Society of Heating, Refrigeration and Air-Conditioning Engineers, ASHRAE publishes a model for estimating solar beam irradiance, solar diffuse irradiance and solar global irradiance at locations in the Northern Hemisphere. This model represents the solar irradiance at the Earth's surface and under clear sky conditions (Moon 1940).

Beam normal solar irradiance G_{bn}

$$G_{bn} = A \times \mathrm{e}^{\left(-\frac{\mathrm{B}}{\cos\theta z}\right)}$$

Where A: Apparent solar constant

B: Atmospheric extinction coefficient

θ_z: Zenith angle (the angle between the vertical and the line to the sun, that is, the angle of incidence of beam radiation on a horizontal surface).

Diffuse solar irradiance on horizontal surface G_{dh}

$$G_{dh} = C \times G_{bn}$$

Where C is the diffuse radiation coefficient.

In handbook of ASHRAE (Fundamental) (Chapter 27 Fenestration 1985), there are related parameters of ASHRAE clear-sky model on the 21st of each month and also the corresponding Extraterrestrial solar irradiance, Equation of time and Declination angle.

Table 2Related parameters of ASHRAE clear sky days model on the 21st day of each month

Month	G_o	Equation of time	Declination angle	A	B	C
	W/m^2	min	°	W/m^2	-	-
Jan	1416	-11.2	-20	1229	0.142	0.058
Feb	1404	-13.9	-10.8	1213	0.144	0.06
Mar	1383	-7.5	0	1185	0.156	0.071
Apr	1360	1.1	11.6	1134	0.18	0.097
May	1339	3.3	20	1103	0.196	0.121
Jun	1330	-1.4	23.45	1087	0.205	0.134
Jul	1328	-6.2	20.6	1084	0.207	0.136
Aug	1343	-2.4	12.3	1106	0.201	0.122
Sep	1364	7.5	0	1150	0.177	0.092

Oct	1386	15.4	-10.5	1191	0.16	0.073
Nov	1408	13.8	-19.8	1220	0.149	0.063
Dec	1417	1.6	-23.45	1232	0.142	0.057

Curve fitting:

Through the process of constructing a curve and mathematical function, for the whole year, coefficients A, B and C can be shown as curves which have a good fit to the series of coefficients A, B and C given by ASHRAE (shown in Figures as follows):

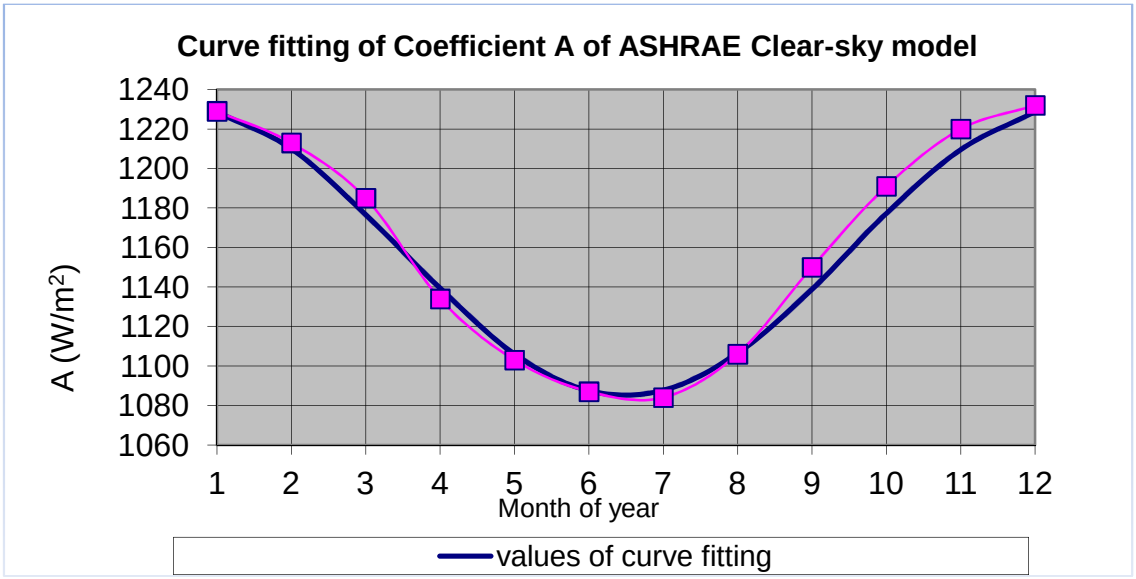

Figure 27Curve fitting of coefficient A of ASHRAE Clear-sky model

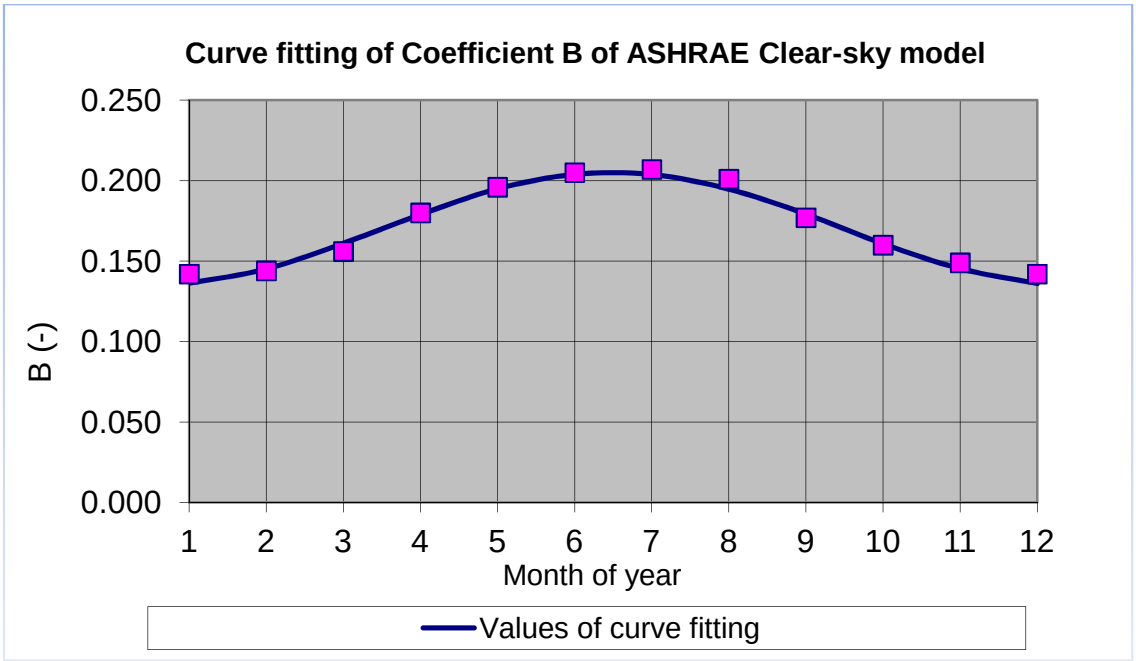

Figure 28Curve fitting of coefficient B of ASHRAE Clear-sky model

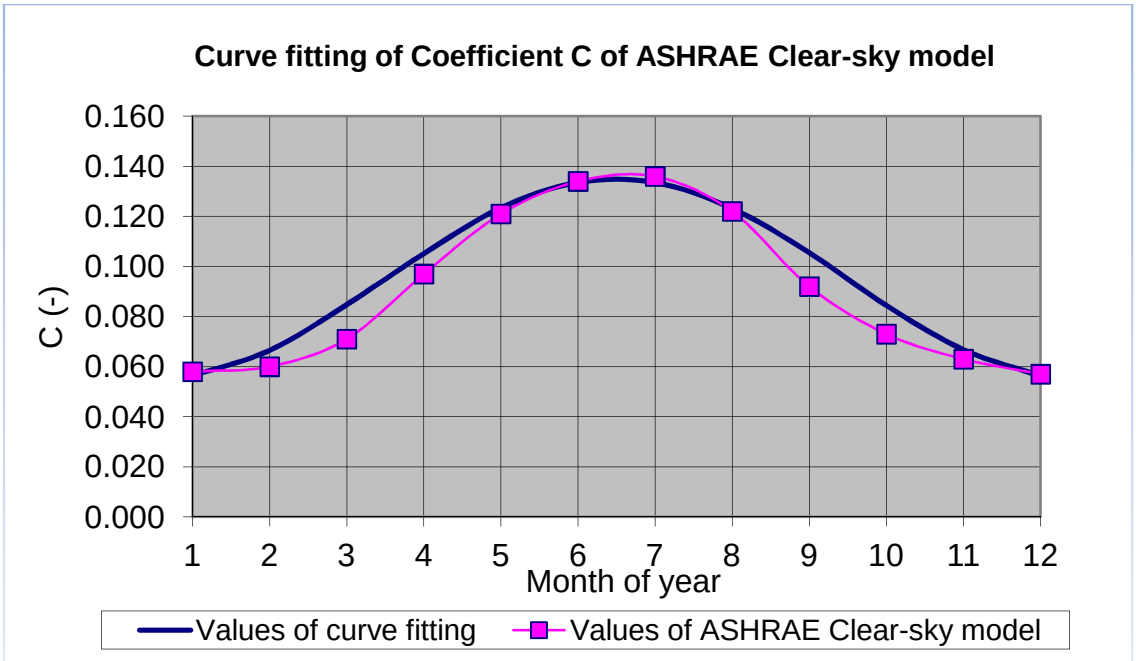

Figure 29Curve fitting of coefficient C of ASHRAE Clear-sky model

The ASHRAE coefficients A, B and C are functions of the n^{th} day of year. As shown from the figures above, generally, the curves fit and for each day of year, the coefficients are constants respectively.

Also the curve fitting method created functions as follows:

$$A = 1158 - 73 \times \sin\left(2\pi \frac{268 + n}{365}\right)$$

$$B = 0.17 + 0.035 \times \sin\left(2\pi \frac{268 + n}{365}\right)$$

$$C = 0.095 + 0.04 \times \sin\left(2\pi \frac{268 + n}{365}\right)$$

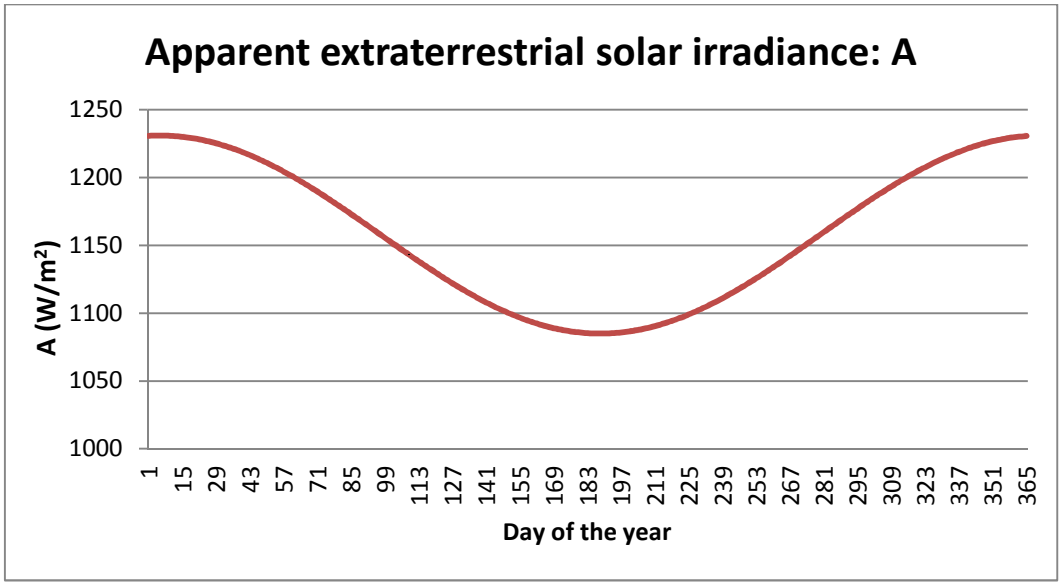

Figure 30Apparent extraterrestrial solar irradiance A as function of day of year

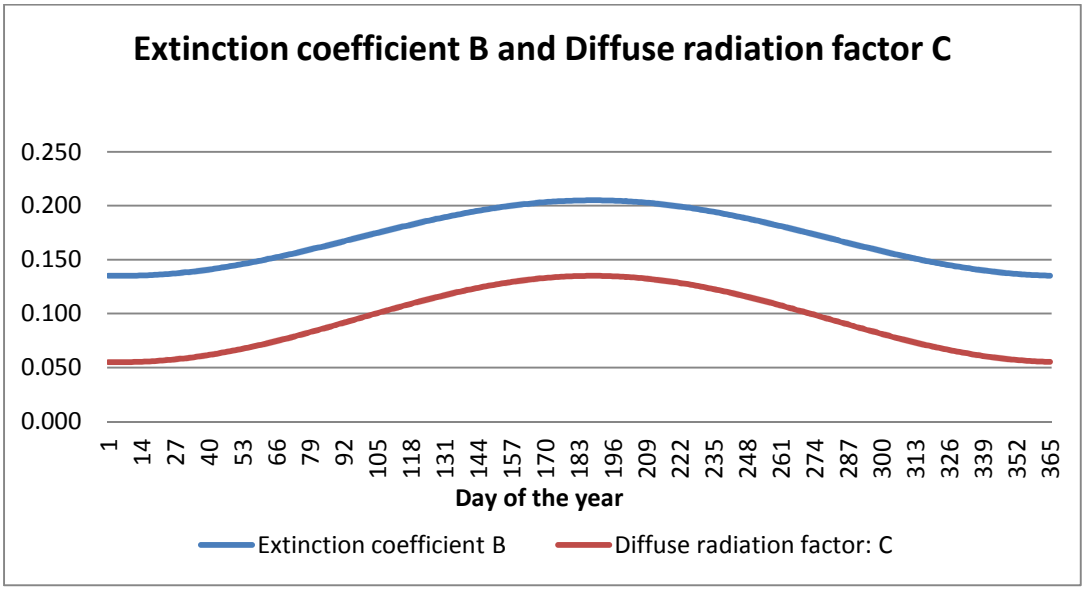

Figure 31Extinction coefficient B and diffuse radiation factor C as function of day of year

With the daily values of A, B and C, it is possible to calculate beam normal solar irradiance G_{bn} and diffuse solar irradiance on horizontal surface G_{dh} for each day of the year with Sun at different solar zenith angles.

2.3.2 Hottel clear sky model

In 1976, Hottel presented his method to estimate the beam radiation under clear atmospheric conditions (Hottel 1976).

The atmospheric transmittance for beam radiation τ_b:

$$\tau_b = \frac{G_{bn}}{G_{on}} = a_0 + a_1 \times e^{\frac{-k}{cos\theta_z}}$$

To calculate the constants a_0, a_1 and k for the standard atmosphere with 23 *km* visibility, the correction factors $r_0 = \frac{a_0}{a_0^*}$, $r_1 = \frac{a_1}{a_1^*}$, and $r_k = \frac{k}{k^*}$ are needed to allow for changes in climate types.

Table 3Correction factors for different climate types

Climate type	r_0	r_1	r_k
Tropical	0.95	0.98	1.02
Mid-latitude summer	0.97	0.99	1.02
Subarctic summer	0.99	0.99	1.01
Mid-latitude winter	1.03	1.01	1

$$a_0^* = 0.4237 - 0.00821 \times (6 - A)^2$$
$$a_1^* = 0.5055 + 0.00595 \times (6.5 - A)^2$$
$$k^* = 0.2711 + 0.01858 \times (2.5 - A)^2$$

Where A is the altitude of the observer up to 2.5 *km*.

Then the clear-sky beam normal irradiance can be calculated:

$$G_{bn} = \tau_b \times G_{on}$$

As τ_b is always bigger than a_0, which is a positive value, the clear-sky beam normal irradiance G_{bn} calculated from Hottel model is always positive even during sunrise and sunset.

2.4 Measurements of solar beam and global horizontal irradiance

Measuring direct normal solar irradiance is of great importance in the development of concentrating solar power plants. For technological utilization of solar energy, study of solar radiation under cloudless skies is very important, particularly for solar systems using concentrators. Maximum insolation is obtained when the skies are absolutely clean and dry, and relatively less radiation is received when aerosols are also present. (A.Louche s.d.)

Accurate direct normal solar irradiance measurements reduce uncertainty in predicting plant performance, thus lowering the perceived risk of investment in such projects, facilitating more rapid acceptance and growth of the industry as a whole. However, accurate direct normal solar irradiance measurements are costly, both in terms of equipment and maintenance (T. S. al s.d.).

2.4.1 Measurement process

The measurements of solar beam and global horizontal irradiance were carried on through 2010 continuously with a Normal Incidence Pyrheliometer and a Horizontal Pyranometer respectively.

There are several purposes for the measurement of beam and global horizontal solar radiation. Firstly, it is useful in simulation of solar cooling processes, while secondly the data show comparison with those data thirty-five years ago (1975-1976) in Torino to indicate the optical quality of its atmospheric change which was greatly influenced by the implementation of district heating system.

The instruments applied are shown as follows:

Figure 32Normal Incidence Pyrheliometer (NIP) (Pyrheliometer s.d.)

Figure 33Pyranometer

The Pyranometer is used to measure the global horizontal solar irradiance.

2.4.2 Processing of measured solar beam irradiance data

Clear-sky measurements of G_λ as a function of zenith angle θ_z, and plotted as $lnG(\lambda)$ versus $sec\theta_z$, should yield a straight line with slope $-\tau(\lambda)$ and intercept G_o(extrapolated back to $sec\theta_z = 0$). An excellent example, along with a discussion of this process, is shown by Stephens (1994) in his Fig. 6.1 (B. A. al 1999).

With Pyrheliometer and Pyranometer, the signal data are recorded every 10 minutes as an interval and the original data of solar beam irradiance were in unit of voltage, hence, the transform of unit is needed:

$$G_{bn}\,[W/m^2] = ((G_{\ bn}[V] + 0.01) \times 2 \times 1000)\ /\ 7.97$$

The same for solar global horizontal irradiance:

$$G_{th}\,[W/m^2] = ((G_{\ th}[V] + 0.09) \times 2 \times 1000)\ /\ 15$$

2.5 Data analysis and validation of clear sky theoretical models

Direct normal solar irradiance data have been employed to validate some widely spread atmospheric models both for the calculation of direct normal irradiance and for splitting total horizontal radiation into its direct and diffuse components.

Starting from the measured beam and total horizontal irradiance, there are two main goals:

Firstly, to verify the well-known ASHRAE model (ASHRAE, 1985) for clear sky beam normal irradiance Gbn, and ASHRAE model for diffuse horizontal irradiance Gdh; Secondly, to verify total horizontal irradiance G_{th} implicitly.

2.5.1 Validation of clear sky models of solar beam normal irradiance

The ASHRAE clear sky model was originally developed by Moon (1940), and was later modified by Threlkeld and Jordan (1958) and Stephenson (1967). The ASHRAE model is still widely used, especially for engineering calculations, and may be described as follows:

Beam normal solar irradiance G_{bn}

$$G_{bn} = A \times \mathrm{e}^{\left(-\frac{\mathrm{B}}{\cos\theta z}\right)}$$

Where *A*: Apparent solar constant

B: Atmospheric extinction coefficient

θ_z: Zenith angle (the angle between the vertical and the line to the sun, that is, the angle of incidence of beam radiation on a horizontal surface).

Diffuse solar irradiance on horizontal surface G_{dh}

$$G_{dh} = C \times G_{bn}$$

Where C is the diffuse radiation coefficient.

The apparent solar constant (A, W/m^2), the extinction coefficient (B) and the diffuse coefficient (C) vary during the year, as reported by ASHRAE (1985).

As an example, both the measured and calculated data from March 6 have been reported.

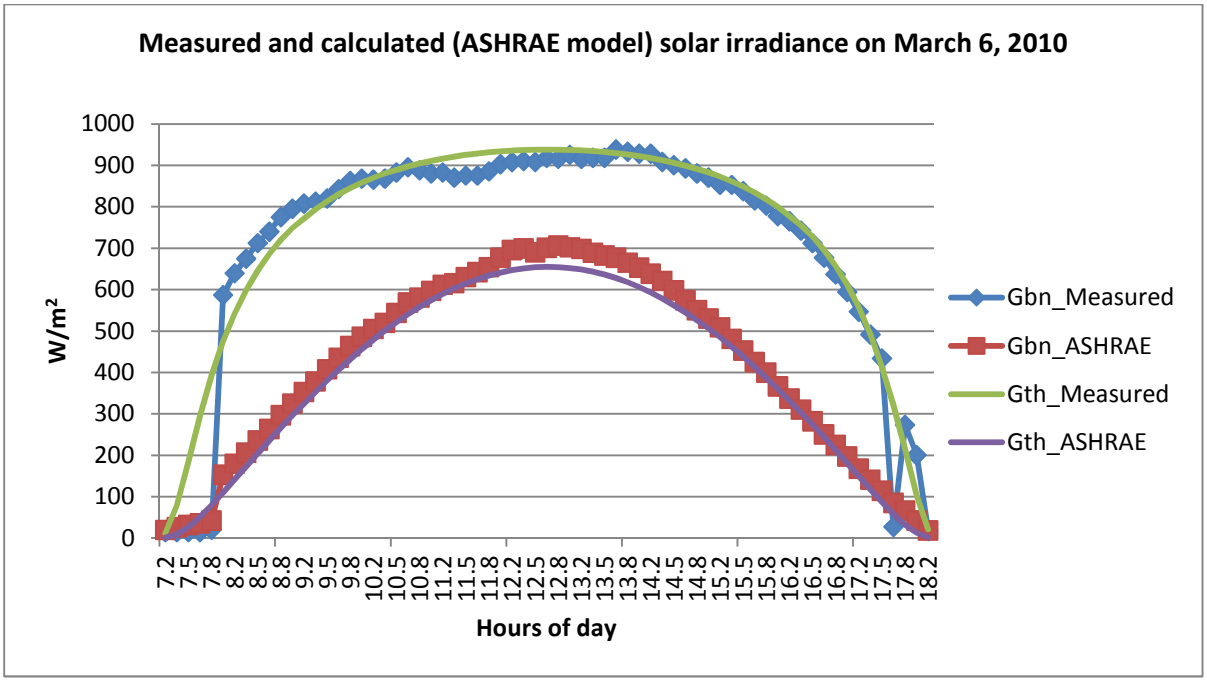

Figure 34Measured and calculated (ASHRAE model) solar irradiances on March 6, 2010

The example above shows that the measured and calculated G_{bn} values look quite similar, except for some shading of both the pyrheliometer and the pyranometer in the morning time. On the other hand, the G_{th} values calculated by the ASHRAE model are in good agreement with data measured at the Department, but they still seem slightly underestimated.

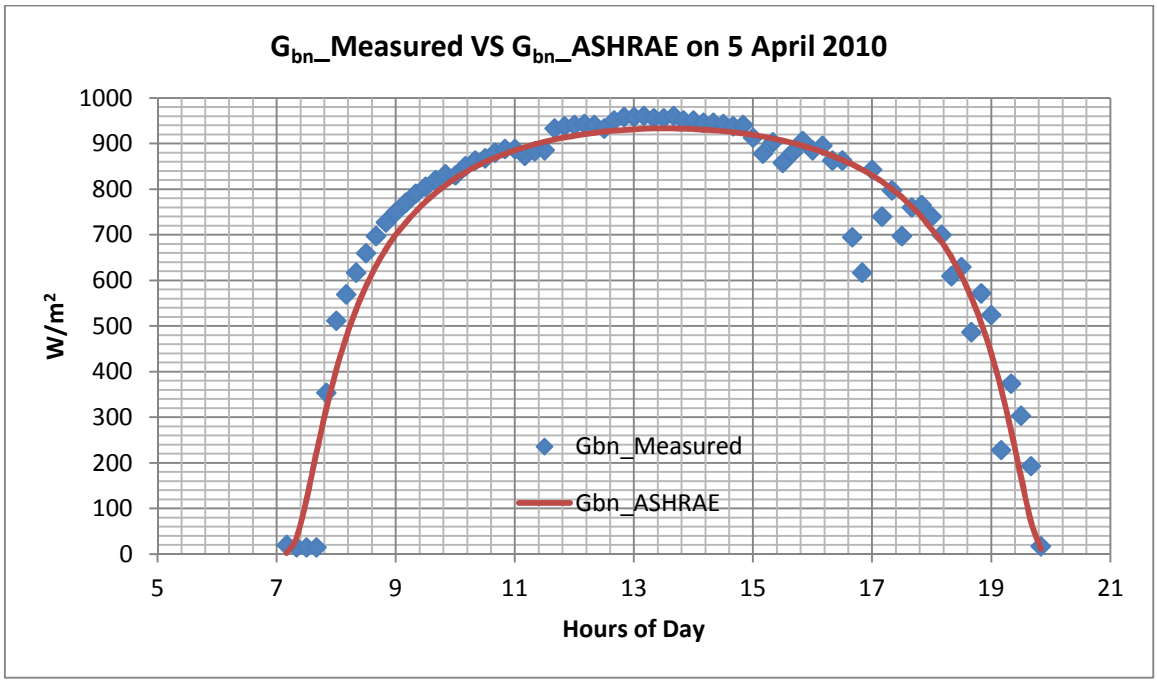

Figure 35Comparison of Gbn between measured data and ASHRAE model on 5 April 2010

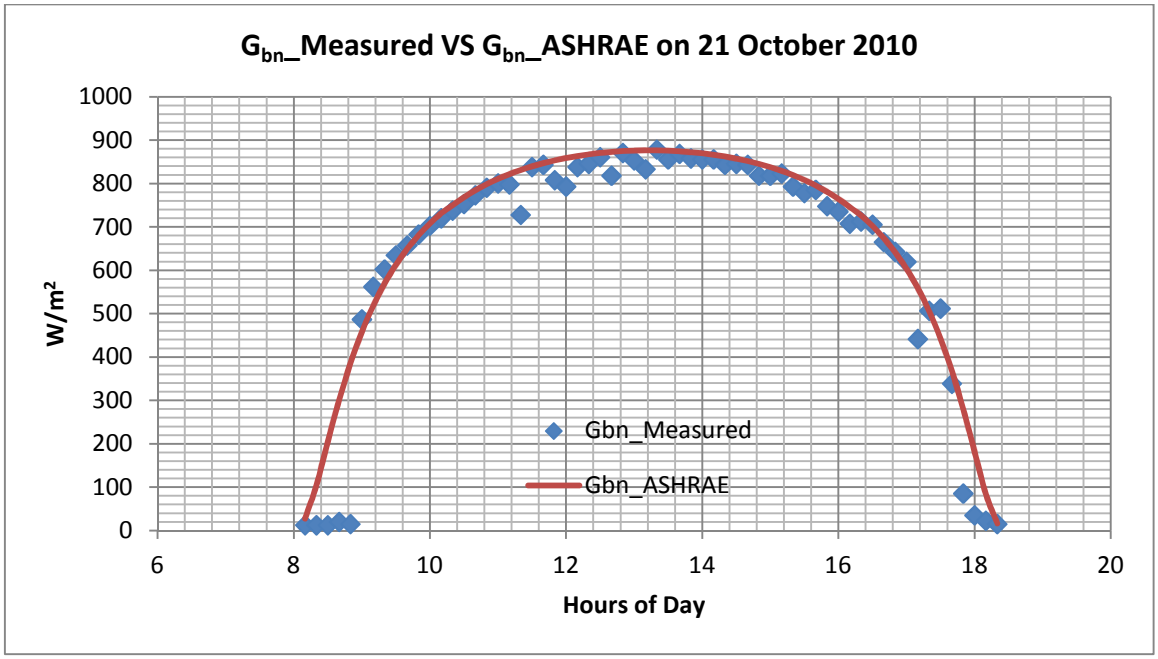

Figure 36Comparison of Gbn between measured data and ASHRAE model on 21 October 2010

For the solar beam normal irradiance Gbn only, the above two examples on clear sky days can show that the ASHRAE clear-sky model mostly fits the solar beam normal irradiance.

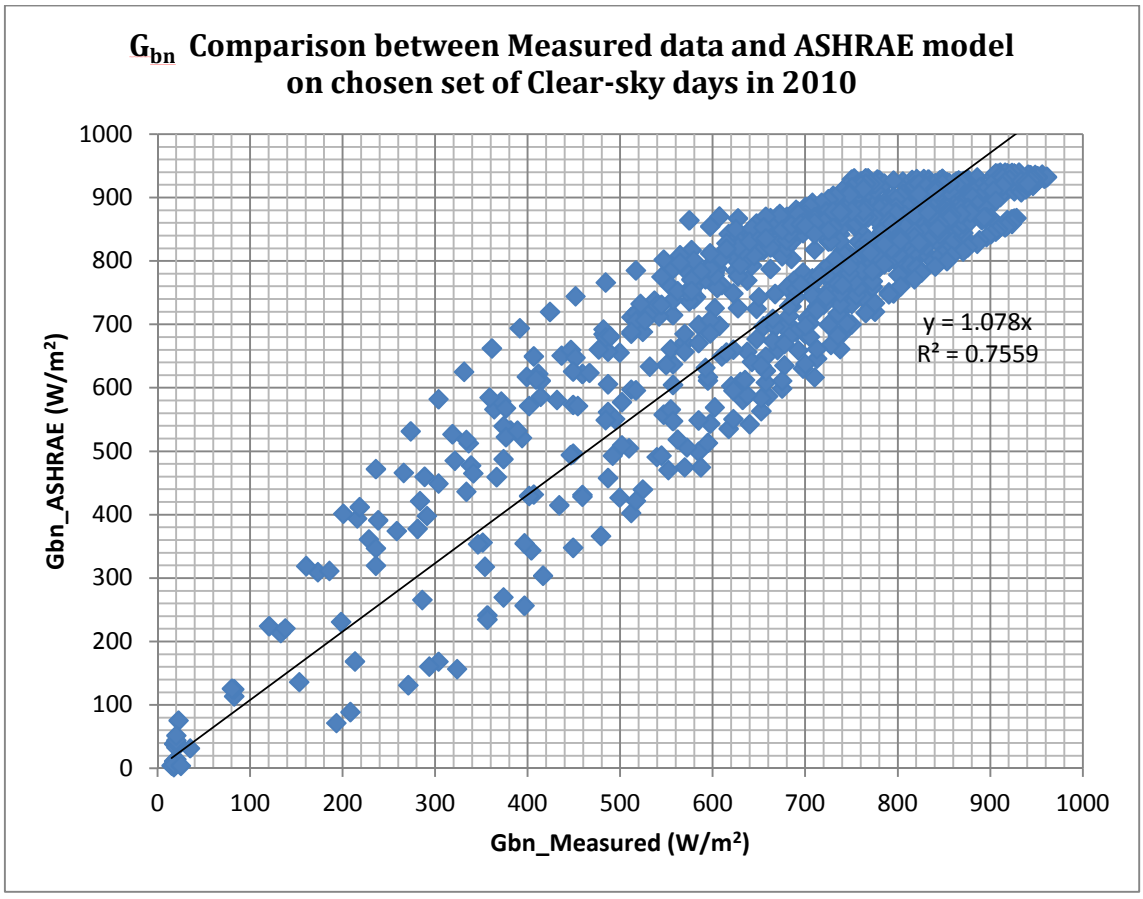

Figure 37Measured and calculated (ASHRAE model) Gbn values

The figure above shows the comparison between measured and calculated values of G_{bn} for the 18 clear sky days. A regression coefficient of 0.76 and a slight overestimate (7.8%) are an evidence of the substantial acceptability of the ASHRAE model for most engineering purposes. The refinement of the method is beyond the scope of this thesis, also due to the modest quality level of measurements performed during this campaign. Main sources of errors were morning shading from buildings, limited duration of the measurement campaign, and non regular calibration of the instrument.

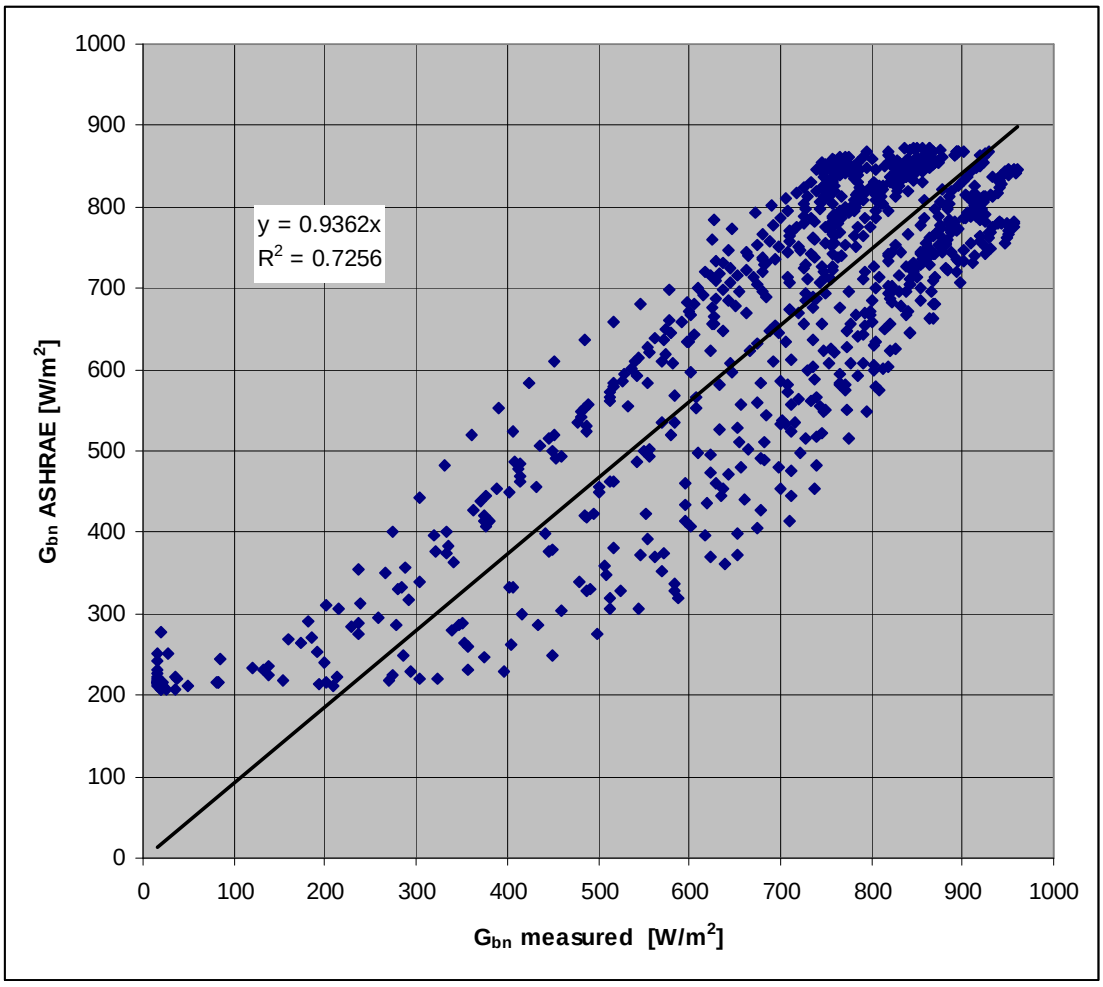

Figure 38Measured and calculated (Hottel model) G_{bn} values

Other models, like Hottel (1976), provided a less satisfactory correlation (r^2 = 0.73), but a similar – in absolute terms - error on the estimate (-6.4%). Its main drawback is the fact that the atmospheric transmittance is never zero, and this leads to a minimum value of around 200 W/m^2, even for very high zenith angles.

2.5.2 Validation of clear sky models of solar diffuse horizontal irradiance

Similarly, the diffuse horizontal irradiance values G_{dh}, have been calculated from G_{th} and G_{bn} measurements as follows:

$$G_{dh} = G_{th} - G_{bn}cos\theta_z$$

G_{dh} values have been compared to those predicted by the ASHRAE model of diffuse horizontal irradiance not in absolute terms, but through its ratio to beam irradiance (namely, constant C in the ASHRAE model). The first comparison led to the results shown as follows:

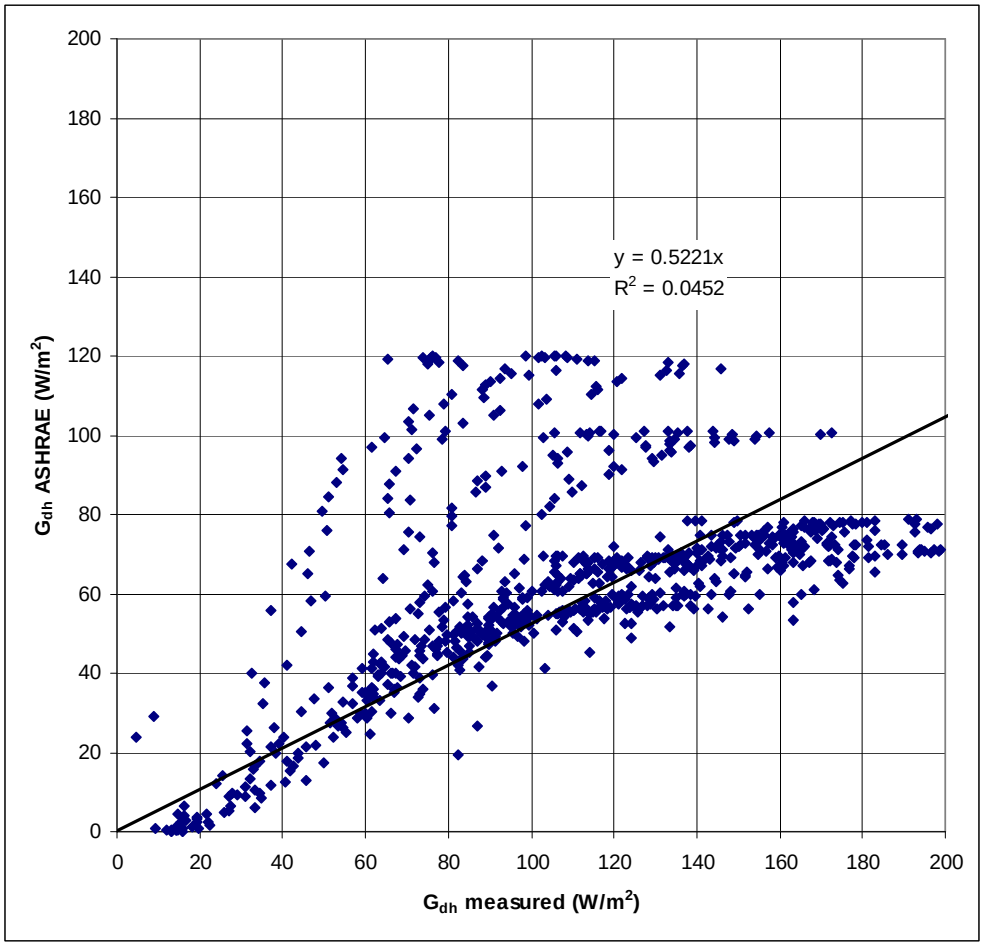

Figure 39Measured and calculated (ASHRAE model) diffuse horizontal irradiance G_{dh}

The figure above is self commented: the large spread of the data (very low regression coefficient) and the systematic error (50% underestimate from theory) are immediately visible.

Similar - although slightly better - results were obtained by the Liu-Jordan model (1960), shown in next figure.

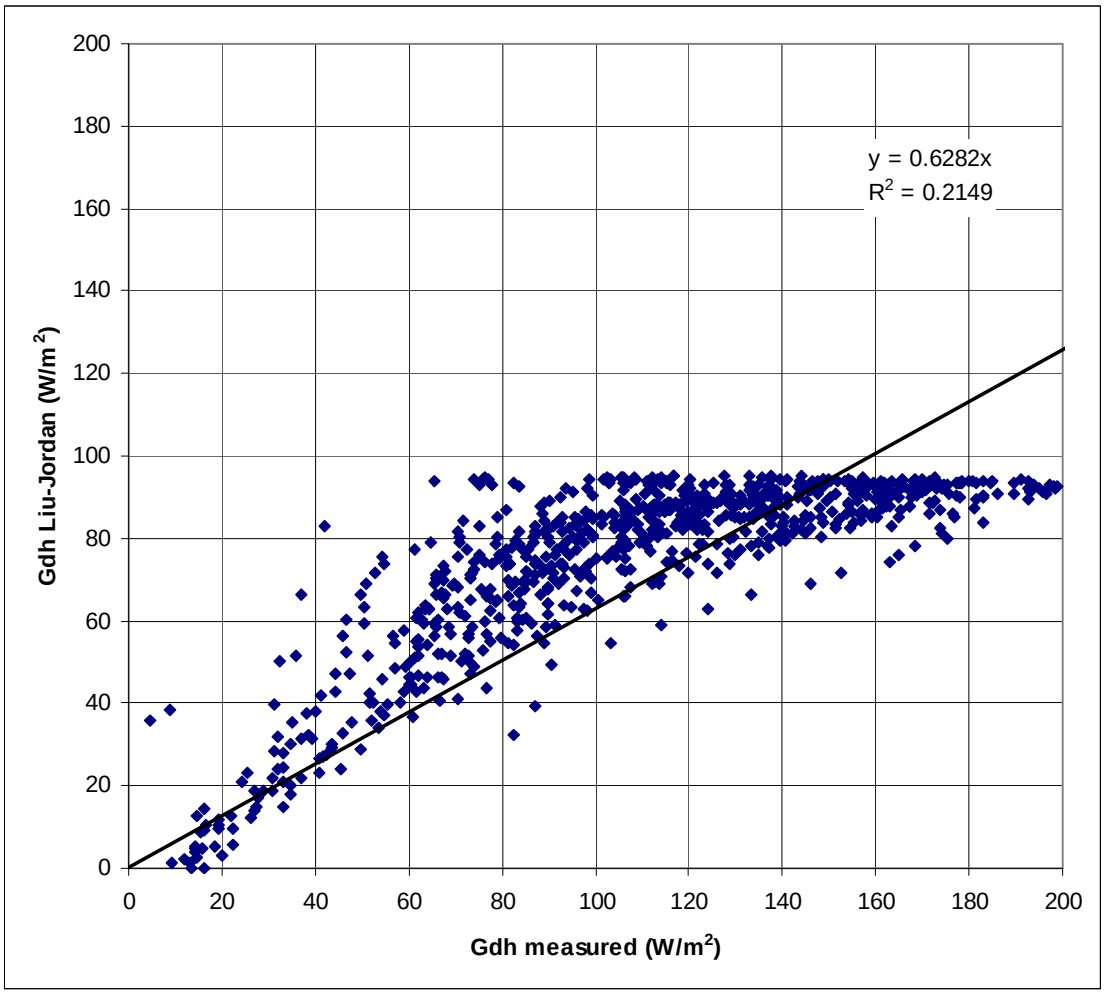

Figure 40Measured and calculated (Threlkeld 1958) diffuse horizontal irradiance G_{dh}

Additionally, the hourly E_{dh} comparison between measured data and ASHRAE model on chosen set of clear-sky days in 2010 are also taken, both the measured data taken from the department of Energy and the data from meteo station in Politecnico di Torino.

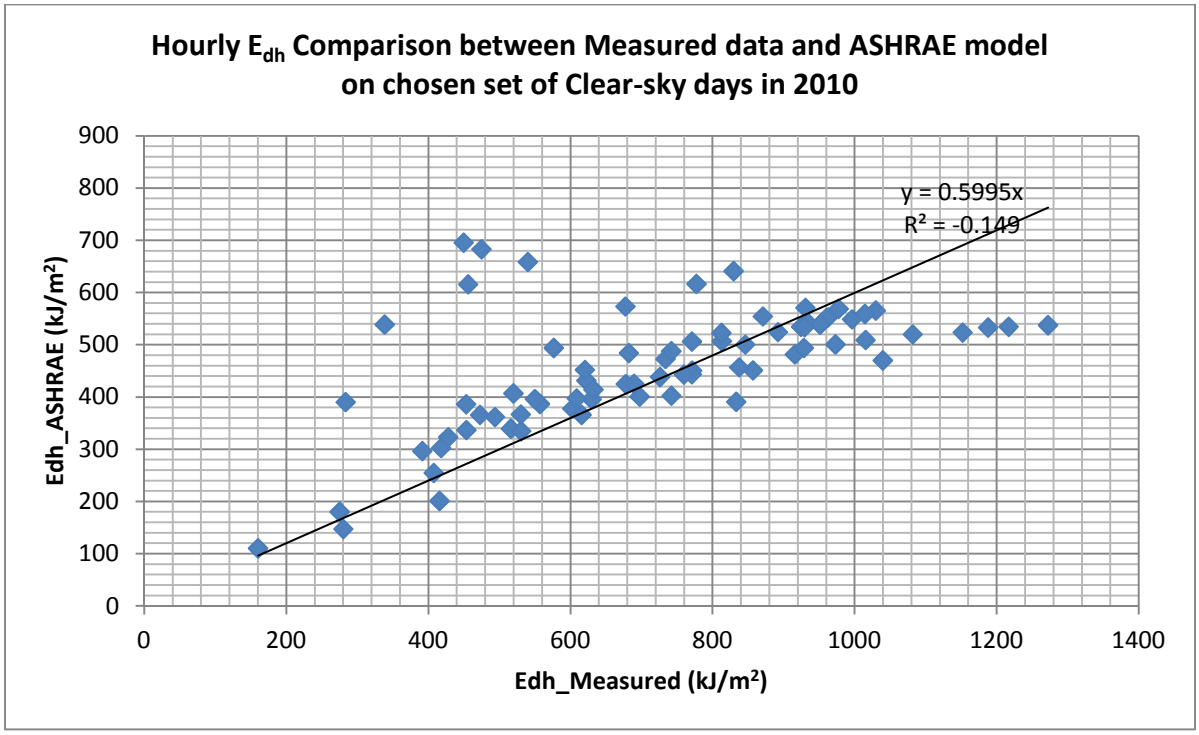

Figure 41Hourly E_{dh} comparison between measured data and ASHRAE model on chosen set of clear-sky days in 2010

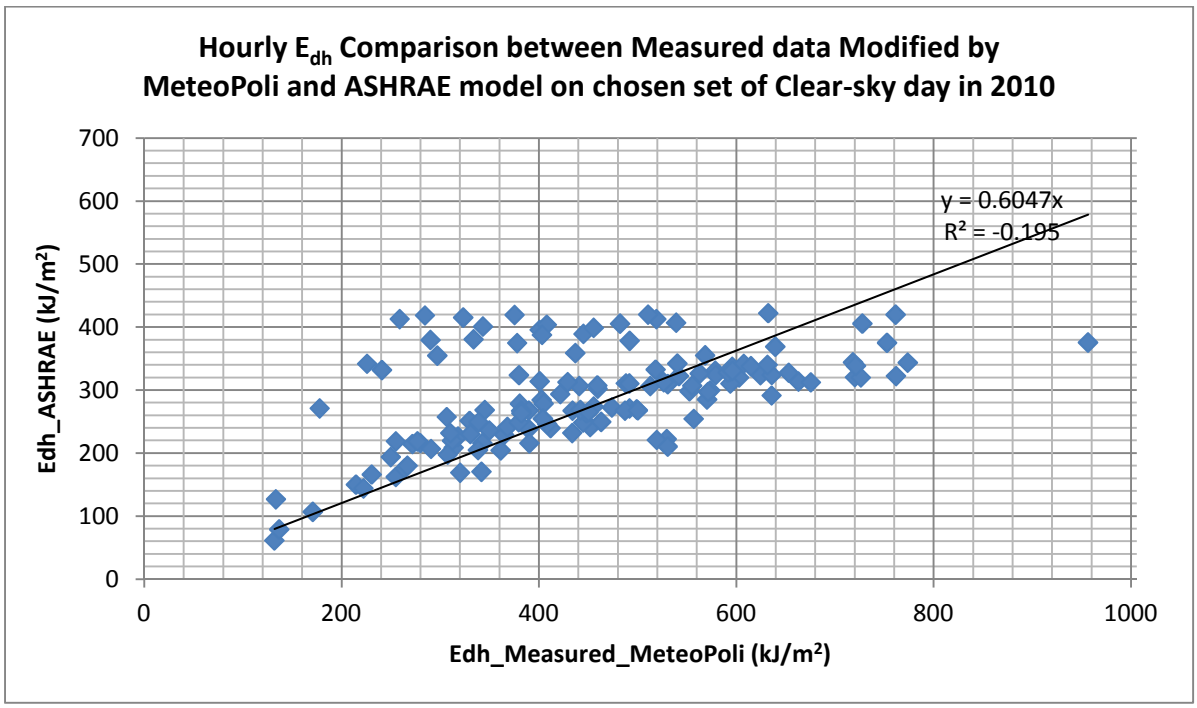

Figure 42Hourly E_{dh} comparison between measured data in MeteoPoli and ASHRAE model on chosen set of clear-sky days in 2010

The ratio of solar diffuse horizontal irradiance to solar beam normal irradiance (namely, constant C in the ASHRAE model) is calculated. Between measured G_{dh} and calculated G_{bn}

(C, blue lozenges, ASHRAE model), or between measured G_{dh} and measured G_{bn} (C', purple squares).

As an example, the daily variations of C for the same day on March, 6 2010 and on April 9 are shown in next two figures.

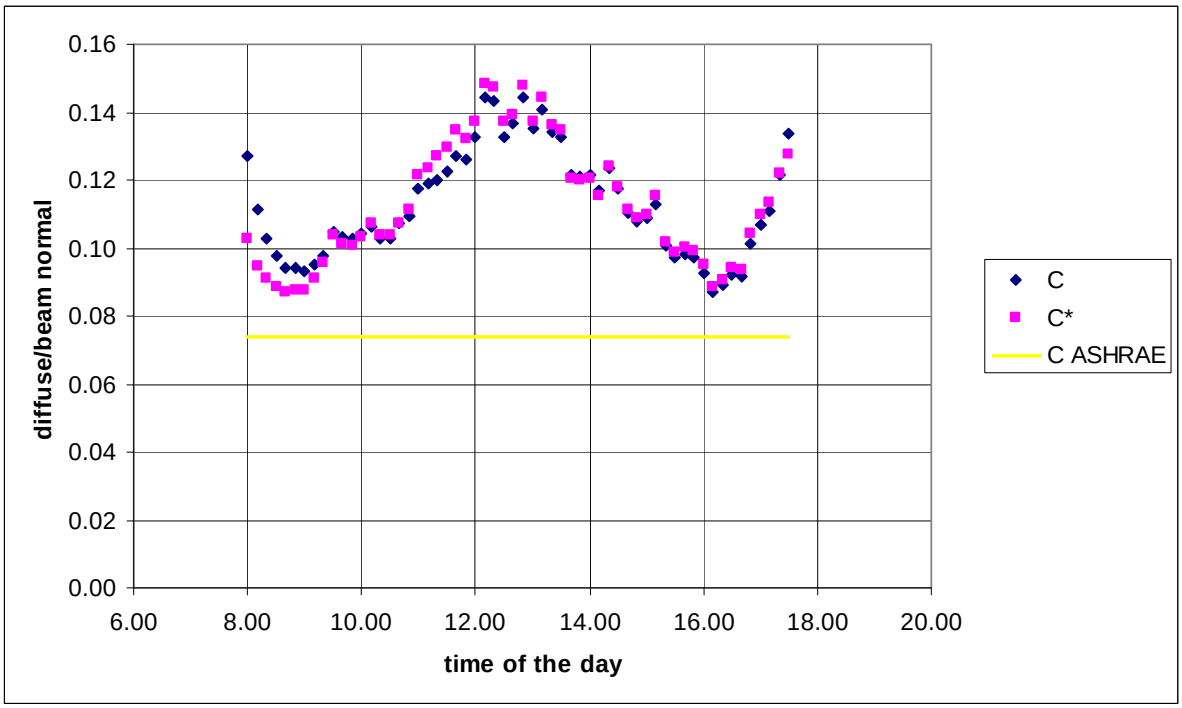

Figure 43Daily variation of diffuse horizontal to beam normal ratio for March, 6 2010

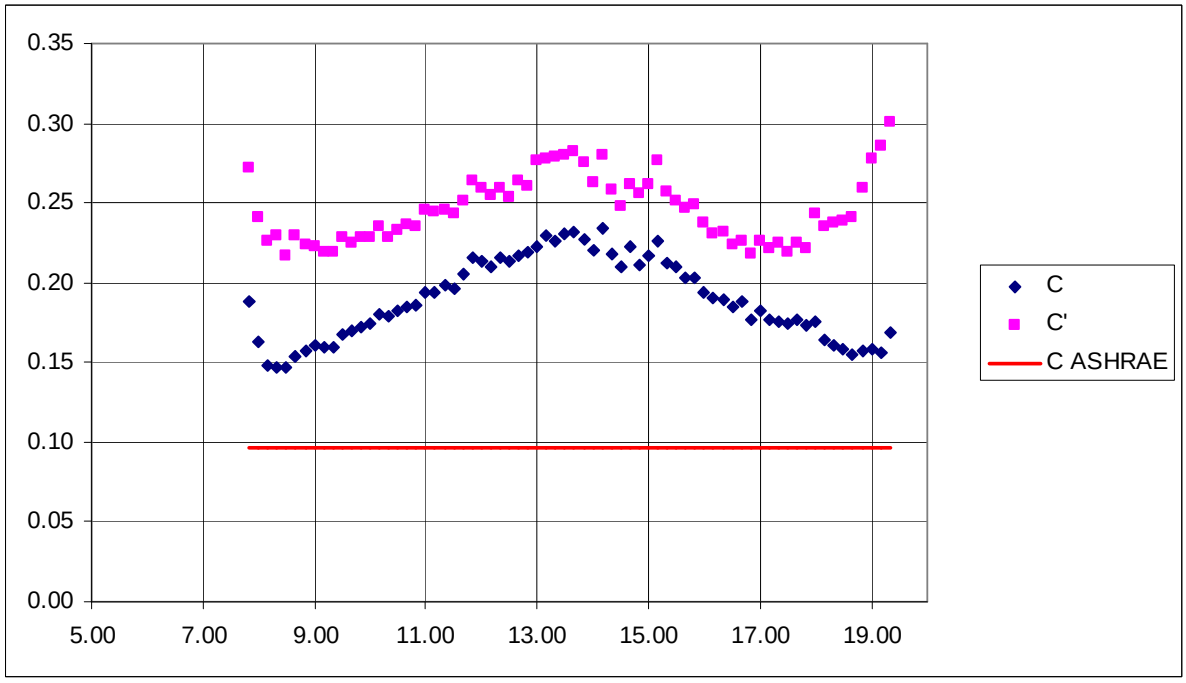

Figure 44Daily variation of diffuse horizontal to beam normal ratio for April, 9 2010

When G_{bn} ASHRAE values almost coincide with measured values, C and C' almost coincide as on March 6, while this does not happen on April 9.

The experimental C and C' values are in the average well above the C predicted by the ASHRAE model, as it could be expected from the results shown in figure of 'Measured and calculated (ASHRAE model) diffuse horizontal irradiance G_{dh}'.

The most interesting finding is however that a daily regular oscillation of experimental C values, symmetrical to noon time, occurs, with very high values at the extremities of the day and at noon.

The last findings may be explained by the limits of the isotropy assumption implicit in the ASHRAE model: as the sun rises, circumsolar sky radiation increases in altitude, and therefore its vertical component tends to become more relevant. On the other hand, for very low altitude angles the vertical component of G_{bn} in equation $G_{dh} = G_{th} - G_{bn}cos\theta_z$ tends to decrease faster than G_{dh}, producing an asymptotical increase of C ratio up to an infinite value for $\theta_z = 90°$.

The author has no clear explanation of the relative maximum at noon. But the regular symmetrical trend is still visible, and with further sets of data could lead to a satisfying explanation and maybe to a new "clear sky diffuse irradiance" model.

2.6 Atmospheric turbidity measurements in 2010 and comparison with data in 1975-1976

2.6.1 Background introduction

Torino is a large industrial city located in Northwestern Italy. It is the seat of the largest Italian car factory, although recently most production plants have been moved to other sites. In the last 35 years coal and heavy oil-fuelled heating systems have been progressively replaced by district heating and natural gas installations. Private and public transportation on the other hand has hugely increased, although the specific pollutant emissions in terms of CO, NO_x, SO_x and particulates have been dramatically reduced with enforcing of more and more stringent euro limits. A comparison between nowadays and 1975 situation under the chemical and health points of view can be easily made because concentrations of the main pollutants are regularly monitored since a long time. However, it is interesting to evaluate how changing emission patterns have affected the optical quality of the atmosphere, namely its turbidity.

In order to make this comparison, direct normal solar irradiance has been continuously measured during year 2010 at the Polytechnic site in Torino city centre and its values have

been compared to those measured by one of the authors during the period September 1975 – July 1976.

2.6.2 Definition of turbidity

The intensity of a monochromatic beam of solar radiation crossing a homogeneous plane-parallel atmospheric layer is given by the so called Bouguer-Lambert Law:

$$G_\lambda = G_{0\lambda} e^{-\tau_\lambda sec\theta_z}$$

Where

G_λ is monochromatic solar irradiance at the ground,

$G_{0\lambda}$ is monochromatic extra-atmospheric solar irradiance,

τ_λ is optical thickness of the atmospheric layers,

θ_z is Zenith angle of the Sun (angle between the solar beam and the local Zenith).

An ideal atmosphere in which only molecular scattering from nitrogen and oxygen occurs would have an optical thickness which has been determined by Rayleigh in his fundamental works in the early 1870's giving an explanation for the blue colour of the sky.

He showed that the optical thickness of this ideal atmosphere, called "Rayleigh atmosphere" can be determined as a function of wavelength and height above sea level by the following formula (Fracastoro, Attenuazione della radiazione solare diretta ad opera di un'atmosfera industriale 1976):

$$\tau_{m\lambda} = \frac{32\pi^3 (n-1)^2 H_0}{3\lambda^4 N_0}$$

Where

n is refraction index of the air (function of wavelength),

H_0 is thickness of the homogeneous atmospheric layers,

N_0 is number of molecules per unit volume.

Introducing the values for H_0, π and N_0 one obtains:

$$\tau_{m\lambda} = 1.04410^5 (n-1)^2 \lambda^{-4}$$

From the above one may obtain the value of the ideal beam irradiance through a Rayleigh atmosphere, once the values of monochromatic extra-atmospheric irradiance $G_{0\lambda}$ are known (Coulson 1975).

$$G_R = G_0 e^{-\bar{\tau}_m sec\theta_z} = \int_0^\infty G_{0\lambda} e^{(-\tau_{m\lambda} sec\theta_z)}\, d\lambda$$

For a real atmosphere in clear sky conditions the following applies:

$$G_{bn} = \frac{1}{S} G_0 e^{-\bar{\tau} sec\theta_z} = \frac{1}{S} G_0 e^{-T\bar{\tau}_m sec\theta_z}$$

Where S takes into account the yearly variation of the solar constant G_0 and T is the number of Rayleigh atmospheres producing the same beam radiation extinction as the real atmosphere, and is called "Linke turbidity factor". In spite of its limits, namely its slight variation with air mass due to wavelength-dependent water-vapour and aerosol absorption, the Linke turbidity factor is useful for comparison of atmospheric conditions under different conditions (Coulson, 1975).

2.6.3 Atmospheric turbidity measurements in 1975-76 (Torino and Pino Torinese)

Starting from October 1975 until July 1976 a measurement campaign (Fracastoro, Misure di radiazione diretta a Pino Torinese e a Torino, 1977) of beam solar radiation was simultaneously carried on in Torino (1.17 million inhabitants, 240 m above sea level) and Pino Torinese (about 5,000 inhabitants, 620 m a.s.l). Two Kipp & Zonen Moll thermopiles previously calibrated at the "Colonnetti" Metrological Institute were used. One was placed on top of the main Politecnico building (Torino), while the other was placed at the Astronomical Observatory of Torino, located in Pino Torinese.

Pino Torinese is a small location on the hills about 10 km East of Torino centre, 380 m above the city. Its atmosphere tends to be unaffected by typical pollution problems which used to characterize the industrial city of Torino.

The summary of these results is shown in figure of SO_2 variation during three decades.

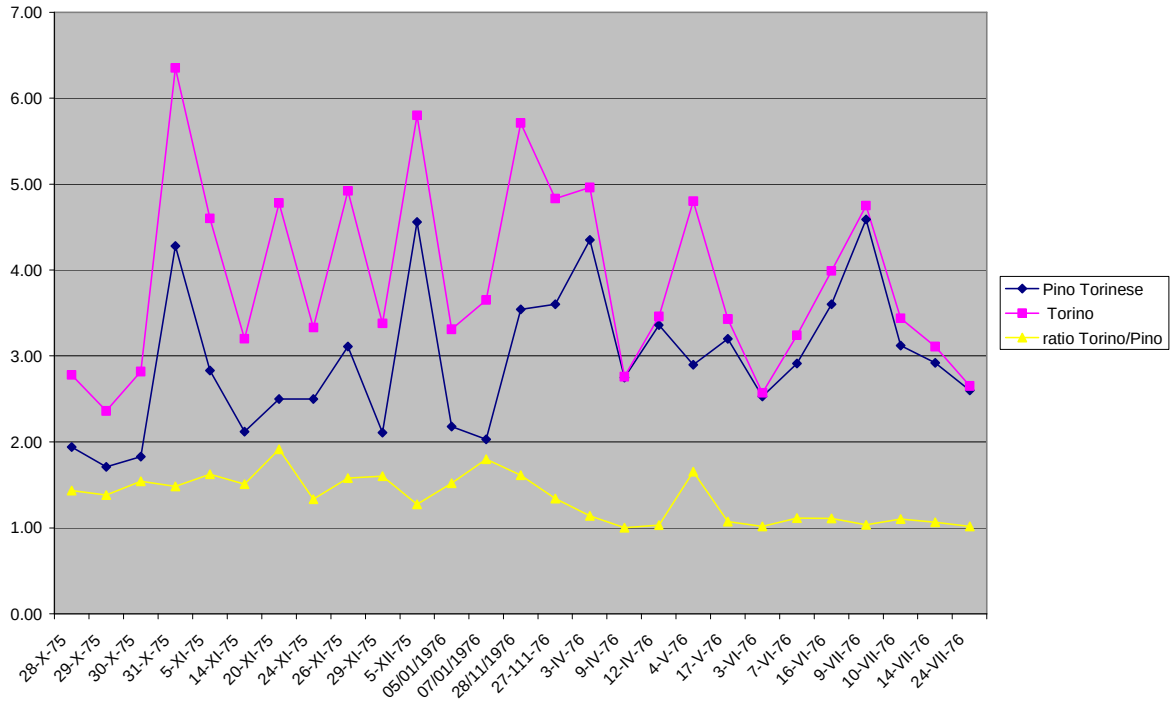

Figure 45Turbidity values in Torino and Pino Torinese during1975-1976

As it could be expected, turbidity data in Pino Torinese were always lower than in Torino. However, while in the late spring and summer months the difference was "physiological" (less than 5%), i.e., justified by the different thickness of the atmospheric layers, during the heating season (from October to April) the difference between the two locations was much higher than in the rest of the year (up to 100% for November 20). This different seasonal behaviour may be explained with the heavy polluting combustion appliances (heavy oil and coal) used for heating and industrial premises in those years in Torino.

2.6.4 Comparison of atmospheric turbidity data in 1975 and 2010

From February 2010 to December 2010 solar beam radiation was regularly measured every day at Torino, exactly at the same location as in 1975-76 measurement campaign. The measurement instrument was an Eppley Pyrheliometer with solar tracker. Unfortunately, this time no beam radiation data were available at Pino Torinese, a useful reference for the new data.

In 1975 Torino was still the seat of both the headquarters and the productive plants of the largest Italian carmaker. Population was reaching its peak value (around 1.2 million inhabitants), and private transportation was booming. The main energy sources for industries, and residential and commercial buildings were coal and heavy oil. Moreover, the specific climatic conditions of the Torino area, with very low winds and frequent winter thermal

inversions, are rather unfavourable to pollutants dispersion. As a result, air quality was very poor, and would absolutely be considered unacceptable under the present, both legal and socio-environmental, points of view.

During the period 1975 to 2010, the city of Torino experienced a profound change in its socio-economical situation: the largest Italian carmaker left only a few productive premises and its headquarters in its birthplace, and moved most of its plants to Southern Italy and abroad (Brazil, Poland, etc.). The population in its turn decreased by about 250,000 inhabitants (from 1.15 to 0.9 million). On the other hand, mobility increased by about 30% (from 415,000 to 545,000 private cars in the same period), reaching more than 600 private cars every 1000 inhabitants.

Moreover, Torino energy structure radically changed: while mobility increase was compensated by more and more stringent pollutant emission limits, the switch to natural gas and district heating (nowadays, 410,000 Torino inhabitants are district-heated) led to consistent reduction of pollutant emissions. As an example, the SO2 time history is shown in figure below (Comune di Torino s.d.).

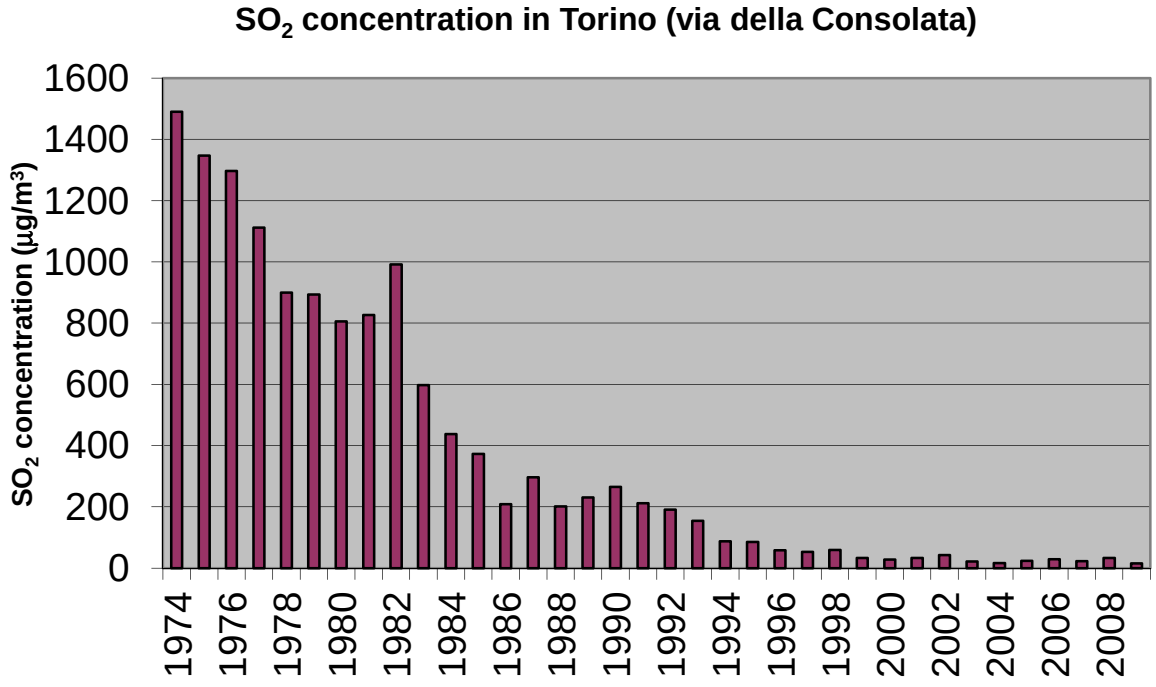

Figure 46SO_2 Concentration time history in Torino

While SO_2 concentration is now just 1% of 35 years ago levels, the air quality in Torino is still poor, compared to other Italian and European cities, with higher than acceptable

frequency of days in which pollution levels are beyond threshold, especially in terms of NO_x, and particulate matter.

For instance, Particulate Matter decreased only by a factor four from 190 μg/m^3 in 1974 to values around 40-50 μg/m^3 in these last years.

A comparison of the measurements in Torino and Pino (1975-6) and Torino (February 2010-December 2010) is shown in figure below. Eighteen daily sets of data were chosen from this measurement campaign as examples of clear sky days.

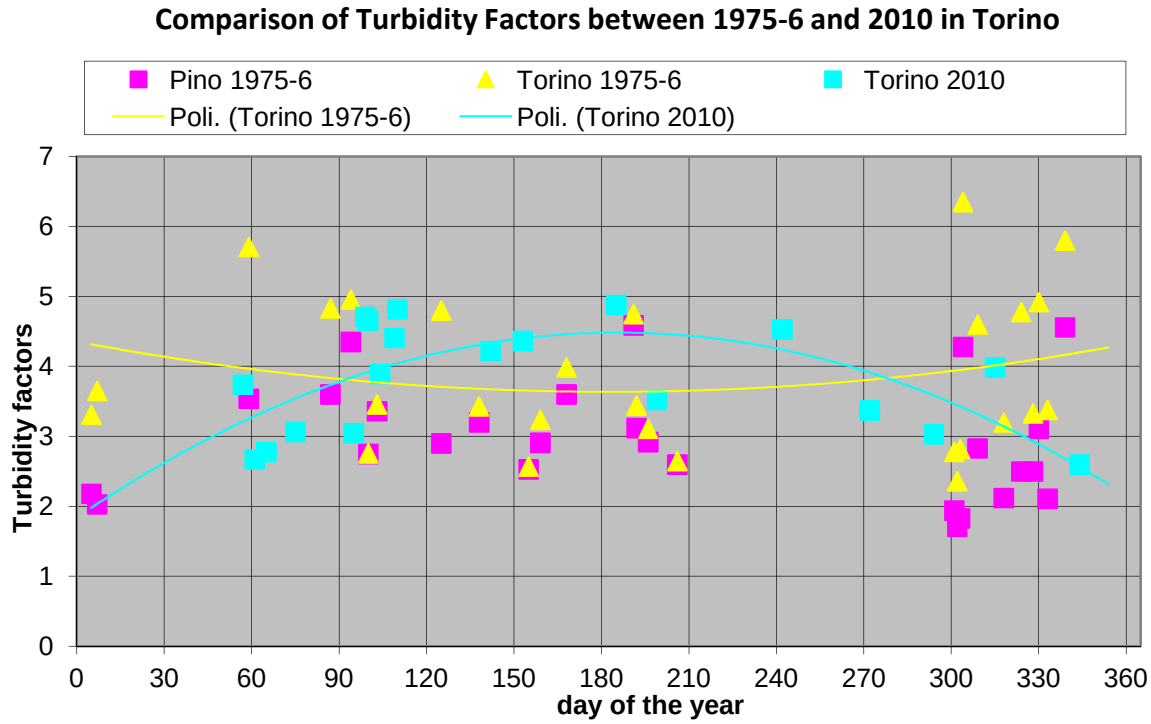

Figure 47Turbidity factors in 1975-6 and in 2010 in Torino

The conclusion which may be drawn is that turbidity data have not radically changed during the last 35 years. They appear slightly below the old data during the heating season, while they seem somehow higher during the rest of the year (April 15 to October 15, or days 105-288).

2.6.5 Conclusions

Turbidity measurements carried out 35 years ago showed a strong seasonal variation, with higher values during the heating season. Torino turbidity values are two Rayleigh atmospheres above those of the reference station (Pino Torinese) during winter time, while they are just a few percentage points above the reference in the late spring and summer.

The new measurements performed during 2010 have shown values comparable to those of 1975-76, but without an apparent seasonal variation: the optical quality of the atmosphere seems to have improved in the winter time, and remained the same during the rest of the year.

CHAPTER 3 COMPONENTS AND PERFORMANCE OF SOLAR COOLING SYSTEM

3.1 Holistic view

The use of solar energy comprises a wide range of uses. First of all, there is the conversion of energy from solar rays into thermal (heat) energy. This thermal energy can be used for many different purposes: for the production of electrical energy (by means of thermoelectric solar power stations), as process heat for industrial use, for the generation of cold (for example by means of absorption cooling) or for domestic use. This thesis is concerned primarily with domestic use, therefore the production of heat for

- hot water (DHW)
- space heating and
- space cooling (air conditioning).

Solar assisted domestic hot water (DHW) and space heating technologies use solar radiation to produce usable heat for water directly. Solar assisted domestic hot water demand can be met all through the year whenever there is sunlight, while space heating is required during winter season. During summer, the demand for air-conditioning for residential buildings, offices, hotels, public offices, etc., is considerable. As solar radiation is maximum in summer time, when there is the greatest need for air-conditioning, therefore the interest in solar cooling is growing. The study in this thesis is relating to the whole instead of a separation into parts, hence, it is called the holistic point of view. When a solar thermal system is designed, the demand for domestic hot water, space heating and cooling are all considered so as to make full use of the solar radiation all through the year, instead of letting the solar thermal collectors useless during winter or summer. This is also for the best use of the investment of solar thermal installation.

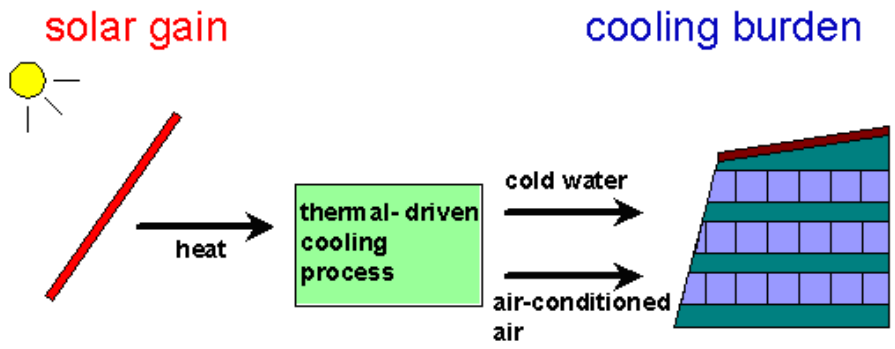

Figure 48A typical solar cooling system

Solar cooling systems are comprised of three key stages mainly: solar thermal collector circuit, cooling process and chilled water or air circuit. A typical solar cooling installation consists of solar collector, pipes and pumps, storage tank, control unit, a thermal driven cooling machine.

To collect the most possible energy coming from solar rays, collectors are oriented at an optimum angle with respect to the sun. Solar radiation is converted into heat by means of a highly absorbent layer (absorber) inside of the collector. A glass covering prevents the thermal energy from being dispersed into the environment. The absorber is passed through by a liquid, which transmits the heat directly to the user, or to a storage tank.

From the periods of sunshine which rarely coincides with those of hot water consumption, thermal energy is temporarily stored in a tank. The thermal tank used is possibly sized in a way that allows the satisfaction of hot water demand (energy demand) of 2-4 days. In this way it is possible to easily make it through even less sunny summer periods. In the winter season it is necessary in many cases to employ additional energy sources, such as oil, gas, or wood. If a system is well designed, it allows for proper functioning with the least possible use of additional energy.

3.2 Solar thermal collectors

3.2.1 Typologies of solar thermal collector

There are some ways to classify solar thermal collectors. According to the temperature of fluid inside of the collector produced, solar thermal collectors are classified by the United States Energy Information Administration as low-, medium-, or high-temperature collectors. Low-temperature collectors are flat plates generally used to heat swimming pools. Medium-temperature collectors are also usually flat plates but are used for heating water or air for

residential and commercial use. High-temperature collectors concentrate sunlight using mirrors or lenses and are generally used for electric power production.

Low temperature solar collector produce fluid of 40-90°C, including flat plate (glazed, unglazed), and vacuum tube. Average temperature solar collector produce fluid of 60-250°C, including vacuum tubes heat pipes Compound Parabolic Concentration (CPC). While high temperature solar collectors can produce working fluid with temperature higher than 250°C, and those collectors are for concentration tower (central receiver) systems or they are liner or trough-type Concentrators.

For small scale of solar heating and cooling systems, the temperature of fluid inside the solar collectors is usually not that high as 250°C. And according to the type of collectors, there are unglazed collectors, glazed collectors, and vacuum tube collectors. Among different types of collectors, the most suitable one depends on user needs.

Unglazed collectors: uncovered flat-plate collector type. Unglazed collectors are ideal for heating pools and for certain uses of pre-heating hot water. In regions where strong winds prevail, there are greater convective losses. On the other hand, unglazed collectors are low in cost and do not cause reflection.

Glass-covered flat-plate collectors: are the most widely used collectors. They are suitable for pre-heating water, for the production of hot water and for space heating. They are a somewhat more expensive than uncovered collectors. Thanks to their good thermal insulation, they are suitable for integration in facades.

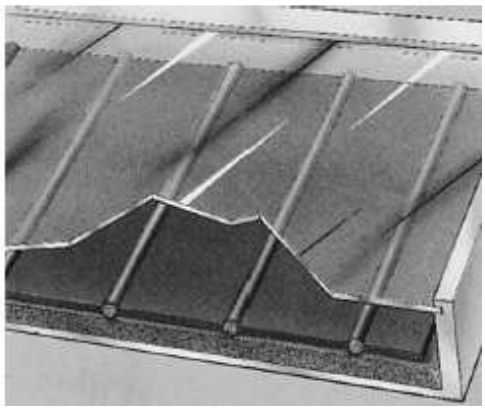

Figure 49Schematic drawing of a glazed flat-plate collector

In this figure above, the heat transfer fluid flows through the thin longitudinal pipes.

Vacuum tube collectors: are especially ideal for the production of hot water or where external temperatures are generally low (or when a considerable part of solar irradiation takes place in winter). This is based on the idea that the absorber in a vacuum tube only loses energy for thermal irradiation. In addition, the reflective behavior of light and the geometry

of the tube in glass contributes to making the obliquely falling light arrive more efficiently to the absorber compared to what happens in flat-plate collectors. Overall, tube collectors are the most expensive though, and for certain uses are not always as suitable as flat-plate collectors.

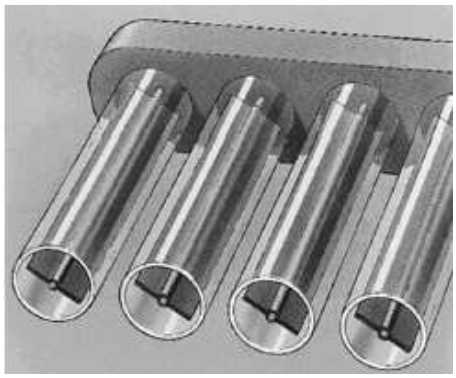

Figure 50Schematic drawing of a vacuum tube collector (Polysun user manual s.d.)

In the figure above, the heat transfer fluid flows through the thin longitudinal pipes.

Type of fluid

There are several types of fluid flowing inside the solar thermal collectors. According to the state, they are divided into liquid, Freons, and air.

The liquid fluid includes water or water plus antifreeze (glycol ethylene or propylene). The specific heat is high, so there is a good heat transfer, but this kind of fluid causes corrosion, viscosity variations, and thermal expansion.

It is dangerous to have freezing in winter. Considering the external temperature can reach below zero, an anti-freeze product would be used, normally glycol. The higher the quantity of glycol, the lower the thermal capacity of the fluid. Ethylene glycol is normally used at a concentration of 33% (propylene glycol at 38%). As a result, the fluid will only freezes like gelatin, without causing explosive effects inside the collector (Polysun user manual s.d.).

Freons (HCFC) is used in heat pipe installations, which has an excellent efficiency, but it also causes corrosion.

Air is usually used inside the solar-wall. There are several advantages such as: lower cost, lower weight, no corrosion, no heat exchangers for space heating, and the heat transfer process is quick. While there are also problems, for example, the ductwork is large, the heat transfer effect is bad, and there is the dust transportation, etc.

The liquid fluid of water plus antifreeze is quite common for small scale solar heating and cooling system.

3.2.2 Thermal balance of solar collectors

The solar irradiation values naturally cannot be entirely utilized by a collector. The thermal performance of a solar thermal collector is determined based on its optical properties and its insulating capacity. When solar radiation falls on the solar thermal collector, there are optical losses, such as the reflection and absorption in the glazing, and the reflections in the absorber; also between the glazing and the absorber, there are multiple reflexes. The remaining solar radiation is absorbed in the absorber, from where the heat is transferred mainly through heat conduction and convection, to the heat transfer fluid medium. Thereafter, the heated liquid is pumped to a heat storage tank. There are also heat losses from absorber, mainly through convection and radiation, but also due to conductive heat losses. To reduce the heat losses, it is very important to build good insulation of both the collector and the piping (Gajbert 2008).

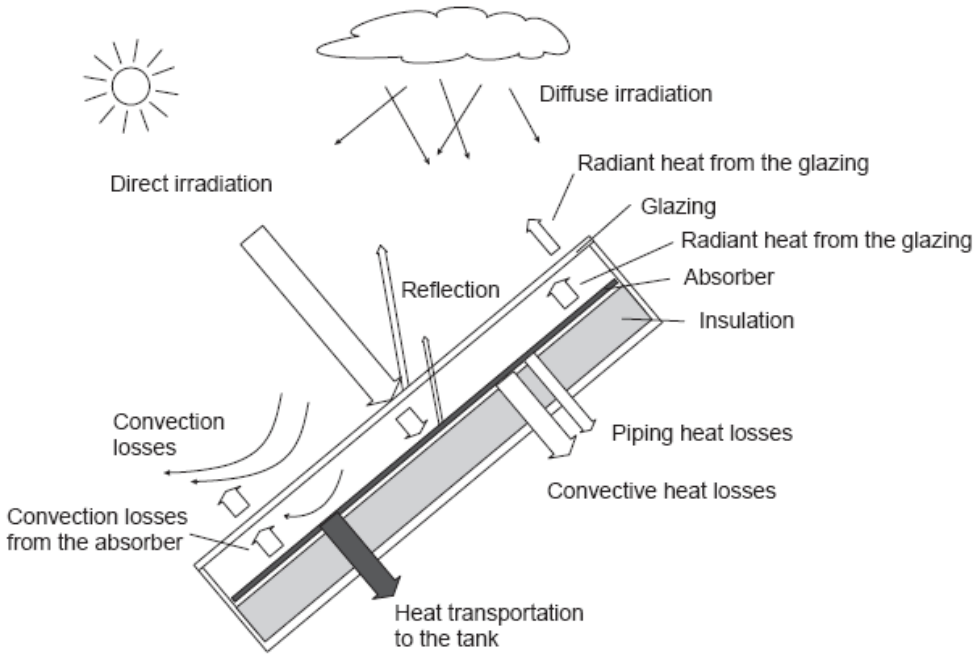

Figure 51Heat transfer in the solar thermal collector

There are various factors which contribute to cause one part of the energy not to be transmitted to the heat transfer fluid.

1) The partial reflection on the cover glass (approx. 8%), except for uncovered collectors,
2) The partial absorption by the collector, depending on the coating: minus 4-10%,
3) The incomplete cooling of the absorber, the so-called factor F': minus 3-10%,
4) The emission of heat by thermal radiation, depending on the coating and the temperature,
5) The loss of heat by means of thermal conduction and convection, losses depending on temperature.

The efficiency of a collector greatly depends on the difference between the average temperature of the collector and the external temperature. If this difference is substantial (i.e. 80°C), there are great losses because of thermal radiation and convection. In case of small temperature differences, the efficiency can reach up to approx. 90%. When the temperature of the collector, due to cold fluid, is less than the surrounding ambient temperature, efficiency could result even greater than 100%. In this case the heat transfer fluid becomes heated not only by the sun, but also by the heat from the surrounding environment.

From the energy balance point of view, for a flat plate, the conservation law states:

$$\dot{Q}_U = \dot{Q}_S - \dot{Q}_L - \dot{Q}_s$$

Where

$\dot{Q}_U$ is net enthalpy flow of the collector, W

$\dot{Q}_S$ is net solar irradiation, W

$\dot{Q}_L$ is the heat loss, W

$\dot{Q}_s$ is heat storage in the collector, W

In many cases, the thermal capacity of the collector is small, or the transients are moderate. In these cases the last term drops out. In steady-state analyses, the last term is zero, and the rest of the terms are assumed to be quasi-invariant with time (Lior 1990).

$$\dot{Q}_U = \dot{m} c_p (T_o - T_i)$$

$$\dot{Q}_S = \tau \alpha A G = SA$$

$$\dot{Q}_L = U_L A (T_m - T_a)$$

Where

T_i and T_o are inlet and outlet temperature of the fluid, $°C$,

A is the collector area, m^2,

G is the solar total irradiance, W/m^2,

$U_L$is collector overall heat loss coefficient, W/m^2,

τ is transmission coefficient of glazing,

α is absorption coefficient of plate,

T_m is mean fluid temperature, $°C$:

$$T_m = \frac{T_o + T_i}{2}$$

$T_a$is outdoor temperature, $°C$.

The efficiency of collector can be calculated is:

$$\eta = \frac{\dot{Q}_U}{AG} = \tau\alpha - U_L \frac{T_m - T_a}{G}$$

As seen from the equation above, the efficiency decreases with increasing operating temperature.

It is somewhat inconvenient to use the equations above because of the difficulty in defining the collector average temperature. It is convenient to define the collector heat removal factor F_R which relates the actual useful energy gain of a collector to the useful gain if the whole collector surface is at the fluid inlet temperature:

$$F_R = \frac{\dot{m}c_p(T_o - T_i)}{A(G\tau\alpha - U_L(T_I - T_a))}$$

So, the actual useful energy gain is found by multiplying the collector heat removal factor by the maximum possible useful energy gain:

$$\dot{Q}_U = F_R A(G\tau\alpha - U_L(T_I - T_a))$$

This equation is a widely used relationship for measuring collector energy gain and generally known as the Hottel-Whillier-Bliss equation (Struckmann 2008).

Thus, the instantaneous thermal efficiency of a collector can be written as:

$$\eta = F_R\tau\alpha - F_R U_L \left(\frac{T_I - T_a}{G}\right)$$

3.2.3 Collector efficiency according to European standards (EN)

The efficiency of a collector is represented by the so-called efficiency curve.

The difference in temperature, between the average collector temperature T_m and the outdoor temperature T_a, is divided by the total solar irradiance *G*:

$$x = (T_m - T_a)/G$$

The trend of the curve can be described by means of a polynomial of the second order, clearly determined by three parameters η_0, $a_1$and a_2. The efficiency is a function of total solar irradiance *G*, average temperature T_m, and outdorr temperature T_a:

$$\eta = \eta_0 - a_1 x - a_2 x^2 G$$

Where

η_0 is conversion factor,

a_1 and a_2 are the loss coefficients.

Assuming $G = 1000\ W/m^2$, $T_a = 20°C$, a normal glass-covered flat-plate collector has the parameters as follows:

$$\eta_0 = 0.83$$

$$a_1 = 4.23$$

$$a_2 = 0.012$$

The efficiency curve of this kind of collector is:

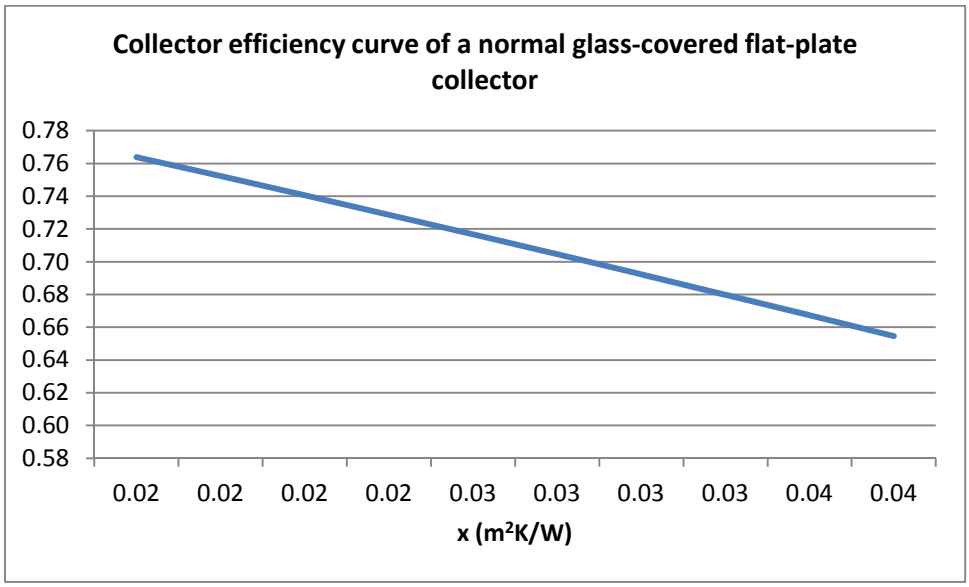

Figure 52Efficiency curve of a normal glass-covered flat-plate collector

η_0 is the efficiency rate achieved when the average temperature of the collector and the outdoor temperature are equal. This value should be as high as possible. a_1 and a_2 are combinations of different loss factors. In a well insulated collector, these values should be as low as possible.

The operation of a solar energy system requires a certain compromises. On one hand, the collector is needed to work at the highest efficiency level, on the other hand, the generated hot water should have a temperature of 50-60°C. So, this means having the collector operate at these temperatures, and that is why solar energy is often used for the pre-heating of water in large buildings. When cold water is heated from 10°C to 30°C, the collector works at a high level of efficiency. In terms of energy demand, it is of little importance that the water is heated from 10°C to 30°C or from 30°C to 50°C. Therefore, the efficiency rate of collectors is quite high in pre-heating. These kinds of systems can be profitable already after a few years (Polysun user manual s.d.).

3.3 Technologies of solar cooling

From a thermodynamic point of view, there are many processes conceivable for the transformation of solar radiation in cooling. See the figure as follows:

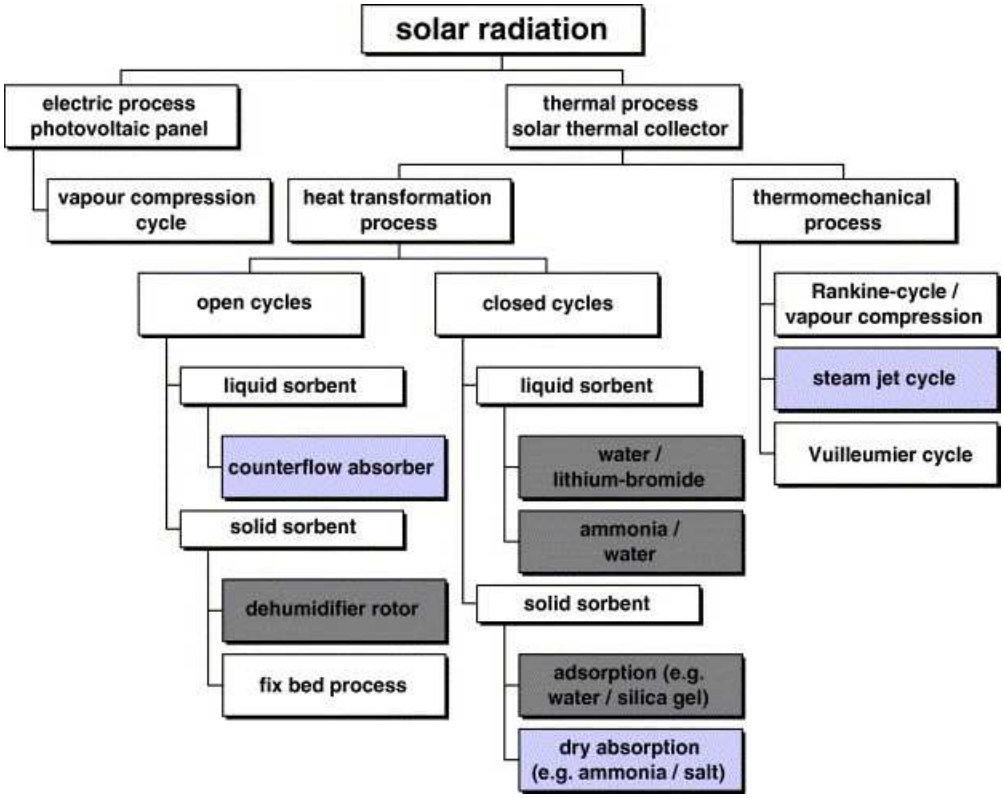

Figure 53Physical ways to convert solar radiation into cooling or air-conditioning

In the figure above, the processes marked in dark grey are those with market available technologies for solar cooling or air-conditioning, while the processes marked in light purple are the technologies in status of pilot projects or system testing (H.-M. Henning, Solar assisted air conditioning of buildings - an overview 2007).

The systems of solar cooling technologies under consideration are generally divided into two main categories: closed and open cycles. Close cycle technologies apply thermally driven chillers to produce chilled water which can be used for any type of cooling equipment. Open cycles are referred to direct treatment of fresh air in ventilation system such as the temperature and humidity (H.-M. Henning, Focus point 2: Solar assisted cooling 2008).

The focus of this thesis is on solar cooling and air-conditioning systems in small and medium size capacity range. Small applications are systems with a nominal chilling capacity below 20 kW, while medium size systems may range up to approx. 100 kW. Systems in small capacity range are usually consist of thermally driven chilled water systems, where the distribution medium, chilled water in a closed loop to remove the loads from the building, whereas medium sized systems may be open cycle desiccant evaporative cooling systems, where the supply air is directly handled in humidity and temperature respectively in an open process.

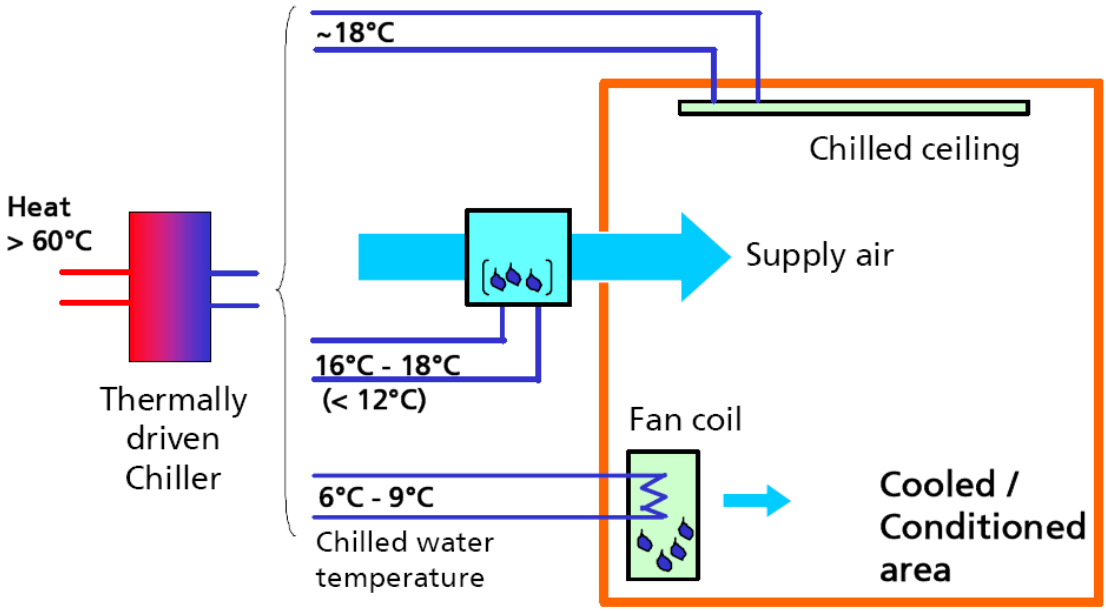

Figure 54General type of thermally driven cooling and air-conditioning technology

In chilled water systems, the central chilled water distribution grid may serve decentralized cooling units such as fan coils, chilled ceilings, walls or floors. It is also possible to make the chilled water used for supply air cooling in a central air handling unit.

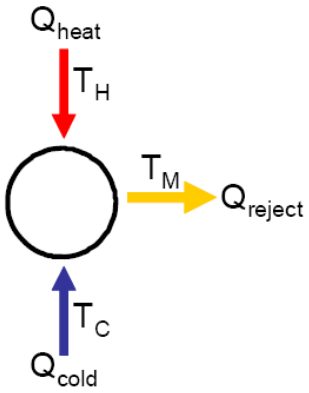

Figure 55Basic scheme of a thermally driven cooling process

Any thermally driven cooling process operates at three different temperature levels. The driving heat Q_{heat} is supplied to the process at a temperature level of T_H, while the heat is removed from the cold side producing the useful cold Q_{cold} at temperature level T_C. Both amount of heat are rejected as $Q_{rejected}$ at a medium temperature level T_M. The driving heat Q_{heat} may be provided by the solar thermal collector alone, or in combination with auxiliary heating system.

A basic parameter to quantify the thermal process quality is the coefficient of performance COP, which is defined as:

$$COP = \frac{Q_{cold}}{Q_{heat}}$$

COP indicates the amount of heat required for producing unit of cold, namely per unit of removed heat from the load side.

The COP and the chilling capacity depends strongly on the temperature levels of T_H, T_C and T_M.

In market available products of thermally driven chillers, the COP range is from 0.5 to 0.8 in single-effect machines, while it can be up to 1.2 in double-effect machines.

3.3.1 Absorption chillers

The dominating technology of thermally driven water chillers is based on absorption.

Absorption chillers are available on the market in a wide range of capacities and designed for different applications. The majority systems available are in a range above 100 kW of cooling capacity, while, also a few commercial systems for small power, below 30 kW, are available at present.

There are at least two chemical components for the basic physical process, refrigerant and the sorbent. For air-conditioning applications, the absorption chillers mainly use the sorption pair water-LiBr, where water is the refrigerant and LiBr is the sorbent. The basic construction is called single effect machine, in which for each unit mass of refrigerant evaporating in the evaporator, one unit mass of refrigerant has to be desorbed from the refrigerant-sorbent solution in the generator.

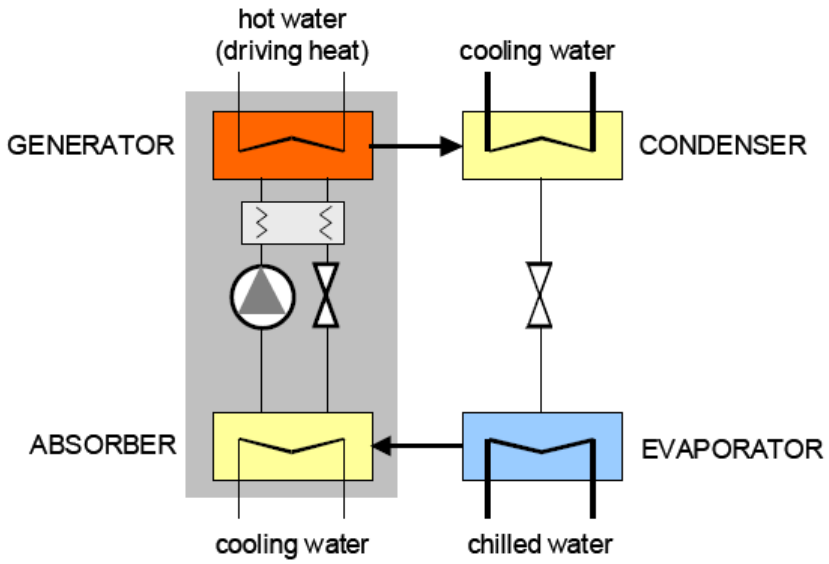

Figure 56Scheme of a thermally driven absorption chiller (SOLAIR 2008)

Under normal operation conditions, a single effect absorption machine needs driving heat at temperatures of 80-100 ° C and the COP can achieve around 0.7 (H.-M. Henning, Solar assisted air conditioning of buildings - an overview 2007).

Chillers using a double effect cycle are also available. Two generators working at different temperatures are operated in series, thus the condenser heat of the refrigerant desorbed from the first generator is used to heat the second generator. The COP of a double effect absorption chiller may achieve a range of 1.1-1.2, with much higher driving temperatures in the range of 140-160°C required. This kind of systems is only available in the range of large capacities.

In recent years, there is a number of new chiller products entering the market in the small and medium capacity range. These products are designed to be operated with low driving temperatures generally speaking so as to be applicable for stationary solar thermal collectors. The lowest chiller capacity available is now 4.5 kW. Some examples of small and medium sized absorption chillers are shown in the figures below:

Figure 57Examples of small size absorption chillers (water-LiBr) (Rotartica, Sonnenklima, EAW s.d.)

3.3.2 Adsorption chillers

Solid sorption materials are used in adsorption chillers and this kind of materials adsorbs the refrigerant while it releases the refrigerant under heat input. A quasi-continuous operation requires that at least two compartments, the evaporator and the condenser, with sorption material. The figure below shows the components of an adsorption chiller.

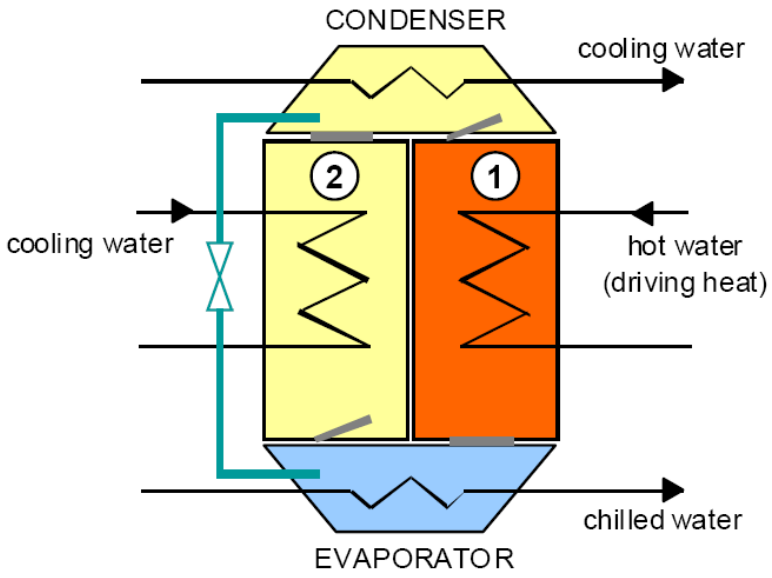

Figure 58Scheme of an adsorption chiller

While the sorbent in the first compartment is regenerated using hot water from the external heat source, e.g. solar collector, the sorbent in the second compartment adsorbs the refrigerant vapor entering from the evaporator; this compartment has to be cooled in order to enable a continuous adsorption. The refrigerant, condensed in the cooled condenser and transferred into the evaporator, is vaporized under low pressure in the evaporator. Here, the useful cooling is produced. Periodically, the compartments are switched over in their functions if the cooling capacity reduces to a certain value due to the loading of the sorbent in the adsorber, and this is usually done through a switch control of external located valve (SOLAIR 2008).

Until now, there are only few manufacturers worldwide, from Japan, China and from Germany produce adsorption chillers. Typical COP values of adsorption chillers are 0.5-0.6. The figure below shows two examples of adsorption chillers:

Figure 59Examples of adsorption chillers (Nishiyodo (Japan), SorTech (Germany) s.d.)

One advantage to use adsorption chillers is that there are low driving temperatures, beginning from 60°C, and the solution pump is not needed with a comparatively noiseless operation.

3.3.3 Desiccant cooling

Open cooling cycles produce directly conditioned air. Any type of thermally driven open cooling cycle is based on a combination of evaporative cooling with air dehumidification by a desiccant, for example, a hygroscopic material.

Desiccant cooling processes are divided into two types, solid sorption and liquid sorption. Solid sorption uses rotating desiccant wheels, equipped either with silica gel or lithium-chloride as sorption material. All required components are standard and have been used in air-conditioning and air-drying applications for buildings or factories since many years (H.-M. Henning, Task 38 Solar Air-conditioning and refrigeration 2010).

Figure 60Open cycles-desiccant air handling units

The standard solid desiccant cooling cycle using a desiccant wheel is shown in the figure as follows:

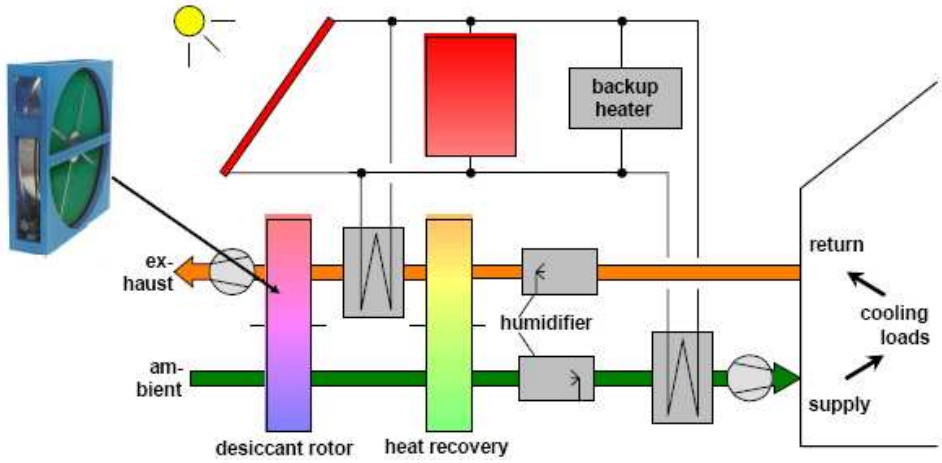

Figure 61Schematic of a solar solid desiccant evaporative cooling system (DEC) using rotating sorption and heat recovery wheels (ISE s.d.)

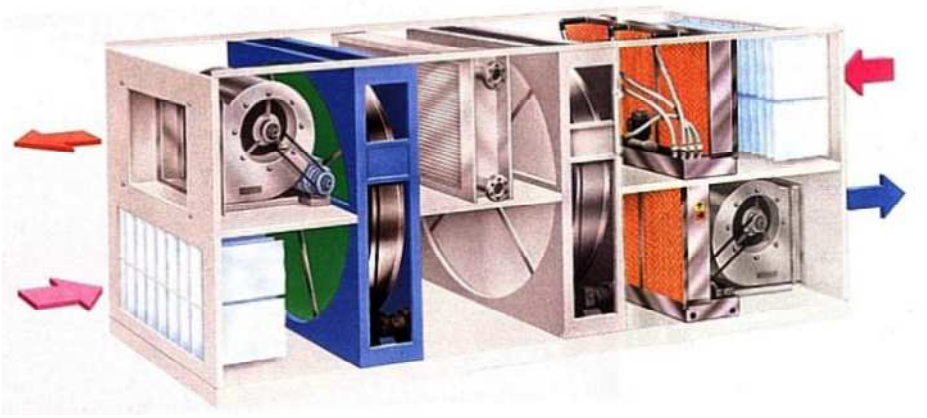

Figure 62Sketch of a DEC unit (Munters s.d.)

The application of this cycle is limited to temperate climates, because if the ambient air is with far higher values of humidity, the possible dehumidification is not high enough to enable evaporative cooling of the supplied air, for example, the climates like those in the Mediterranean countries (SOLAIR 2008).

Systems employing liquid sorption have packed bed and plate exchanger, using LiCl-solution. Liquid sorption materials have higher air dehumidification at the same driving temperature and it is possible to have high energy storage by means of concentrated hygroscopic solutions. These systems are not yet market available but close to the market introduction. There are several demonstration projects carried out in order to test the applicability of this solar cooling technology. A possible general scheme of a liquid desiccant cooling system is shown in the figure as follows:

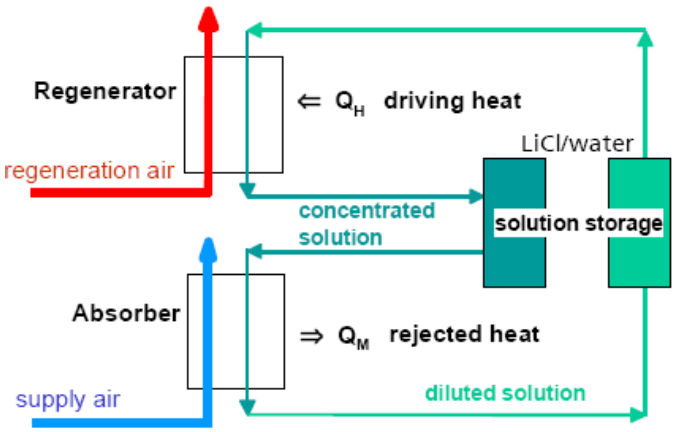

Figure 63General scheme of a liquid desiccant cooling system (ISE s.d.)

The supply air is dehumidified in a special configured spray zone of the absorber, where a concentrated salt solution is diluted by the humidity of the supply air. The process efficiency is increased through heat rejection of the sorption heat, e.g., by means of indirect evaporative cooling of the return air and heat recovery. A subsequent evaporative cooling of the supply

air may be applied, if necessary (heat recovery and evaporative cooling is not shown in the figure). In a regenerator, heat e.g. from a solar collector is applied, to concentrate the solution again. The concentrated and diluted solution may be stored in high energy storages, thus allowing a decoupling in time between cooling and regeneration to a certain extent.
In open cycle desiccant cooling systems, the COP is much more difficult to assess, because it depends more strongly on the system operation.

3.3.4 Ejector cooling

Solar ejector cooling technology is used for air conditioning of trains or large buildings. The generator temperature is between 85 and 95°C, and COPs reported are in the range of 0.2-0.33 for a condenser temperature between 28 and 32°C. There was a report of a much higher COP of 0.85 for a pilot steam ejector plant, but this can only be possible with a heat source temperature at 200°C. The solar ejector cooling has a great advantage which is the simple construction of the ejector systems, while the COP makes it difficult to compete with other solar driven technologies. It is unlikely that COP could be improved to a competitive level due to the inevitable energy dissipation in the working mechanism of conventional ejectors (D.S.Kim 2008).

3.4 Market available standardized solar cooling kits in Europe

The solar cooling kits usually include solar thermal collectors with attachments, hot water storage, pump sets, sorption chiller, re-cooler, chilled water storage and a system controller. The potential for solar cooling in Europe is huge, while there are only a small number of companies develop and offer standardized small-scale (up to 30 kW cooling capacity) solar cooling kits so far. The great challenge is to integrate the cooling system into a standard solution.
The cost of a solar cooling kit is still fairly high. SolarNext for example, the market pioneer in this segment, the specific total costs of the installed solar cooling systems in Europe have been between 5000 and 8000 €/kW cooling capacity, and depending on the application and the site, the prices of average system have reached around 4000 to 4500 €/kW. Hence, to reach a reasonable payback time, an all-season use of solar energy for domestic hot water, space heating and solar cooling is indispensable, which is also called the holistic point of view.
The other three main companies are also striving to reduce costs, while sometimes, the cost of a solar cooling kit does not include the re-cooler. The average value of specific collector surface of listed kits is 4.2 m^2/kW cooling capacity. If the solar fraction for the solar cooling

system is set to be more than 70%, the collector areas should be supplied with 4.5 m^2/kW or more. The average value of all installed small to large solar cooling systems in Europe is increasing. Until year 2006, it was 3 m^2/kW (Solar cooling kits for Europe s.d.).

Table 4Market available standardized solar cooling kits in Europe

Company	**Technology /working pair**	**Cooling capacity [kW]**	**COP**	**Cold buffer storage [l]**	**Collector area [m^2]**	**Hot buffer storage [l]**	**Recooler**
Solarnext AG, Germany	Adsorption, water/silica gel	7.5	0.56	-	34	1825	Dry recooler with water spraying
	Adsorption, water/zeolith	10	0.50	-	46	2475	Dry recooler with water spraying
	Absorption, ammonia/water	12	0.62	1000	52	2825	Wet cooling tower
	Adsorption, water/silica gel	15	0.56	-	68	3650	Dry recooler with water spraying
	Absorption, water/LiBr	17.5	0.70	1000	78	4300	Wet cooling tower
Schüco International KG, Germany	Absorption, water/LiBr	15	0.71	1000	48	2000	Wet cooling tower
	Absorption, water/LiBr	30	0.75	1500	96	4000	Wet cooling tower
Solution Solartechnik GmbH, Austria	Adsorption, water/silica gel	7.5	0.56	-	32	1500	Dry recooler with water spraying
	Adsorption, water/silica gel	15	0.56	-	64	3000	Dry recooler with water spraying
	Adsorption,	30	n.a	-	124	6000	n.a.

	water/silica gel						
	Absorption, water/LiBr	54	0.75	4000	221	10000	Wet cooling tower
SK Sonnenklima GmbH, Germany	Absorption, water/LiBr	10	0.77	-	30 to 40	1000	Wet or dry cooling tower

3.5 Performance of solar cooling system

3.5.1 Solar fractions

In the simulation or pre-design stage, it is necessary to define solar fractions to analyze the system's behavior and performance. In simulation software Polysun, to evaluate the performance of the solar heating and cooling system, three solar fractions are defined as follows:

$$SF_i = \frac{solar\ energy\ to\ storage\ tank}{solar\ energy\ to\ storage\ tank + auxiliary\ energy\ to\ starage\ tank}$$

$$SF_n = \frac{solar\ energy\ to\ the\ system}{solar\ energy\ to\ the\ system + auxiliary\ energy\ to\ the\ system}$$

$$SF_g = \frac{irradiance\ onto\ collector\ area}{irradiance\ onto\ collector\ area + auxiliary\ energy}$$

The limits for the calculation of each solar fraction are shown in the figure below:

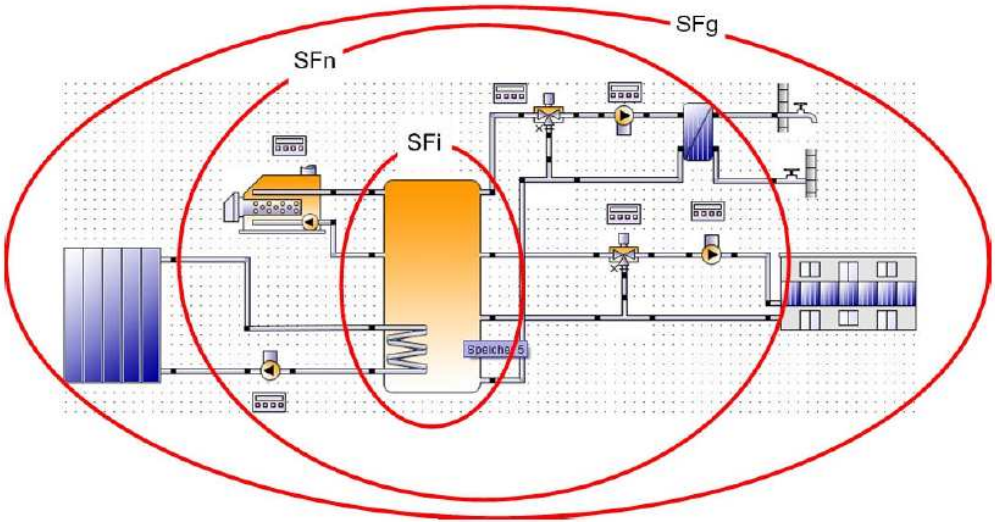

Figure 64Limits for the solar fraction calculation (Polysun user manual s.d.)

To calculate the solar fraction for hot water and heating separately, it is only possible for special system configurations where the heat for heating and hot water are run and stored separately.

3.5.2 Fuel and CO_2 savings

In most cases, solar heating and cooling systems are used as support to conventional systems for the heating of hot water. During the summer auxiliary heating is most often inactive if cooling load can be met, while during the winter it forms the main contribution to heating.
Electric auxiliary heating is often used to lighten the work load of the boiler in summer. Normally, by installing a solar energy system, the use of auxiliary electric heating is canceled.
The use of the solar energy system enables to reduce both fuel demand and CO_2 emissions. For a solar heating and cooling system, the savings can be calculated based on the calorific value and the annual average efficiency of the heat generator.
For fuel saving calculation, the S_{sol} solar energy in the tank is divided by the heating value of the fuel and the total yearly boiler efficiency:

$$Fuel\ saving\ [unit] = \frac{S_{sol}\ [kJ]}{Heating\ value_{fuel}\ \left[\frac{kJ}{unit}\right] \times total\ yearly\ boiler\ efficiency}$$

With reference to CO_2 savings the solar yield to the tank is multiplied by the CO_2 emissions from the fuel and divided by the yearly boiler efficiency:

$$Impeded\ CO_2 = \frac{S_{sol}\ [GJ] \times CO_2 emission}{total\ yearly\ boiler\ efficiency}$$

CHAPTER 4 SENSITIVITY ANALYSIS WITH POLYSUN

4.1 Polysun simulation software

In this chapter, the simulations are focused on the small or medium size solar cooling system with thermally driven sorption chiller, not only because the solar heating and cooling systems are increasingly popular among single and multi families, but also because this simulation research is related on the pre-design stage of a regional solar cooling project and the performance monitoring and evaluation of small size solar cooling system in IPLA, Torino.

The design and dimensioning of a solar cooling system depends not only on the maximum cooling load. Dynamic simulations have shown that it also depends on the characteristics of the cooling load distribution all over the year.

The solar fraction of the required solar heating energy depends on the collector type and area, storage tank volume, specific mass flow rate of the collector field, the control of the collector circuit pump, and the charge and discharge control of the storage tank.

On the side of the thermally driven sorption chiller machine, absorption chiller machine for example, the overall performance of the machine is significantly influenced by the control of the cooling temperature at absorber and condenser inlet, the required chilled water temperature and the heating temperature on the generator side (Ursula Eicker 2009).

Also, the building and its location, along with the control strategies, all have influence on the performance of the solar cooling system.

In the following simulations discussion, the influencing factors such as collector type, area, storage tank volume, control strategies, etc., are analyzed with multi simulations using Polysun, and the performance both from technical and economical side is evaluated.

Polysun is a software that enables users to effectively simulate solar-thermal, photovoltaic and geothermal systems (Polysun user manual s.d.). The program provides dynamical annual simulations of solar thermal systems and makes optimization. The operation is with dynamic time steps from 1 second to 1 hour, so as to make the simulation more stable and exact. Also, this software has a graphic-user interface which permits a clear input of all system parameters required.

The aspects of Polysun are based on physical models which work without empirical correlation term. Furthermore, the economic viability analysis as well as ecological balance, which includes emissions from the eight most significant greenhouse gases, can be performed, hence it is possible to compare the systems working only with conventional fuel

and those with solar thermal driven. Polysun was validated by Gantner, and was found to be accurate to within 5-10% (M. 2000). Accuracy and efficiency is of paramount importance when planning a solar cooling system and Polysun's solar cooling module allows users to reliably predict the performance and energy consumption of every single component through physics-based simulation, as well as effectively calculate energy efficiency.

The modular approach and the hydraulics focus on real available components allow the use of Polysun in the early planning phase and the optimization of system components and control strategies. It has been recognized that a physics based numerical treatment with a fully coupled system of equations is capable of predicting the system behavior and in principle is useful for analysis, design and optimization (Seyed Hossein Rezaei 2009).

In this chapter, simulations of solar cooling are carried on with Polysun combining with domestic hot water and space heating in some cases for the sensitivity analyses of solar cooling installations.

4.2 Template and reference system

4.2.1 Influence of location

The dimensioning of a solar cooling system requires choosing the correct size of the sorption chiller, but this is not sufficient for the dimensioning of the solar cooling system to achieve a certain solar fraction. The reason is that different buildings have various daily cooling load characteristics with maximum cooling power demand at different timing during the day, while there is a fixed timely availability of solar energy. To solve the time shifts problem between maximum cooling load and maximum solar radiation or cloudy days with little solar radiation available, hot water and chilled water storage tank are introduced into the system.

Hence, the location of the building has a clear influence on the required cooling load, and also the performance of the solar cooling system. Absorption chiller for example, apart from the local solar radiation available, the ambient temperature and humidity are the most critical parameters for the efficiency of the system.

In this thesis, the location is always set to be at Torino, Italy, where the pre-design Helios-HP project and IPLA solar cooling installation are located.

4.2.2 Template scheme

In Polysun simulation of solar heating and cooling system, template 71a - Space heating and cooling + hot water (absorption chiller, dry recooler) has the only proper scheme which can be used as an initial design structure of a solar cooling system. During the following simulation analyses, component types, sizes and several parameters will be changed.

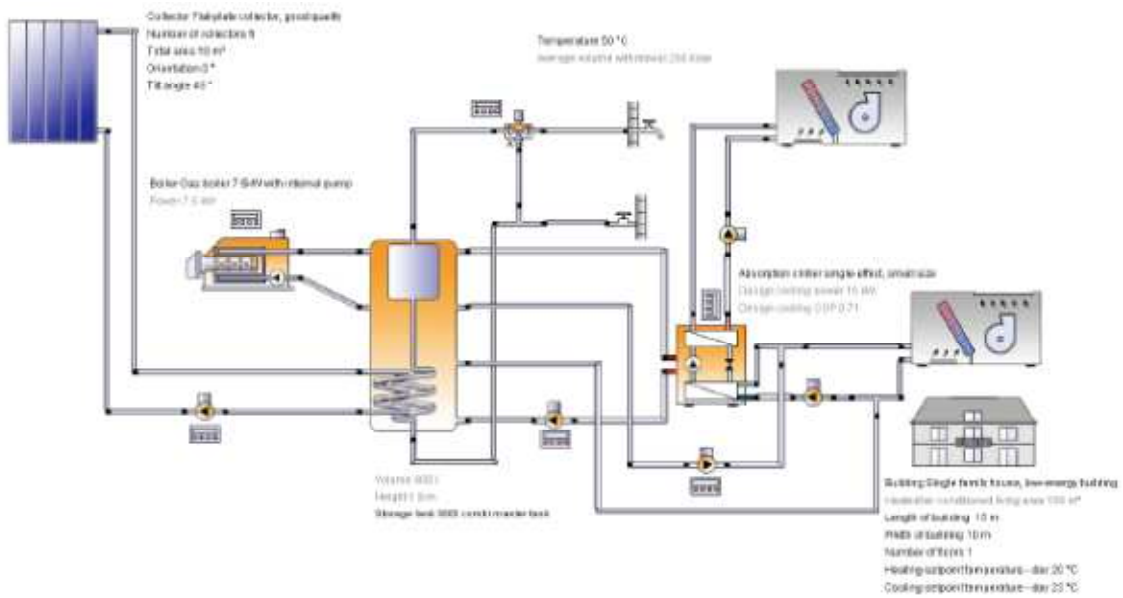

Figure 65Schematic of template 71a - Space heating and cooling + hot water

This solar heating and cooling system combining with domestic hot water includes flat-plate collector, a combi master storage tank, a single-effect small size absorption chiller, an auxiliary gas boiler, fan coils, pumps, etc.

There are some basic parameters which are defined before the simulation in the table below.

Table 5Basic parameters of the template 71a

Location	Torino, Italy, Europe
Electric grid voltage [V]	230
Consumers	Hot water and space heating (Without pool or process heat)
Energy generators	Solar thermal system with boiler (oil, gas, wood); Absorption chiller
System	Small size
	Single field collector
	Potable water: Buffer tank with coil/Tank in tank

4.2.3 Denominations and representation of the results

To evaluate the simulation results of a solar thermal system in Polysun, it is necessary to get an idea of the denominations and representation of the results.

The abbreviations for the energy balances are always based on the same model in Polysun simulations. For the symbol ‘QparS’, it means the heat transferred from the pump to the solar loop. Q stands for the energy transferred to the system or rather to the hydraulic system, and ‘par’ is for parasitic energy, e.g., the pump. S is for the circuit, and in solar thermal systems,

especially for the solar loop. The last index is missing, here S, it is meant to the transferred heat energy to all loops by all available pumps.

Heat loss to interior space ‘Qint’ means the losses of all the components present indoors, also including the chemical energy losses in boilers with less than 100% efficiency.

‘Qdem’ is the energy demand, calculated by Polysun, which should be possibly covered. In the case when the ‘Quse’ (effective energy consumption) is lower than the ‘Qdem’, the energy demand cannot be covered and the corresponding warning appears. The causes are sought primarily in the installation height of the connections in the boiler or of controller settings. The availability of hot water and building heating are shown in the component results indicate what percentage of energy demand is covered.

In case of collector, the end energy ‘Esol’ is referring to the gross collector surface irradiation. ‘Eaux’ means the chemical energy (highest value of heat of combustion) of combustible fuel. In this chapter, the auxiliary energy comes from the gas boiler.

There are usually five letters composing one parameter in the results of Polysun. The table below shows the definitions.

Table 6and representation of the results in Polysun thermal systems

Letter position	***Letter***	***Definition***
1	E	End energy (fuel and electrical power consumption)
	Q	Energy to the system or energy withdrawn from the system
	S	Energy to the tank or energy withdrawn from the tank
2 to 4	sol	Solar energy
	out	Energy withdrawn
	use	Energy consumption
	dem	Energy demand
	aux	Auxiliary energy
	par	Auxiliary or parasitic energy (pumps and fans)
	int	Energy to indoor room
	ext	Energy to surroundings
	def	Energy deficit
	xfr	Transferred energy
	ventil	Energy in ventilation of building
	trans	Energy transmission in building
5	S	Solar
	A	Auxiliary

	X	Heat transmission
	U	User
	M	Midex (Solar and auxiliary)
	-	Total of all loops

For some of the letter in position 2 to 4, here are some additional explanations to demonstrate the meaning of definitions: e.g. Qsol=Energy supplied from collector to fluid; 'use' means amount of energy actually consumed for domestic hot water, building, etc; 'aux' means theoretically calculated value referring to the amount of energy required, for example, to heat the cold water of the cold water piping to the desired hot water temperature.

4.2.4 Configuration of reference system

To evaluate the performance of a solar cooling system, solar fraction is an important parameter, while the specification of separate solar fractions has no significance for design or customer service purposes. A much more crucial role will be played by the use of the reference systems offered as a standard in Polysun. This will enable to elicit the influence of single system components and to optimize the heating and cooling system.

Important values like, e.g. Solar savings (Fractional solar savings F_{SS}) may only be calculated with the aid of the definition of a reference system. Solar savings are defined as follows:

$$F_{SS} = 1 - \frac{(E_{aux} - E_{par})_{sol}}{(E_{aux} - E_{par})_{ref}}$$

Where E_{aux} refers to the Auxiliary energy and E_{par} refers to the Parasitic energy of the respective system. 'sol' means solar energy system, while 'ref' means reference system.

This reference system is defined for 4 persons (200 liters hot water daily consumption) living in a low-energy house.

Table 7Parameters for the domestic hot water (DHW) demand

Parameter	***Value***	***Unit***
Temperature	50	°C
Average volume withdrawal per capita	50	l/day/capita
Availability times	all year around	-

Table 8Parameters for the building (Single family house, low-energy building)

Parameter	***Value***	***Unit***
Heated/air-conditioned living area	150	m²
Number of people	4	-
Heating set point temperature-day	20	°C

Heating set point temperature-night	19	°C
Cooling set point temperature-day	23	°C
Cooling set point temperature-night	24	°C
Heating seasons	Jan-Feb-Mar-Apr-Oct-Nov-Dec	-
Cooling seasons	Jun-Jul-Aug	-

Table 9Parameters for the collector (Flat-place, good quality)

Parameter	***Value***	***Unit***
Collector area	10	m^2

Table 10Parameters for the storage tank (Combi master tank)

Parameter	***Value***	***Unit***
Storage tank volume	800	l

4.2.5 Results of reference system simulation

After simulation of the reference system with the parameters setting above, the system results are shown as follows.

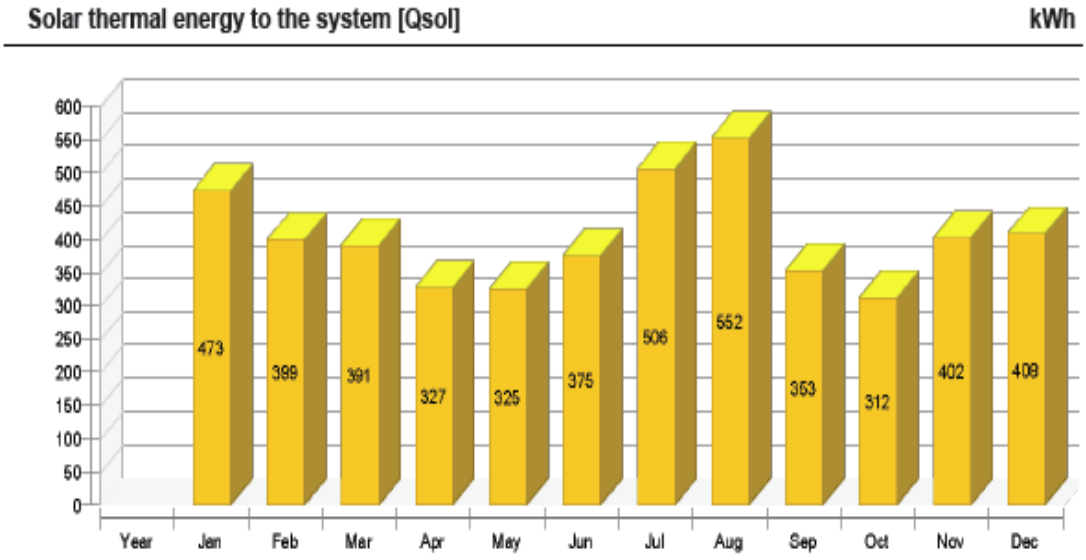

Figure 66Solar thermal energy to the reference system for each month of year

Q_{sol} refers to the energy supplied from collector to fluid.

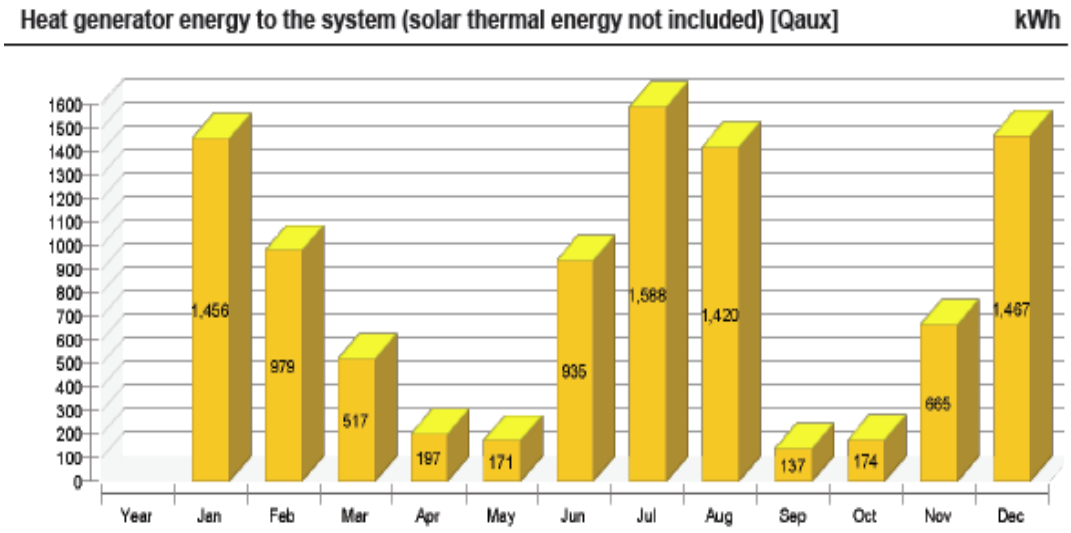

Figure 67Heat generator energy to the system (solar thermal energy not included) for each month of year

In this reference system, the heat generator is mainly the gas boiler as an auxiliary system, and Q_{aux} refers to the energy supplied from heat generator to fluid.

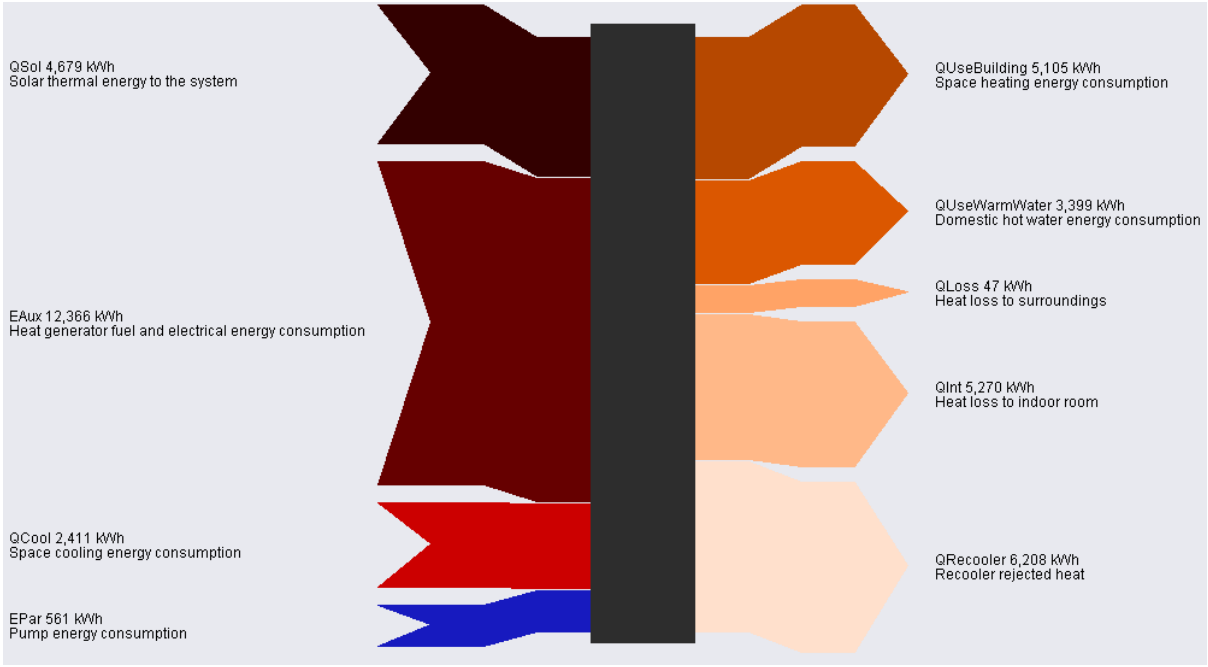

Figure 68Energy flow diagram

The energy flow diagram shows clearly the direction, amount of each energy flow.

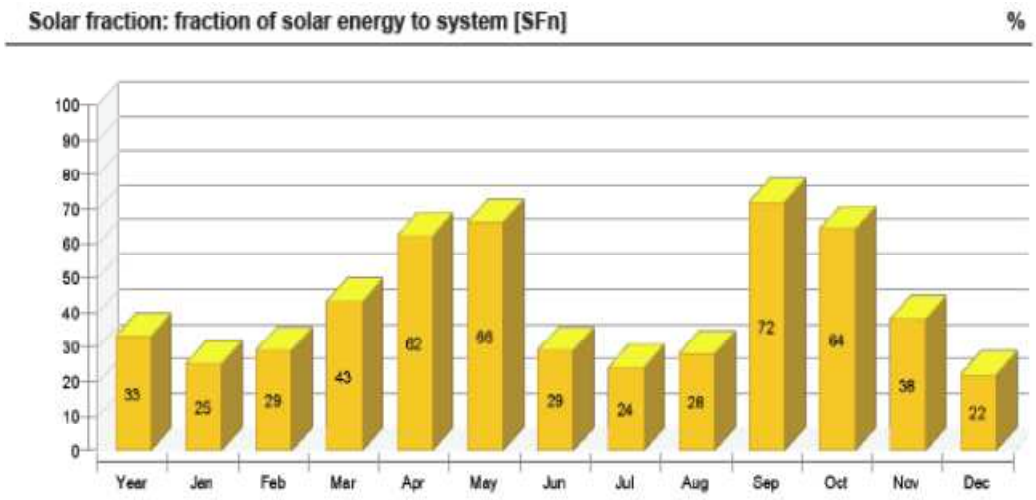

Figure 69Fraction of solar energy to system for each month of year

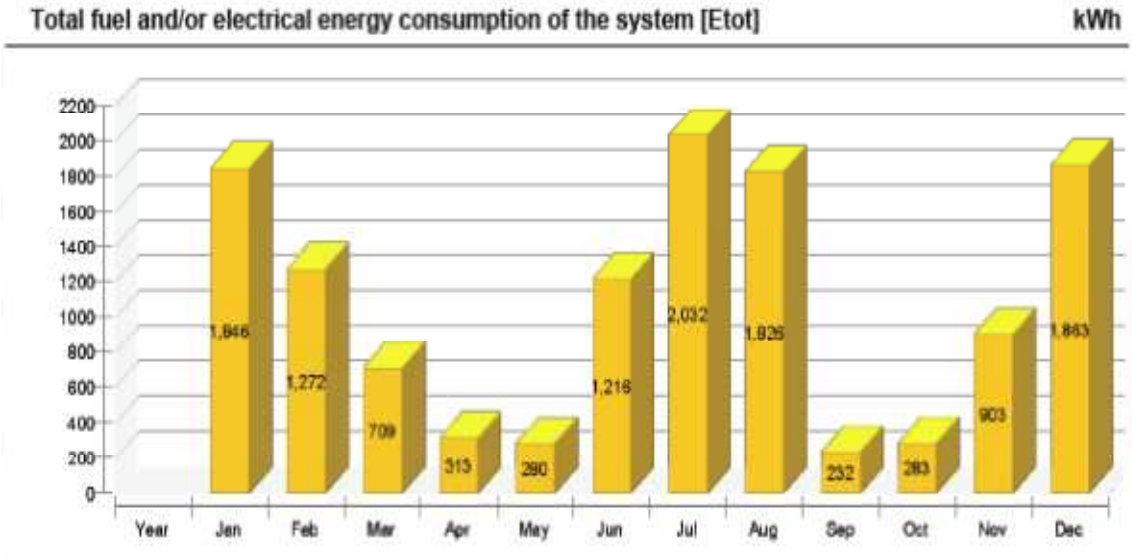

Figure 70Total fuel and/or electrical energy consumption of the system for each month of year

For the annual values of the performance of this reference system, the table below shows the main results.

Table 11Overview of whole energy system (annual values)

Parameter	***Value***	***Unit***
Total fuel and/or electrical energy consumption of the system [Etot]	12,776.5	kWh
Total energy consumption [Quse]	11,118.4	kWh
System performance (Quse / Etot)	0.87	-
Comfort demand	Energy demand covered	-

Table 12Overview of solar thermal system overview (annual values)

Parameter	***Value***	***Unit***
Solar fraction total	33.20	%
Solar fraction hot water [SFnHw]	42.40	%
Solar fraction building [SFnBd]	25.30	%
Total annual field yield	4,823	kWh
Collector field yield relating to gross area	482	kWh/m²/Year
Max. fuel savings	510.4	m³ natural gas
Max. energy savings	5,359.4	kWh
Max. reduction in CO2 emissions	1,241.2	kg

Table 13Table Overview of absorption chiller (annual values)

Parameter	***Value***	***Unit***
Seasonal performance factor - Cooling	0.65	-
Total cooling energy yield	2,436.9	kWh
Heat supplied in generator	3,752.2	kWh

4.3 Sensitivity analysis of reference system

For the configuration of the reference system, the collector area is 10 m^2. If the basic demand from the building side can be met, solar collector area can be changed to different sizes so as to get different performances of the solar circuit, namely, the various contribution of solar energy to the whole energy consumption needed in the reference system with the initial configuration of components.

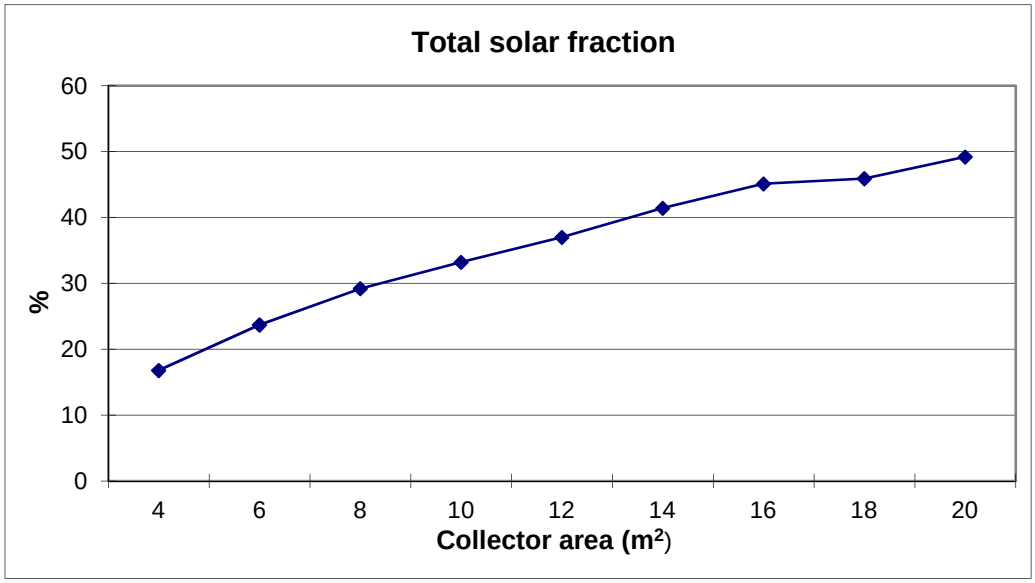

Figure 71Total solar fraction variation with collector area increasing

The total solar fraction of the solar system increases as the collector area is growing, while, the increasing rate is slowing down when the size of the collector field is over sized. And this is also reflected in the variation of the total annual field yield in the figure as follows.

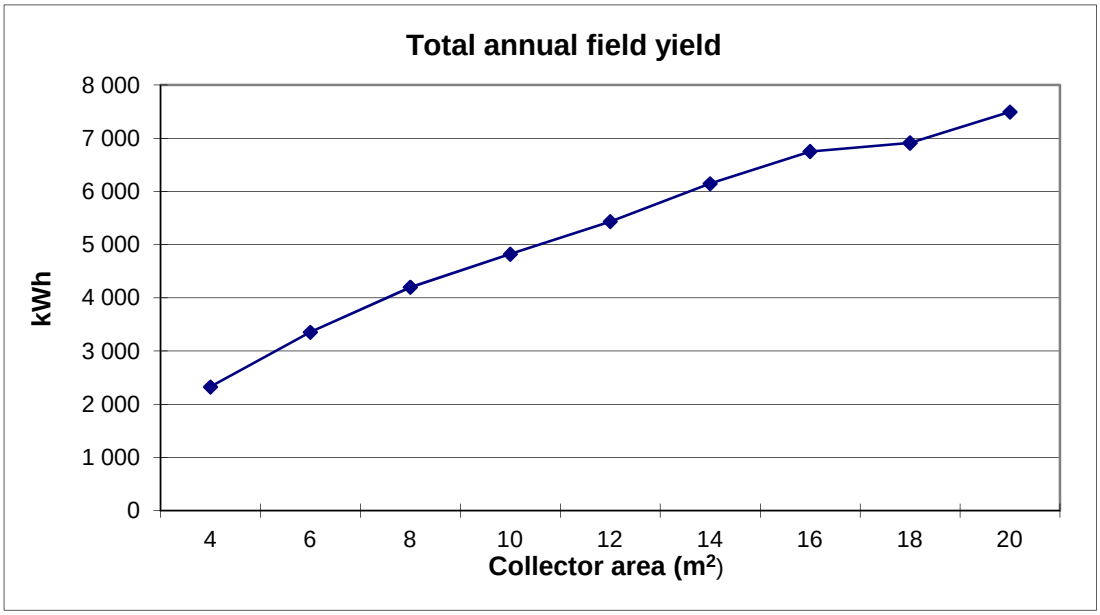

Figure 72Total annual field yield with different collector areas

To enlarge the size of solar collector without limit is not a rational option, not only because of the high investment cost, but also can be explained by the collector yield, which decreases as the solar collector area is increasing. This is because, the amount of cold water to be heated by the solar radiation is becoming much more if the size of the collector is over designed and there would be a great heat loss from the collector to the environment.

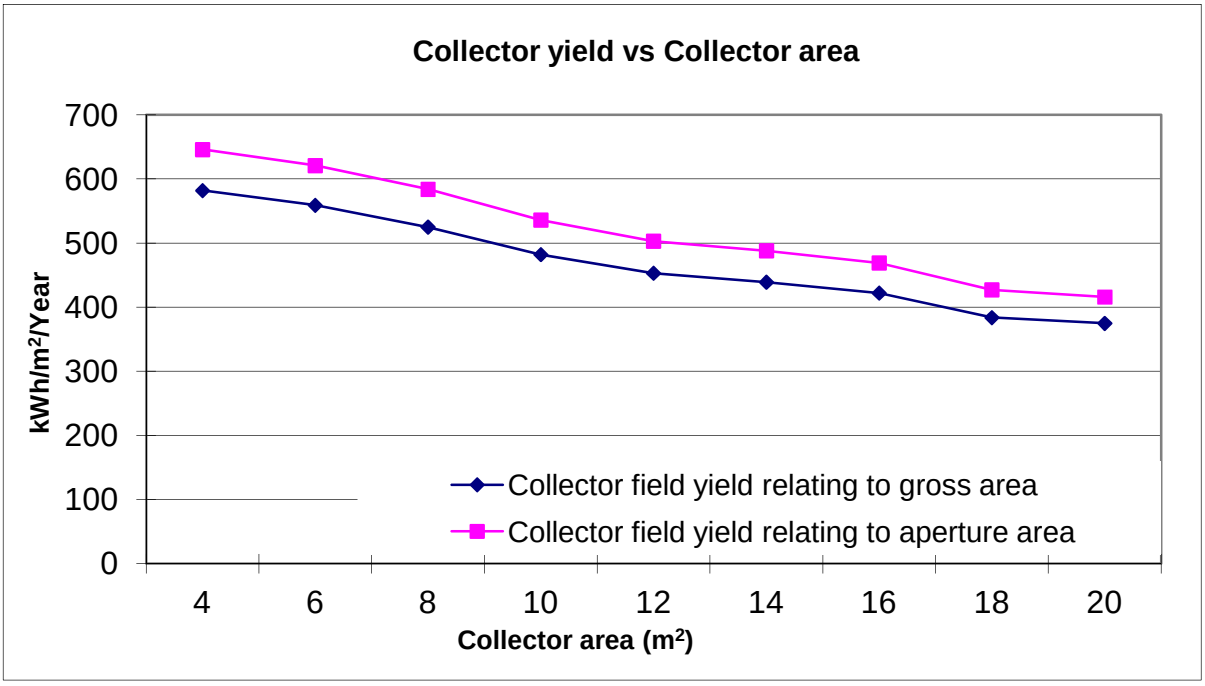

Figure 73Variation of collector yield with increasing collector area

4.4 Sensitivity analysis of solar cooling system

To change the solar collector area, and the combi master buffer storage tank volume, various configurations of solar heating and cooling system can be established, the through corresponding various simulations of the whole system, and the results of parameters such as solar fractions, the performance of solar system can be evaluated. This kind of sensitivity analysis can help to get an idea of pre-design or optimization for a solar heating and cooling installation.

4.4.1 Definition of a solar heating and cooling scheme

As the Polysun solar thermal simulation deals with domestic hot water, space heating and cooling together and there are only schemes for the combi design inside the software, so it is only possible to apply control strategies to make a solar system for cooling during summer season only. This section is for the sensitivity analysis of solar cooing system instead of the solar combi installation design.

To obtain relationship among solar collector area, storage tank volume and solar fraction of cooling, a scheme is needed to be defined. Since the system is also for DHW and space heating, there are control strategies for the analysis of solar cooling.

Most of the components are the same as those in the reference system defined above. The system category 71a: Hot water + space heating + space cooling + absorption chiller + solar thermal + dry recooler + boiler.

A flat-plate collector is chosen here for the small size solar cooling system. The principle is to choose different areas for the collector used and to choose different storage volumes firstly to define several cases of configuration, then, simulate each case to obtain SFcooling factor.

For the domestic hot water demand, the set temperature is 50 °C, with daily hot water demand 200l, while the annual demand is not known. If the temperature can reach to the set point or higher, the DHW demand is assumed to be satisfied.

For the building side, there are several specifications. The building is of Building-Catalog no.2, which is a single family house with low-energy consumption. The length and width are 15m and 10m respectively with only one floor. The annual demand of this building is not known, neither. The heating set point temperature is 20°C during the day.

The solar thermal collector is chosen from the Collector-Catalog no. 3, which is a good-quality flat-plate under European test standard. The tilt angle is 30° with the orientation of 0°S. This kind of solar thermal collector is assumed to create medium solar fraction with the initial collector absorber area of 9 m^2 consisted by 5 number of collectors.

Storage tank is of Storage tank-Catalog no. 578, which is an 800l combi master tank, because at the beginning of the design, due to the building demand, the tank volume is recommended to be 750l.

Gas boiler with internal pump is chosen for the auxiliary heating, which is of Boiler-Catalog no. 100, with the size of 5 kW.

The design cooling power of the absorption chiller (Absorption chiller-Catalog no.1) is 15 kW, and the design COP of the chiller is 0.71.

4.4.2 Control strategy

Different controllers are available in Polysun. There are solar loop controller, variable speed pump controller, mixing valve controller, heating circuit controller, temperature controller with AND/OR Operation, flow rate controller and irradiance controller.

Time controller

The ‘time function’ may be used for all controllers, i.e. the user will be able to define availability times in which the controller should be operating. This function enables to enter time, day and month in which the controller should be ‘active’ as required.

Figure 74Timer controller

Energy demand not covered

A number of controllers, such as temperature and flow rate, allow to set fixed and variable temperature settings. Sometimes after running a simulation, the energy demand will be shown as 'not covered'. This may happen if the temperature settings or flow rates defined within controllers and user profiles are not reached.

In all configurations, the energy demand is required to be covered. Hence, if the 'not covered' happens, it does not mean that Polysun is making wrong calculations or that the hydraulic system is not correctly working, but that the entered temperature levels or flow rates may not be reached.

Main control strategies

To make best use of the gas boiler auxiliary system, several parameters are set in the auxiliary heating controller 5.

Maximum tank temperature: 140 °C;

Sign of output: normal;

Logic relation temperature sensor 1 and 2: None;

Reference for temperature sensors 1: Fixed value;

Cut-in tank temperature 1: 80 °C;

Cut-off tank temperature 1: 100 °C.

As there is no option in Polysun the scheme for solar cooling during summer season only, it is necessary to apply proper control strategies to make this system for solar cooling only.

To get rid of the domestic hot water demand, the availability times of the mixing valve controller 1 (for DHW) is set to be none, which means the valve controlling the flow of domestic hot water is closed for sure.

Also, the same control stratagy is applied to the heating controller 2, with no available times.

For the pump controller in the solar loop, the availability times are during June, July and August only.

For the storage tank volume, when to change the volume from smaller size to larger one, in some level of volume, the type of tank is needed to be changed too, because for the combi

master tank (which is used as a default type in scheme 71a), there are only volumes of 800l and 1000l.

4.4.3 Simulations of cases

The figure below shows the main relationship among solar thermal collector area, storage tank volume, and the solar factor for cooling.

Each point in the figure is a configuration with demand satisfied.

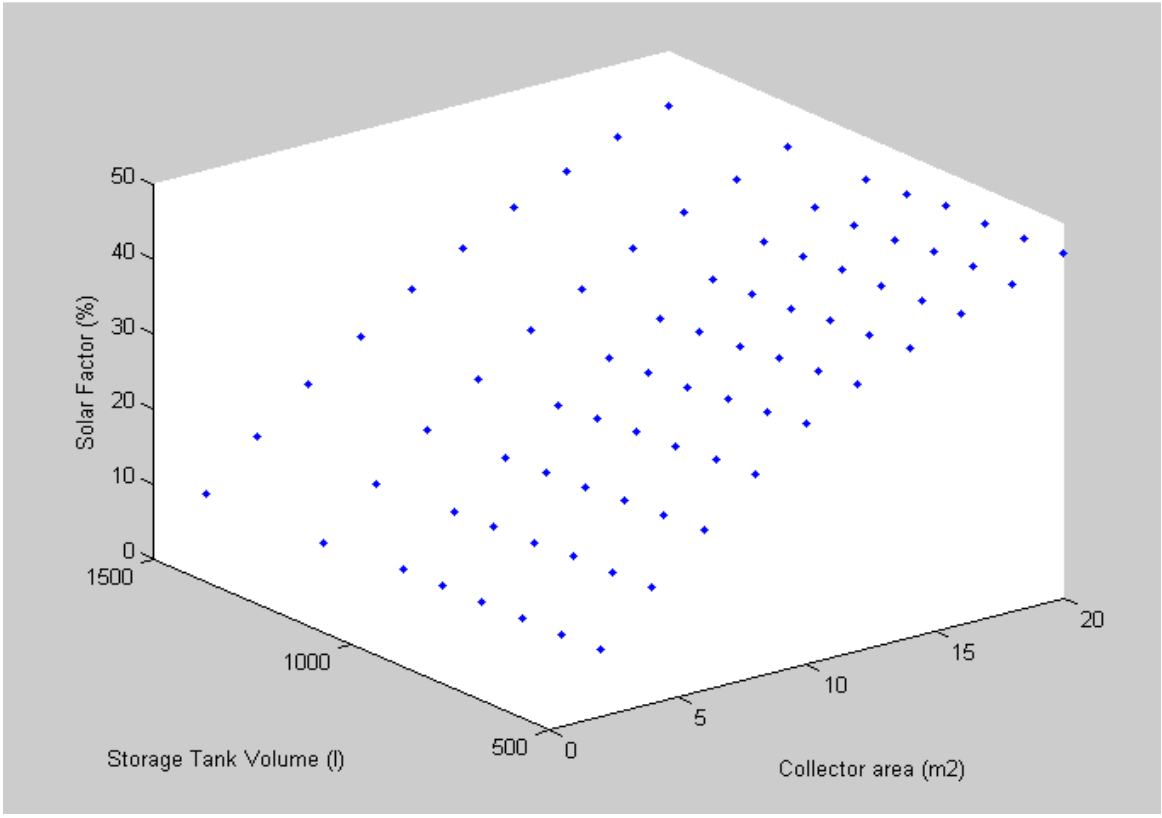

Figure 75Sensitivity analysis among collector area, tank volume and solar factor for cooling

For the result of simulations, it shows that the solar factor (SF) increases as solar collector area is larger, but its increasing ratio is decreasing. As for the storage tank volume, the solar factor for cooing (SF) decreases as volume size of storage tank is bigger after the demand side is satisfied.

CHAPTER 5 HELIOS-HP PROJECT

Helios-HP is a Piemonte regional project which started from 2010 and was planned to be part of this thesis. Since there were several hinders during the development of this project due to technical issues, this thesis will contain only the presently available results, such as planning of working phases and preliminary design of the test rig and the floor plans.

5.1 Introduction of the project

5.1.1 Background of Helios-HP project

Helios-HP (Heat Pumps), a regional project in Piemonte, Italy, which aims at solar heating and cooling, is an industrial research project with experimental development. The main partners are SGI (coordinator), DENER Department of Energetics (now DENERG – Energy Dept.) of Polito, Frigoriferi Bava, and Ecojoule.

SGI is a small consultancy company based in Torino.

Refrigerators BAVA, a brand from 1938, deals with design, production, installation and servicing of industrial thermal-fluid-dynamic plants studied and engineered to customer specification.

Ecojoule was founded in 2005 as a result of the selling of a branch of MG Eco Engineering, which has been on the market since 1999, offering design and consulting in green building, including renewable energy systems. The company is a leading company in the renewable energy sector, and it sells renewable energy systems and components for buildings on national level.

The Helios-HP project is addressed the design and engineering of two kinds of system plants which may have application in existing buildings or new construction.

A complete system with function of test bench will test two types of plants:

1) The first consists of solar thermal collectors with high performance coupled with a group of absorption refrigerators driven by heat from the solar thermal collectors. The goal is to develop a “solar kit” for the production of heat for domestic hot water and integrated space heating and solar cooling, which is intended to be replicated and placed on the market.
2) Additional product will be a direct expansion compression heat pump, in which the evaporator consists of a solar collector made of plastic. Also this system will be implemented through the test bench, following the development of another kit.

All the components and systems studied in this project should be suitable for the use in low-energy houses and are characterized by a high efficiency of energy transformation and based on the use of solar energy.

5.1.2 Activities of industrial research and experimental development

The activities that are carried out during the project can be summarized in:

1) Scouting: extended research of innovative technologies for the solar climate control currently employed on the world market. Identification of types of components suitable for dual purpose design and retrieving performance data.
2) Modeling and simulation: evaluation of performance and outcomes expected by different technological solutions through models of calculus developed at hoc. Optimizing design of the various components
3) Design: detail design of equipment, systems and components, for the mechanical parts, electrical, computer, inherent in the construction of demonstrators and test bench systems. Construction: manufacture and Assembly of components
4) Monitoring: data acquisition systems demonstrators. Exam results: comparison with theoretical simulations, critical analysis time the improvement of systems made, optimization systems.
5) Collection and production results of labor and intellectual property protection (patents, etc.)
6) Organization and operational coordination

5.2 Research and experimental working phases

5.2.1 Scouting and technical feasibility

Find detailed information in the literature and in the institutions, bodies, Institutions and companies actively engaged in applied research and in production of solar air conditioning and refrigeration and integrated solar assisted heat pumps. This working phase is considered the preparatory phase for the subsequent activities. The research is aimed at the acquisition information theoretic and scientific and technical-commercial, and in particular the operating data necessary for the realization of dynamic simulations. The investigation will focus on a bounty of powers around the 5kWf, suitable for residential use.

a. Research of techniques for the production of cold/heat from drying at low temperatures. There will be suspects both prototypes exist, both the machines currently already marketed and produced a documentary on full collection systems: adsorption and absorption, using ammonia and cycles Lithium bromide, etc; adsorbent of silica gel and zeolite, etc. There will

be investigated the primary fluid and/or employees be employable for the thermodynamic cycle, both as a heat transfer fluid in the final use (water plants, for air). The possibility of integration with the most popular plants in the field industrial and residential will be evaluated. Dimensions, integrations Engineering, purchasing and maintenance costs will be studied. The techniques disposal and/or recovery of heat from the condenser will be evaluated in order to define a component as possible efficient and silent, for use in residential area. In particular the subject of discussion is the size < 5 kWf. (DENER; SGI)

b. Similar theoretical and application technique investigation will be carried out as for heat pumps, solar-assisted, meaning this name both the heat pump evaporator with direct expansion outside, both heat pumps coupled in parallel with collection systems solar, through a heat accumulator, dedicated to the production of heat. Of such systems will be studied the feasibility of a reversible system for the production of heat and cold. (DENER; SGI)

c. Particularly in relation to the point b will be investigated the possibility of using CO_2 as a refrigerating fluid in direct expansion system. In particular will be highlighted and suspects the thermodynamic and mechanical problems related to operating pressure. (DENER; SGI)

d. Examples of installations will be sought both prototypes (described in the literature and implemented at universities or research institutions, e.g. a plant absorption at the Politecnico, DENER) is functional. (DENER; SGI)

e. Information collected in support of a campaign to capture data from existing installations, in particular a small solar cooling plant in the service of an office building, powered solely by solar power and if possible an installation of solar cooling in parallel to a boiler plant (e.g. COMO). (DENER; SGI)

f. The potential applications of systems described above will be evaluated, both in the construction sector, both in industry and in transport. In fact we think of solar cooling systems can be inserted both in new buildings and retrofit installations serving residential and commercial users. (DENER; SGI, EJ, BAVA)

g. A survey of potential market and a regional mapping of potential users should be the tool for the assessment of economic impacts (for companies engaged) and environmental (population) of the massive application of these technologies. (DENER; SGI)

h. There will be relations of cooperation and exchange of information through participation in conferences and seminars, but especially from companies and institutions already engaged in this area of the market, especially there is a plan to participate in the work of the " International task Energy Agency Solar Heating and Refrigeration "and" Polymeric materials for solar applications ". (DENER; SGI, EJ, BAVA)

The principal players involved: POLITO and SGI. And there are also other two partners involved: ECOJOULE and BAVA. The expected output is a review of the science and technology system architectures from which flows a shortlist that will be applied mathematical simulation models.

5.2.2 Model development for simulation and optimization

Based on the results of Scouting and technical feasibility, and with the aim of determining the plants to accomplish in design and construction of installations, DENER will develop, in close relationship with industrial partners and leader SGI (which ensures dialogue and harmonization between the scientific approach and the application of different subjects), some mathematic models for the simulation of the operation of individual components (e.g., collectors) integrated into system with numeric codes and not main stream with flexibility to fit experimental developments that will be gotten from the step of monitoring, comparison and evaluation of operational performance, namely, pre-commercial analysis (e.g. Matlab, Simulink, TRNSYS).

In particular, the simulations provide information necessary to design realization of solar collectors optimized for both systems are the subject of the project.

Simulations will aim to identify the best technology choices from the energy point of view, but the final choice for systems to be built will be based on technical feasibility, availability of materials, the cost of construction and maintenance. The development of simulation models allows saving time and money by reducing prototyping materials only two systems most promising results.

Simulations will then validate based on data collected from the exercise equipment made and used in support of the optimization process (especially the part of adjustment and control system).

5.2.3 Design and construction of installations

a. Solar cooling plant

Based on the results of the simulations conducted in model development step, There will be designed a executive level and detailed in all its components, and built a solar plant cooling system complete collection, solar heat storage, group refrigerator powered by heat produced by solar, cold storage, group for heat dissipation, regulating system, monitoring system performance. The plant will have a cooling capacity of approximately 5 kWf, and will powered by an area of about 20 m2 of collectors. It is intended to identify a situation plant representative of a classical audience for test operation continuous, like a real application. The system architecture will be developed in order to test different system solutions: with and

without the use of pond, direct from the fridge, solar collectors with power to the fridge accumulation, with integration from both pellet generators, either through direct the accumulation. At least two systems of heat dissipation from the capacitor will be tested: via convection and evaporation Tower.

Ecojoule develops a solar collector specifically designed to feed a cycle absorption refrigerator (for machines already on the market), preserving high efficiency conversion of solar radiation into heat. It is intended to investigate the technical feasibility of realizing a large manifold double size transparent and partially cover material recyclable. Possess the know-how to build a solar panel, if such realized cost competitive, it would be a good card for development use solar energy for heating purposes is energy-efficient buildings, both in redevelopment of existing buildings. Burr is also affected refrigerators to refrigerating unit to develop a absorption with implant-compatible. The solutions adopted are derived from scouting and model devolopment, which will determine the choice between systems with absorption or adsorption, fluids heat transfer water or air.

The main subjects in working phases are: Ecojoule (buy the components, accomplished the collector, is responsible for developing the control software and SGI (designs) the overall system and the part that simulates the user) with the advice of Refrigerators Burr for the part relating to absorption refrigerating and realization implantation and DENER regards the monitoring system and data acquisition.

b: Prototype of solar-assisted PdC

Another technological solution to accomplish is a heat pump expansion conducted, in which the evaporator consists of a solar collector. The solution proposed integrates an optimal exploitation of solar radiation is directed both widespread uptake system that can be placed on the roof or facade, with the operation of a heat pump for the production of heat for heating of environments. The obstacles to be overcome from a technological point of view regarding the choice of refrigerant gases (and in particular gas natural is favorable, for example, the CO_2), for example, the development of the evaporator, regulator and control of the flow rate and temperature of the cycle, the optimization of operation in the presence of variable and transient loads of sudden solar side and the summer operation.

There will be investigated the technical and economic feasibility for implementation in large series of a solar collector in plastic (possibly uploaded to other materials), incorporated as an element of group system heat pump for solar-assisted direct expansion.

This system will be installed at the test bench, in parallel to the solar system cooling and it is possible to create for user to simulate different conditions of operation.

Players involved: SGI (designing the plant) BAVA (building the facility)-DENER (supervision and specialist advice).

5.2.4 Operational performance monitoring, comparison and evaluation of results, setting up systems (Pre-commercial analysis)

The first part will be devoted to the task of harmonization components, development of management software of complete systems, on the basis of the data resulting from the examination of performance and operational parameters during exercise.

An analysis to verify the cost and feasibility of commercialization of products developed to be carried out, having at this point of data availability functioning in conditions of full systems development. Will also be considered data about market expectations (not just regional) investigated during the Scouting.

5.2.5 Collection and production results of labor and property protection

It is probable and desirable that the prototypes designed to be then placed in production and price lists of DROOL and EJ, as both components are integrated into a pre-engineering system and (possibly) as individual components, also for other applications (such as high-performance solar collectors can also be used for heating or absorption refrigerator group of small size can find application in the field automotive, etc). It considers that such options should be considered, both for increase the level of excellence of the undertakings and of the region in the field of technique, both to provide additional sales markets to industrial products covered by the studio.

The progress and achievement of objectives will be monitored through the production of ongoing reports. At the end of the work will produce a synthesis document of the scouting stage technologies and reporting of data collected on other people's systems and examined on operation of systems and components built.

5.3 Design of test bench

5.3.1 Air-conditioning systems laboratory, helium-assisted functions

The laboratory is designed as a test bench for refrigeration with absorption/adsorption powered by solar thermal heat pumps and solar assisted.

There are 4 main circuits:

- Solar thermal circuit
- Heat supply circuit
- User load circuit
- Dissipation circuit

The whole installation is planned to be in Politecnico di Torino.

For the main components and their dimensions are preliminarily designed.

Solar thermal collector has a radiation capturing surface of 20 m^2, which is provided on two parallel rows of modules, each of about (10x2) m, placed on easels ballast, with variable inclination.

A group of steam compression refrigeration, air cooled, nominal cooling capacity yield 37kW, will be placed on the terrace, in the vicinity of hoardings.

Three storage tanks are needed, all located in the workshop of the 2° floor, and the volumes of these tanks are:

- Solar tank 750 l (850 kg)
- Chilled water storage 500 l (560 kg)
- Hot water storage tank 500 l (560 kg)

To solve the problem of lift of the floor will be positioned on the axis of the beam between the pillar and mainstay and/or appropriate allocation structures, according to the indications of the technical department. The facility is designed to test the operation of heat pumps, absorption/adsorption of size 3-9 kW refrigerators. A typical machine dimensions and weight are: (1.3 * 0.8) m * 1.7 m (height); the weight < 400 kg. Weight distribution structures will be used, according to the indications of the technical department.

The circuits are made with insulated pipes arranged or on the terrace with suitable substrates that allow thermal expansion, or in the lab clamped a pillar during the descent and floor or suspended on support structures. The lab requires a PC and a connection to the network.

All the Spaces needed are: for the terrace, approximately 30 m^2 for positioning the solar collector with related links, and a group of dissipation fridge; while for the lab, an area of 55 m^2 in floor 2 of laboratories for all other components is needed.

Major electric utilities are:

- Electric heater of integration in the solar tank (approx. 10kW)
- Electric heater for heat load simulation (approx. 10kW)
- Compression refrigerating circuit for electrical dissipation positioned on the roof (about 16kW)
- Heat pump test solar-assisted (about 5kW)
- Absorption chiller in test (< 200W)
- Pumping test circuits (3kW)
- Power control systems

5.3.2 All norms consulted for the project

During the pre-design stage, it is important to know all the available standards relating to solar cooling system. Here are the norms which were consulted during this process.

UNI 8477-1:1983 Energia solare. Calcolo degli apporti per applicazioni in edilizia. Valutazione dell' energia raggiante ricevuta.

UNI 8477-2:1985 Energia solare. Calcolo degli apporti per applicazioni in edilizia. Valutazione degli apporti ottenibili mediante sistemi attivi o passivi.

UNI EN 12975-1:2006 Impianti termici solari e loro componenti - Collettori solari - Requisiti generali.

Thermal solar systems and components - Solar collectors - Part 1: General requirements

UNI EN 12975-2:2006 Impianti solari termici e loro componenti - Collettori solari - Parte 2: Metodi di prova.

Thermal solar systems and components - Solar collectors - Part 2: Test methods.

UNI CEN/TS 12977-2:2010 Impianti solari termici e loro componenti - Impianti assemblati su specifica - Parte 2: Metodi di prova per collettori solari ad acqua e sistemi combinati.

Thermal solar systems and components - Custom built systems - Part 2: Test methods for solar water heaters and combi-systems.

UNI CEN/TS 12977-4:2010 Impianti solari termici e loro componenti - Impianti assemblati su specifica - Parte 4: Metodi di prova per le prestazioni di accumuli solari combinati.

Thermal solar systems and components - Custom built systems - Part 4: Performance test methods for solar combistores.

UNI CEN/TS 12977-5:2010 Impianti solari termici e loro componenti - Impianti assemblati su specifica - Parte 5: Metodi di prova per le prestazioni dei sistemi di regolazione.

Thermal solar systems and components - Custom built systems - Part 5: Performance test methods for control equipment.

5.3.3 Design of the test bench

The design of this solar cooling system is shown as follows.

The whole system includes the solar thermal collector circuit, the chilled water circuit and the hot water circuit and the heat rejection.

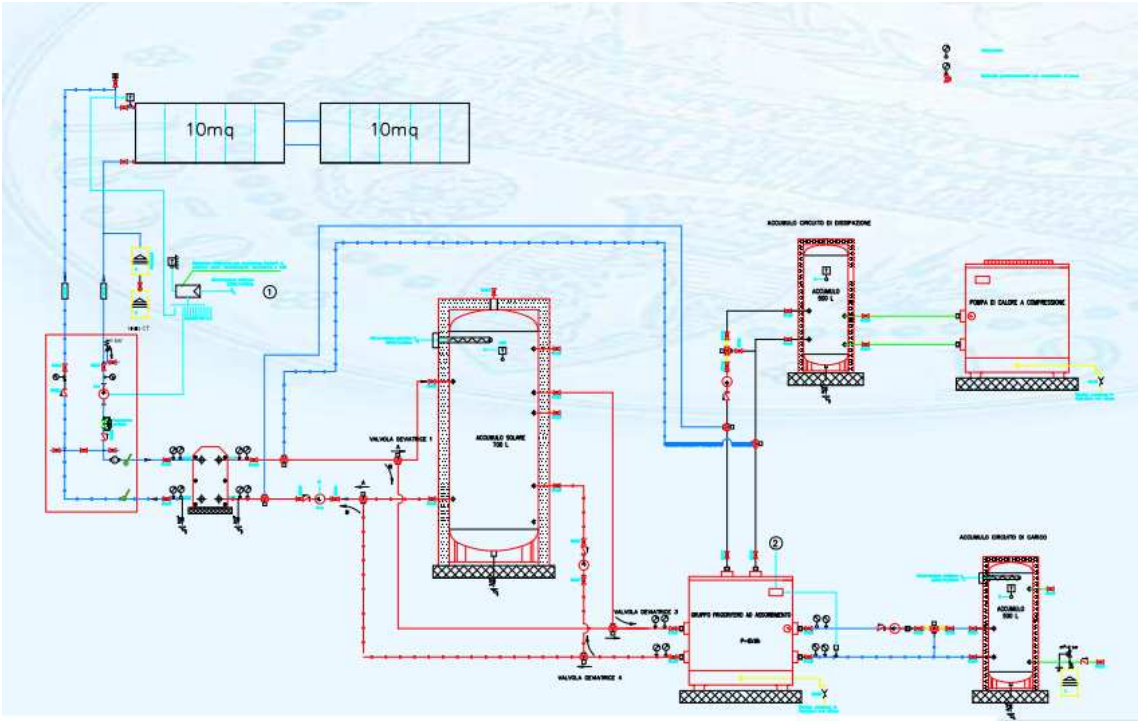

Figure 76Test bench design of Helios-HP project

5.4 Floor plans

The components of this solar cooling system are arranged in part on the flat roof of laboratories (solar thermal collector and refrigerator for dissipation circuit) and part 2° floor in Energy Department in Politecnico di Torino. And the following are the preliminary floor plans for this installation.

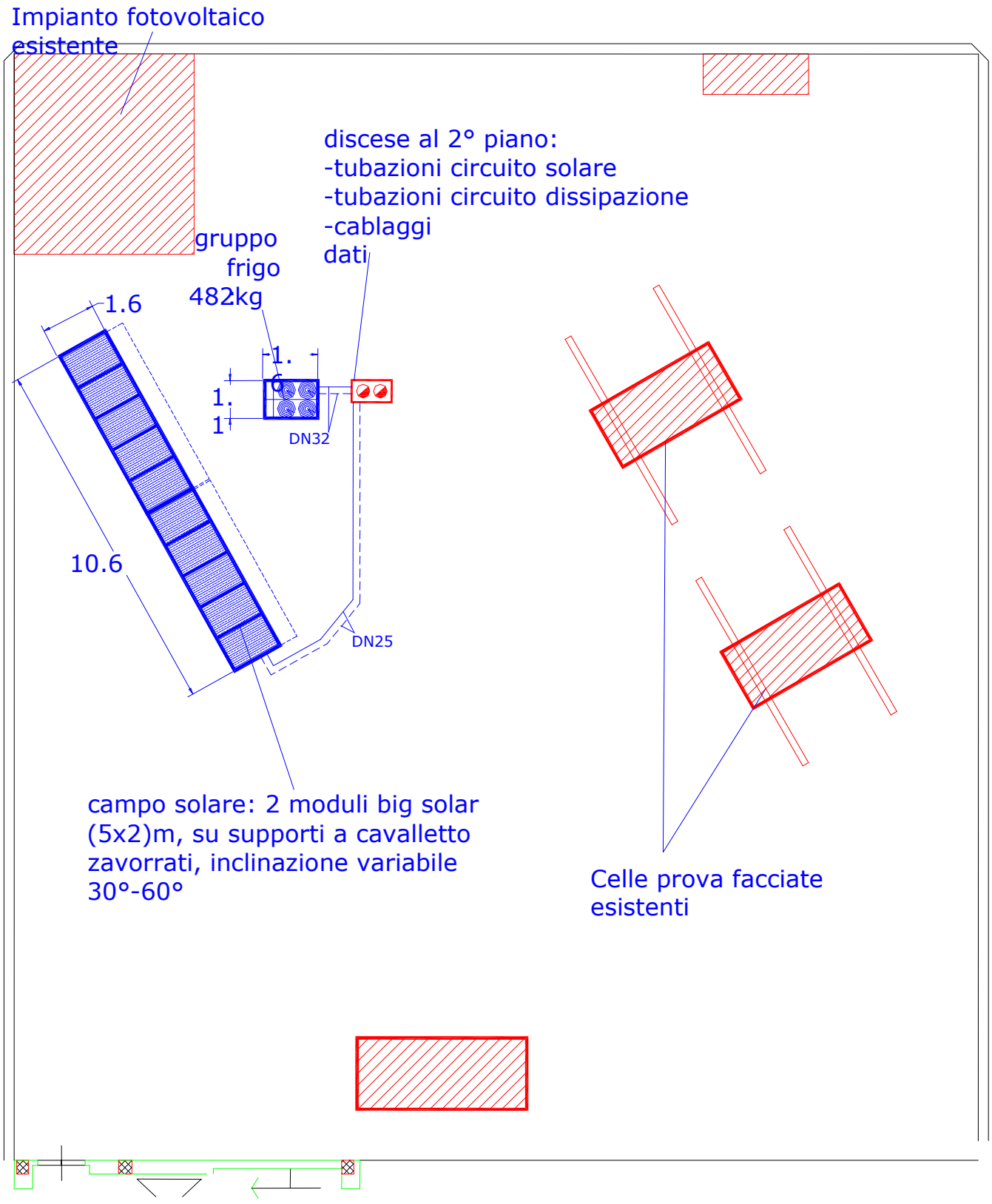

Figure 77Floorplans of solar thermal collector in Helios-HP

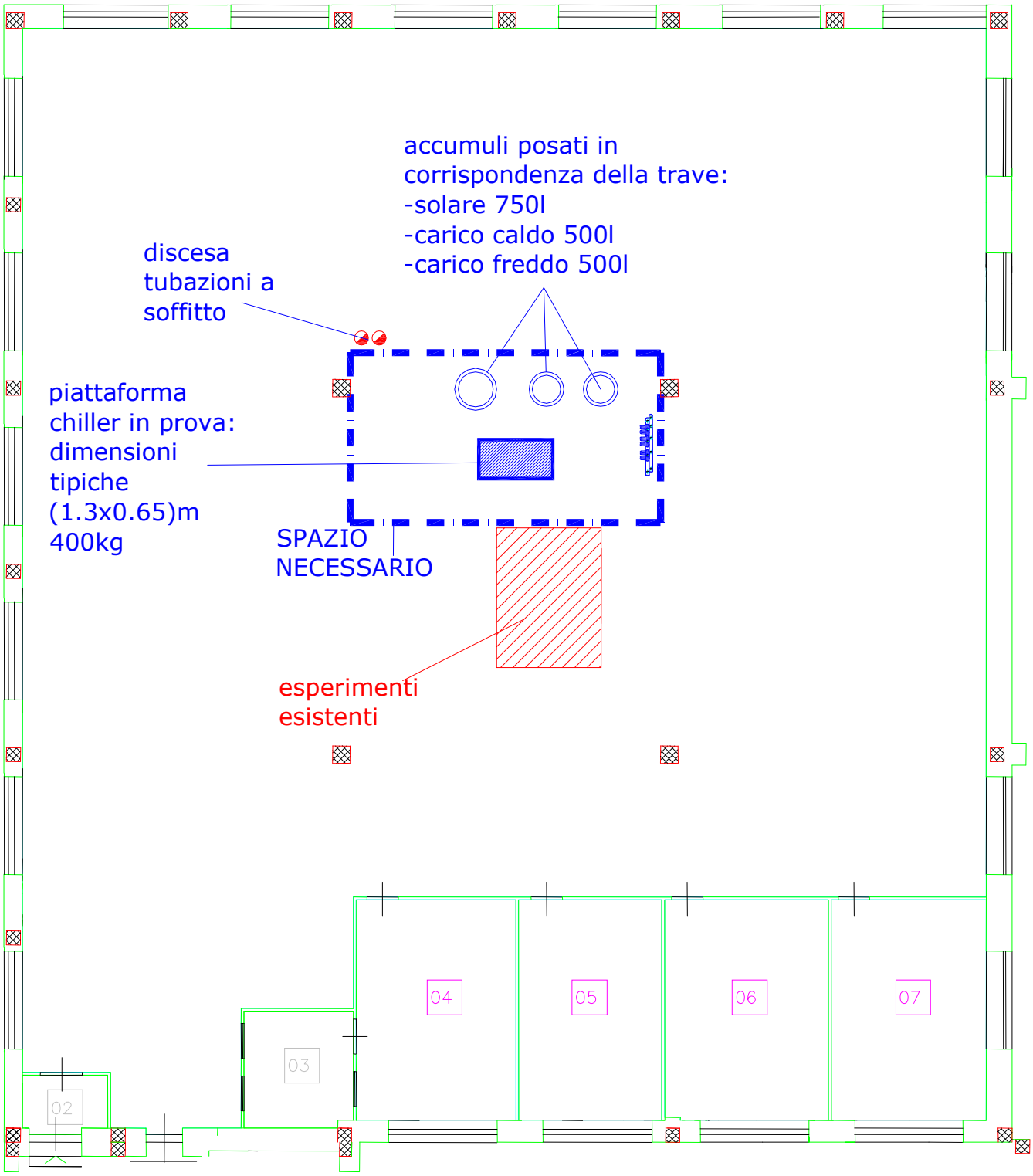

Figure 78Floorplans of sorption chiller and tanks in Helios-HP

CHAPTER 6 IPLA SOLAR COOLING SYSTEM CASE[1]

Solar cooling for small size buildings represents a very interesting trend, while it is still under developed and there are a wide range of uncertainties both on the technological and economical sides. Only a small number of plants have been actually installed and measured so far. Actually, the use of solar thermal collectors for cooling purposes – coupled with winter ambient heating, would widen their application beyond traditional domestic hot water systems.

The small size ready-to-market absorption or adsorption chillers are significantly more expensive than the technically mature compression ones, also the solar thermal collectors are costly, thus, the solar cooling system combining solar collector with sorption chiller turns out unaffordable for a small size project, and the solar cooling system itself requires a thorough design stage to be optimized properly.

A monitoring campaign has been carried on in a new building PUEEL (*Prototipo Uffici ad Elevata Efficienza in Legno*, High Efficiency Wooden Office Prototype) in IPLA in Torino, Italy.

6.1 PUEEL building with solar cooling system in IPLA

The building has a wooden highly insulated envelope, controlled mechanical ventilation with thermodynamic heat recovery, radiant heating/cooling. A solar thermal collector field (upper solar collector in the figure below) is integrated on the building roof used both for the building heating and cooling demand. The adsorption chiller in the solar cooling system has a cooling capacity of 9 kW. There are also photovoltaic collectors on the lower part of the building roof slope.

[1] The following material has been collected during my stay at Politecnico, although I was only partially involved in this research activity, thanks to the availability of Prof. Fracastoro, and the other persons involved in Helios-HP project.

Figure 79Solar thermal collectors and PV collectors on the roof of PUEEL building

The solar cooling system of PUEEL building at IPLA institute in Turin, Italy, is the first of this kind in the nearly 1-million-inhabitant city, and one of the few cases of entire Italy.

The solar collector circuit and the dry recooler are shown in the figures below.

Figure 80Solar collector circuit in PUEEL

Figure 81Dry recooler in PUEEL

6.2 Monitoring of solar cooling system in PUEEL

6.2.1 Scheme of the plant

The PUEEL building solar cooling system is based on a simple scheme. The 28 m^2 solar collector field supplies heat to a 4 m^3 water storage tank. The storage tank is fitted with a thermostatically controlled auxiliary heat source (electrical resistance). A 9 kW peak power chiller, based on an adsorption cycle with zeolite, is driven by the heat flow coming from the hot water storage tank and refrigerates the building by mean of a radiant panel cooling system. A chilled water storage tank with volume of 0.5 m^3 is installed in the cooling circuit. Heat rejection from the chiller is based on a fan driven dry recooler.

During the design stage, an adsorption chiller with a low nominal driven temperature value (70°C) has been selected and coupled with water-glycol double-glazed solar collectors. Due to budget reasons, during the construction phase this type of collector has been replaced with single glazed one.

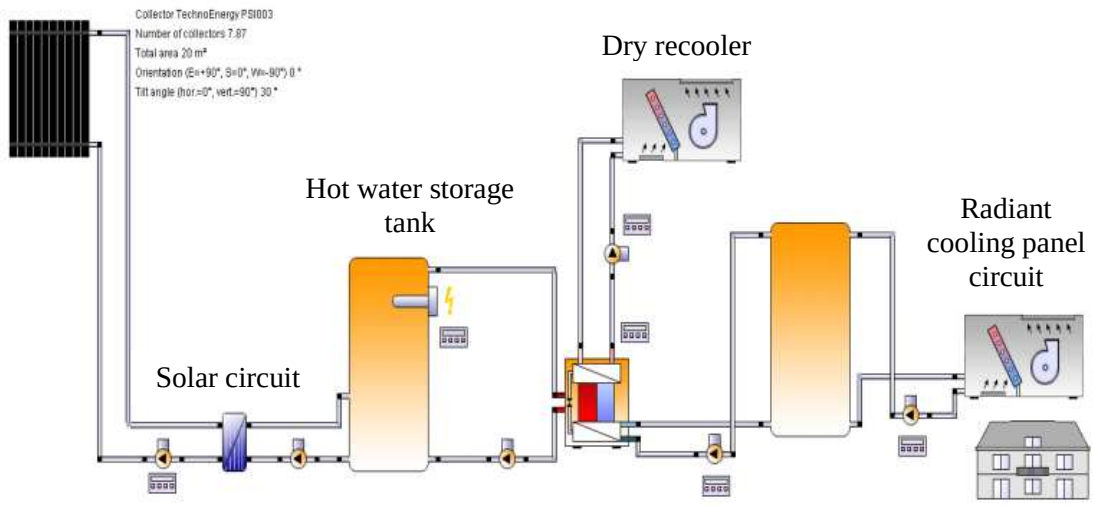

Figure 82Scheme of the solar cooling system in PUEEL building

6.2.2 Parameters monitored

For the performance evaluation of the solar cooling system in PUEEL, several meteorological parameters are monitored with hourly samples, such as the solar global horizontal irradiance, the outdoor air temperature, humidity, wind speed and direction.

As for the solar cooling installation itself, there are several related parameters for evaluation were monitored, shown in the table below.

Table 14Parameters monitored in the solar cooling system in PUEEL building

Circuit	***Variable***	***Unit***	***Precision***
Solar collector circuit	Water return temperature	[°C]	±0.5
	Water supply temperature	[°C]	±0.5
	Flow rate	[m^3/h]	±0.01
Hot water storage tank	Water return temperature	[°C]	±0.5
	Water supply temperature	[°C]	±0.5
	Flow rate	[m^3/h]	±0.01
Radiant cooling panels	Water return temperature	[°C]	±0.5
	Water supply temperature	[°C]	±0.5
	Flow rate	[m^3/h]	±0.01
Dry recooler heat rejection	Water return temperature	[°C]	±0.5
	Water supply temperature	[°C]	±0.5
	Flow rate	[m^3/h]	±0.01

6.3 Performance evaluation of the solar cooling system

6.3.1 Global efficiency of solar cooling system

During the monitoring time the auxiliary electrical heater was set off, all thermal power coming from solar energy.

The global efficiency of the solar cooling system COP_{sol} and the efficiency of the adsorption chiller COP_{ch} (L. Schnabel 2010) are two main indicators for evaluating the performance of this solar cooling system.

The global efficiency of the solar cooling system, COP_{sol}, is defined as:

$$COP_{sol} = \frac{Q_C}{G \times A}$$

Where

Q_C is the cooling energy produced, kWh,

G is solar global irradiance on the collector plane, kWh/m^2,

A is the net aperture area of collector field, m^2.

The efficiency of the adsorption chiller COP_{ch} is defined as:

$$COP_{ch} = \frac{Q_C}{Q_{th}}$$

Where

Q_{th} is the thermal energy from the hot water storage tank to the adsorption chiller, kWh (F.Agyenim 2010).

COP_{sol} and COP_{ch} have been derived from daily monitored parameters and shown in the figure as follows.

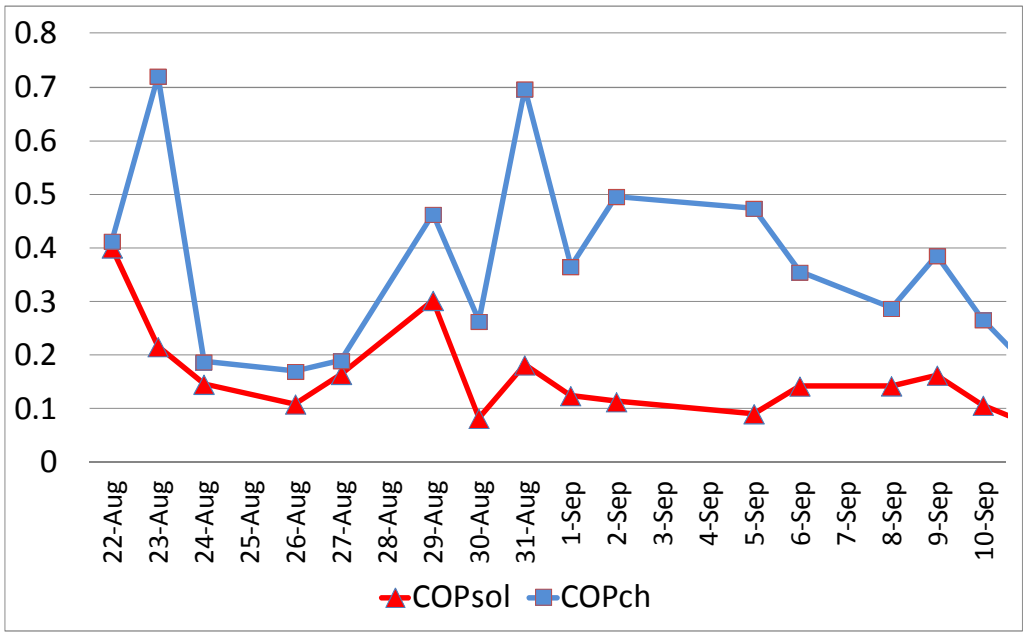

Figure 83Daily COPsol and COPch of solar cooling system in PUEEL during August 21 and September 23, 2011

The COP_{ch} presents a wide spread of values, from 0.1 to 0.7, while COP_{sol} is within a range of 0.1-0.4, with an average value of nearly 0.14.

In terms of power profile, the day of August 26, for example, is shown in figure below.

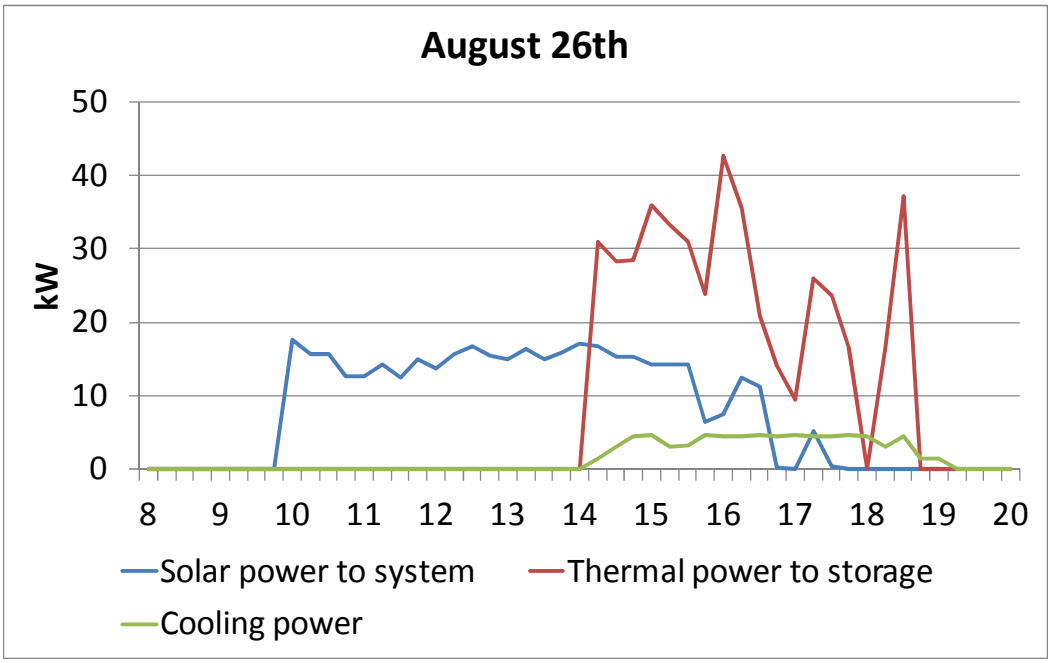

Figure 84Hourly measured thermal power in PUEEL on August 26, 2011

The figure above shows how the hot water storage tank was charged from 10 to 14 during the day 26 August 2011, while it was used as heat source during the afternoon. Its sizing should take into account the eventual shift of thermal power from peak solar radiation to peak cooling demand times.

The thermally driven temperature and the chilled water temperature were also monitored, which are shown in the figure below.

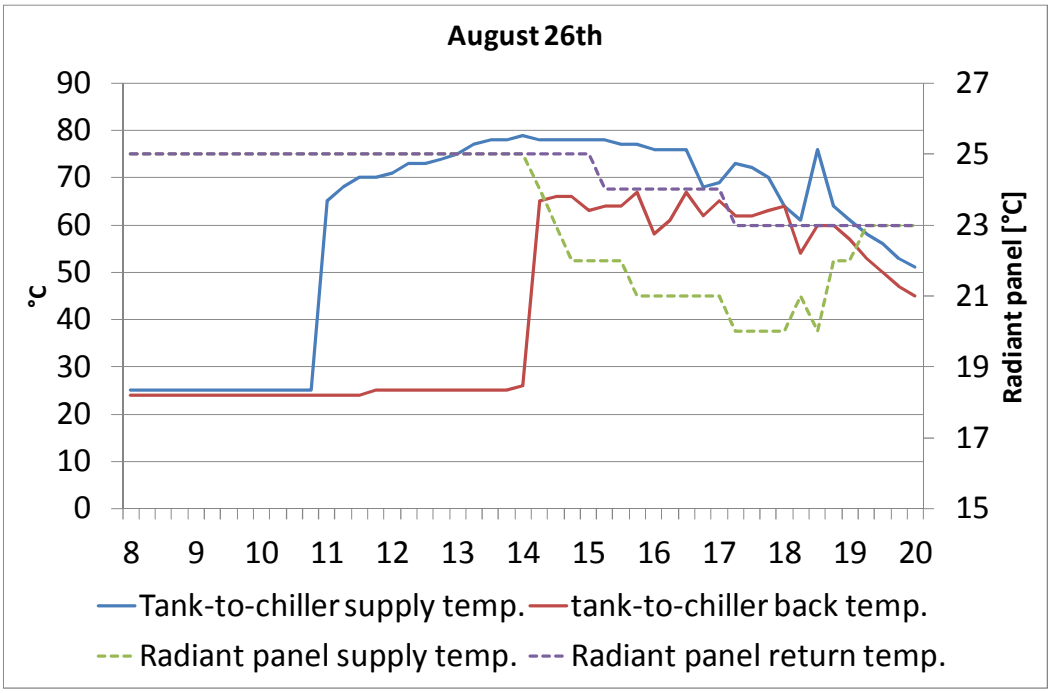

Figure 85Hourly measured temperature in driving hot water circuit and radiant panel cooling circuit (both at constant flow rate) on August 26, 2011

This figure above reports typical range of operability of the system, in term of temperatures on the two sides of the chiller, tank to chiller circuit, and radiant cooling panels circuit. The inlet temperature to the chiller, coming from the storage, is around 80°C, while its nominal value is 70 °C. During the evening, when solar power lowers down, the temperature of the storage decreases too, and this will lead to a lower COP_{ch}value than nominal one.

The daily solar energy collected and heat to the chiller is illustrated in Figure below. The difference between these data includes both tank losses and tank internal energy variations. In the long term they account only for tank losses.

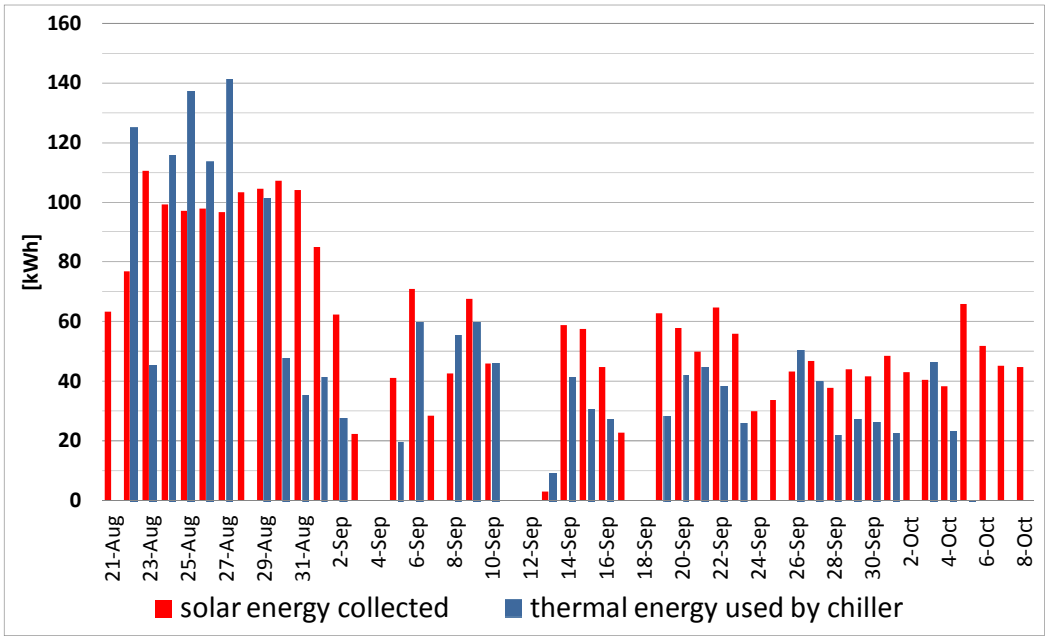

Figure 86Energy balance of the system: solar energy collected compared to heat used by the chiller

The following figure reports the net daily balance between solar energy collected and heat to the chiller and its cumulated value, compared to the cumulated daily cooling energy of the system.

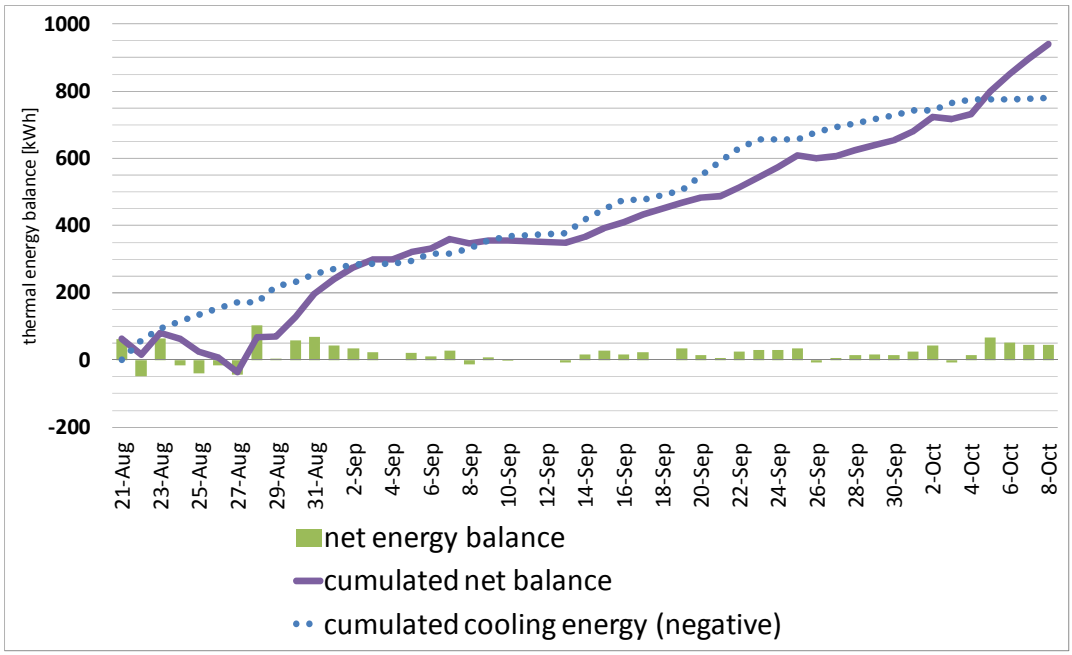

Figure 87Energy balance of the system: daily balance, cumulate curve of daily balance compared to cumulated cooling energy (to be considered with negative sign)

The overall tank losses equal the cooling energy, thus indicating an over sizing of the solar collector circuit.

The figure above also suggests that the system efficiency is significantly low, since tank losses are of the same order of magnitude of the building cooling energy.

Assuming that (as far as the auxiliary heater is off):

$$COP_{sol} = \eta_{BOS} \times \eta_{coll} \times COP_{ch}$$

Where η_{BOS} is the balance of system efficiency, it is possible to calculate this efficiency, which takes into account overall thermal losses of the system, excluding the solar circuit.

To do so, it is necessary to evaluate the efficiency of solar collectors. The measured mean value of η_{coll} (solar collector efficiency) is 0.45, while the value calculated from catalogue performance data, using as input the x-parameter calculated through the measured water temperature and weather data, is 0.52.

Figure below shows the 19 days of daily averaged measured η_{coll} values compared to expected ones.

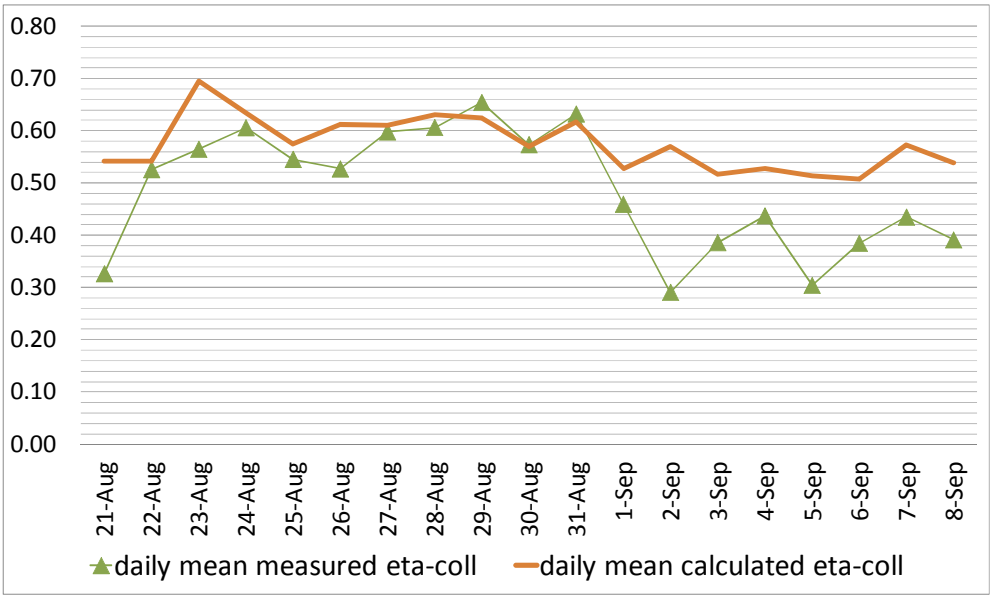

Figure 88Daily mean solar collector efficiency of central hours of the days 21 August - 8 September

Considering these values, the mean efficiency of the system η_{syst} is 0.82, meaning that almost 20% of the collected solar energy is lost.

6.4 Comments on monitored results

The monitoring campaign has helped to evaluate the performance of the solar cooling system in PUEEL, and there are some key points to mention.

The thermal storage plays a very important role and its design size should consider the expected shift of solar irradiation and cooling demand profiles.

The averaged daily values of COP_{ch} present a wide spread, likely due to a too low sampling frequency of the monitoring system. Mean values are, nonetheless, on the same order of the credited official values. Adsorption chiller presents unsteady performance, for its own nature of intermittent cyclic system. The assessment of the chiller instantaneous performance needs a sampling time-step lower than one minute.

The solar thermal system efficiency presents some discrepancies with catalogue values, but average values are only slightly lower than expected ones.

The averaged daily values of COP_{sol} is about 0.14. This value, considering the mean values of COP_{ch} and of η_{coll}, is due to an unexpected low value of BOS efficiency. A significant part of the collected solar energy is lost. This can suggest an oversizing of the solar collector system related to the cooling demand in the monitored period.

In a word, this three-week monitoring campaign has shown a satisfactory performance of this solar cooling system in PUEEL, although the solar installation appears oversized.

CHAPTER 7 CONCLUSIONS AND OUTLOOK

7.1 Clear-sky Models of solar irradiance in Torino

From the comparison between measured solar beam normal irradiance and solar global horizontal irradiance, the results shown that the ASHRAE clear-sky model mostly fits the solar beam normal irradiance while the experimental C and C' values are in the average well above the C predicted by the ASHRAE model.

The most interesting finding is however that a daily regular oscillation of experimental C values, symmetrical to noon time, occurs, with very high values at the extremities of the day and at noon. These findings may be explained by the limits of the isotropy assumption implicit in the ASHRAE model: as the sun rises, circumsolar sky radiation increases in altitude, and therefore its vertical component tends to become more relevant. On the other hand, for very low altitude angles the vertical component of G_{bn} in equation $G_{dh} = G_{th} - G_{bn}cos\theta_z$ tends to decrease faster than G_{dh}, producing an asymptotical increase of C ratio up to an infinite value for θ_z = 90°. The regular symmetrical trend is visible in all clear sky days, and further sets of data could lead to a new "clear sky diffuse irradiance" model.

7.2 Atmospheric turbidity factors in 2010 in Torino and comparison with that during 1975-1976

Turbidity measurements carried out 35 years ago showed a strong seasonal variation, with higher values during the heating season. Torino turbidity values used to be two Rayleigh atmospheres above those of the reference station (Pino Torinese) during winter time, while they are just a few percentage points above the reference in the late spring and summer.

The new measurements performed during 2010 have shown values comparable to those of 1975-76, but without an apparent seasonal variation: the optical quality of the atmosphere seems to have improved in the winter time due to usage of cleaner fuels and district heating, and remained the same during the rest of the year.

7.3 Sensitivity analyses of solar cooling with Polysun

The sensitivity analyses are based on the solar cooling system category 71a in Polysun, namely, space heating and cooling system with absorption chiller. Through control strategies, the solar system only works for space cooling during summer, in June, July and August.

The principle is to choose different areas for the collector used and to choose different storage volumes firstly to define several cases of configuration, then, simulate each case to obtain SFcooling factor.

After various change of the collector area and hot water storage tank volume, the result of simulations shows that the solar factor (SF) increases as solar collector area is larger, but its increasing ratio is decreasing, as expected. As for the storage tank volume, the solar factor for cooing (SF) decreases as volume size of storage tank is bigger after the demand side is satisfied.

7.4 Field data monitoring of solar cooling system in IPLA

The monitoring campaign has helped to evaluate the performance of the solar cooling system in PUEEL.

The thermal storage plays a very important role and its design size should consider the expected shift of solar irradiation and cooling demand profiles.

The averaged daily values of COP_{ch} present a wide spread, likely due to a too low sampling frequency of the monitoring system. Mean values are, nonetheless, on the same order of the credited official values. Adsorption chiller presents unsteady performance, for its own nature of intermittent cyclic system. The assessment of the chiller instantaneous performance needs a sampling time-step lower than one minute.

The solar thermal system efficiency presents some discrepancies with catalogue values, but average values are only slightly lower than expected ones.

The averaged daily values of $\mathrm{COP_{sol}}$ can suggest an oversizing of the solar collector system related to the cooling demand in the monitored period.

In a word, this three-week monitoring campaign has shown a rather satisfactory performance of this solar cooling system in PUEEL, and a continuous monitoring in future for better working of the solar system is recommended.

BIBLIOGRAPHY

http://rredc.nrel.gov/solar/spectra/am0/.
http://www.humanethology.org.uk/c-chart.html.
http://calgary.rasc.ca/howfast.htm.
www.eyesolarlux.com/Solar-simulation-energy.htm .
A.Louche, et al. "An analysis of linke turbidity factor."
al, Barry A. Bodhaine et. "On Rayleigh Optical Depth Calculations." *Journal of atmospheric and oceanic technology*, 1999: 1854-1861.
al, Tom Stoffel et. "Improving the accuracy of low cost measurement of direct normal solar irradiance."
Atmosphere. http://en.wikipedia.org/wiki/Atmosphere.
Bason, Frank. "Diffuse solar irradiance and atmospheric turbidity." *SolData instruments.*
"Chapter 27 Fenestration." In *ASHRAE, Handbook of Fundamentals*. New York: ASHRAE, 1985.
Comune di Torino. http://www.comune.torino.it/ambiente/aria/aria_cielo/andamento-inquinanti.shtml.
Coulson, K.L. *Solar and Terrestrial Radiation.* New York: Academic Press, 1975.
D.S.Kim, C.A. Infante Ferreira. "Solar refrigeration options - a state-of-the-art review." *International journal of Refrigeration*, 2008: 3-15.
Daylight Hours . http://www.worldmapsonline.com/LESSON-PLANS/6-daylight-hours-globe-lesson-16.htm.
Declination. http://en.wikipedia.org/wiki/Declination .
Direction of Earth's Rotation. http://www.sci.uidaho.edu/scripter/geog100/lect/01-foundations-of-geography/earth-rotation.htm.
Earth's Atmosphere. http://www.windows2universe.org/earth/Atmosphere/overview.html.
Earth-Sun Geometry. http://www.physicalgeography.net/fundamentals/6h.html.
"Energy and Communications." *Swedish Ministry of Enterprise.* 2007.
Ennis, Dwight. *The Ecliptic System and the Zodiac.*
http://www.astrologyclub.org/articles/ecliptic/ecliptic.htm.
ESTIF. *European Solar Thermal Industry Federation.*
ESTIF. *Solar thermal markets in Europe: Trends and market statistics 2010.* 2011.
F.Agyenim, I.Knight, M.Rhodes. " Design and experimental testing of the performance of an outdoor LiBr/H2O solar thermal absorption cooling system with a cold store." *Solar Energy*, 2010: 735–744.
Fracastoro, G.V. *Attenuazione della radiazione solare diretta ad opera di un'atmosfera industriale.* Torino: Politecnico di Torino, 1976.
Fracastoro, G.V. "Misure di radiazione diretta a Pino Torinese e a Torino,." *Annuario dell'Osservatorio Astronomico di Torino*, 1977.
Gajbert, Helena. "Solar thermal energy systems for building integration." 2008.
Henning.
Henning, Hans-Martin. *Focus point 2: Solar assisted cooling.* Freiburg, 2008.
Henning, Hans-Martin. *Solar air-conditioning and refrigeration-Introduction.* 2007.
Henning, Hans-Martin. "Solar assisted air conditioning of buildings - an overview." *Applied thermal engineering*, 2007: Volume 27, Issue 10, July 2007, Pages 1734–1749.
Henning, Hans-Martin. *Task 38 Solar Air-conditioning and refrigeration.* Cape town, November 15, 2010.
Hottel, H.C. "A simple model for estimating the transmittance of direct solar Radiation through clear atmospheres." *Solar Energy*, 1976.
Introduction to Solar Radiation. http://www.newport.com/Introduction-to-Solar-Radiation/411919/1033/content.aspx.

ISE, Fraunhofer.
"ISES Membership newsletter." 2011 (No.6).
John A. Duffie, William A. Beckman. "Solar engineering of thermal processes."
L. Schnabel, M. Tatlier, F. Schmidt, A. E. Senatalar. "Adsorption kinetics of zeolite coatings directly crystallized on metal supports for heat pump applications (adsorption kinetics of zeolite coatings)." *Applied Thermal Engineering*, 2010: 1409.
L.T.Wong, W.K.Chow. "Solar radiation model." *Applied Energy*, 2001: 191-224.
Lior, Noam. "Thermal theory and modeling of solar collectors." In *Solar collectors, energy storage, and materials*, by F. de Winter, MIT Press. Cambridge MA, 1990.
M., Gantner. *Dynamicsche simulation thermischer solaranlagen.* 2000.
Moon, P.J. "Proposed Standard Solar Radiation Curves for Engineering Use." *J.Franklin Institute*, 1940.
Movements of the Earth.
Munters.
newsletter, ISES.
Perihelion and Aphelion.
Perihelion and Aphelion.
http://www.windows2universe.org/physical_science/physics/mechanics/orbit/perihelion_aphelion.html.
Polysun user manual.
Pyrheliometer. http://www.ncpre.iitb.ac.in/page.php?pageid=47&pgtitle=Solar-Energy.
"Renewable Energy Essentials: Solar Heating and Cooling." *International Energy Agency.*
Roselund, Christian. "The Sleeping Giant: Solar Cooling and Heating Market Trends." *SolarServer.* http://www.solarserver.com/solar-magazine/solar-report/solar-report/the-sleeping-giant-solar-cooling-and-heating-market-trends.html.
Selfe, Dave. "A History of the Solar System." *The Journal of the Derby and District Astronomical Society* . January - April 2006. http://www.derbyastronomy.org/AriesJanApr06HistorySolarSystem.htm.
Seyed Hossein Rezaei, Andreas Witzig, Jorg Marti. "Deign methodology for combined solar and geothermal heating system." *ESTEC.* Munich, 2009.
SOLAIR. *Best practice catalogue on successful running solar air-conditioning appliances.* 2008.
Solar cooling kits for Europe. http://www.solarthermalworld.org/node/386.
Solar keymark. http://www.estif.org/solarkeymark/.
"Solar Keymark brochure."
Struckmann, Fabio. "Analysisi of a flat-plate solar collector." 2008.
Sunpath. http://kcorreia.com/2010/sunpath/.
The solar system: A brief glance. http://www.youtube.com/watch?v=fmxi3HvK2Js.
Threlkeld, J.L. and R.C. Jordan. " Direct solar radiation available on clear days." *ASHRAE Trans*, 1958: 45-48.
Ursula Eicker, Dirk Pietruschka. "Optimisation and economics of solar cooling systems." *Advances in building energy research*, 2009: 45-82.
Wiki: Ecliptic.
Wiki:Celestial sphere.